

Medical University of South Carolina

MEDICA

MUSC Theses and Dissertations

2014

Discovery of Pharmacological Compounds that Stimulate Renal Mitochondrial Biogenesis and Restore Kidney Function

Sean Robert Jesinkey

Medical University of South Carolina

Follow this and additional works at: <https://medica-musc.researchcommons.org/theses>

Recommended Citation

Jesinkey, Sean Robert, "Discovery of Pharmacological Compounds that Stimulate Renal Mitochondrial Biogenesis and Restore Kidney Function" (2014). *MUSC Theses and Dissertations*. 505.

<https://medica-musc.researchcommons.org/theses/505>

This Dissertation is brought to you for free and open access by MEDICA. It has been accepted for inclusion in MUSC Theses and Dissertations by an authorized administrator of MEDICA. For more information, please contact medica@musc.edu.

**Discovery of Pharmacological Compounds that Stimulate
Renal Mitochondrial Biogenesis and Restore Kidney
Function**

By

Sean Robert Jesinkey

A dissertation submitted to the faculty of the Medical University of
South Carolina in partial fulfillment of the requirements for the
degree of Doctor of Philosophy in the College of Graduate Studies.

Program in Drug Discovery and Biomedical

Sciences

2014

Approved by:

Chairman, Advisory Committee

ACKNOWLEDGEMENTS

Personally, I would like to acknowledge my wife Carrie and family (Leslie Jesinkey, Brian Jesinkey, Shannon Jesinkey, Alison Jesinkey, Courtney Barnett and David Barnett). If it were not for their unconditional support, encouragement, and vast imaginations none of this would be possible.

Professionally, I would like to acknowledge Dr. David R. Wiseman for planting the seed for me to become an eclectic autodidactic polymath, Drs. Thomas A. Dix and Craig C. Beeson whose continued support allowed me to grow, and the tenacious leadership of Dr. Rick G. Schnellmann, which not only brought the aforementioned to fruition, but also ripened my ability simplify complexity. I would also like to thank my committee members: Dr. Zhi Zhong, Dr. Robin Muise-Helmericks, and Dr. Mike Wyatt for their guidance and direction. In addition, I want to acknowledge Kyle Rasbach who has provided years of invaluable advice and my colleagues Jason Funk, Ryan Whitaker, Jenny Blakely, and Matt Smith for the constant challenge to be creative.

Finally, it is imperative to acknowledge that all of those mentioned have influenced the distortion of my boundaries, leading me to accomplish more than I ever thought I was capable.

TABLE OF CONTENTS

Chapter 1: ACUTE KIDNEY INJURY AND MITOCHONDRIAL BIOGENESIS

Renal anatomy and physiology	1
Overview	1
The Nephron	2
Renal Corpuscle: filtration	4
Proximal Tubule: reabsorption and secretion	5
Loop of Henle, distal tubule, and collecting duct: reabsorption and secretion	6
Acute kidney injury	6
Definition	6
Epidemiology, outcomes, and economics	10
Etiology	14
Pathophysiology: prerenal, intrinsic, and postrenal	20
Pathophysiology of ischemic AKI	17
Simulating I/R induced AKI in animal models	27
AKI Biomarkers: traditional and emerging	29
Mitochondria	34
Mitochondrial structure and function	34
Mitochondrial dysfunction in AKI	38
Mitochondrial biogenesis	41
Definition of mitochondrial biogenesis	41
Nuclear control of mitochondrial biogenesis and function	42
Physiological mechanisms controlling mitochondrial biogenesis	49
Mitochondrial biogenesis in renal cell injury	53
Alternative splice variants of PGC-1 α	57
Biotechnology: drug discovery and mitochondrial biogenesis	58

G-protein coupled receptors: biological targets for mitochondrial biogenesis	58
Drug discovery: AKI and mitochondrial biogenesis	60
Chapter 2: RENAL MITOCHONDRIAL BIOGENESIS VIA A₁ ADENOSINE RECEPTOR ACTIVATION.....	68
Abstract	68
Introduction	69
Experimental Procedures	71
Animal Dosing	71
Immunoblot analysis	72
Quantitative real-time polymerase chain reaction (qPCR).....	72
Respirometry assay	73
Pharmacophore modeling	74
Statistical analysis	74
Results	74
Discussion	102
Chapter 3: FORMOTEROL RESTORES MITOCHONDRIAL AND RENAL FUNCTION AFTER ISCHEMIC/REPERFUSION INJURY.....	105
Abstract	105
Introduction	106
Experimental Procedures	108
Ischemia/reperfusion model of AKI	108
Assessing renal function	109
Immunoblot analysis	109
Immunohistochemistry	109
Mitochondrial isolation and oxygen consumption	110
Statistical analysis	110
Results	111
Discussion	120
Chapter 4: ATOMOXETINE PREVENTS DEXAMETHASONE-INDUCED SKELETAL MUSCLE ATROPHY IN MICE.....	122

Abstract	122
Introduction	123
Experimental Procedures	126
Dexamethasone induced model of skeletal muscle atrophy.....	126
Assessing skeletal muscle atrophy	126
mRNA analysis	127
Mitochondrial DNA content	128
Immunoblot analysis.....	128
Statistical analysis	129
Results	129
Discussion	150
Chapter 5: CONCLUSIONS AND FUTURE DIRECTIONS	154
Conclusions	154
Future Directions.....	160
References	167

ABSTRACT

SEAN ROBERT JESINKEY. Discovery of Pharmacological Compounds that Stimulate Renal Mitochondrial Biogenesis and Restore Kidney Function (Under the direction of Drs. Rick G. Schnellmann and Craig C. Beeson)

Dysfunctional mitochondria are a primary pathological consequence of acute kidney injury (AKI). Mitochondrial homeostasis is disrupted up to 144 h after ischemia-reperfusion (I/R) induced-AKI in the renal cortical tissue of mice. Stimulation of mitochondrial biogenesis in renal cells after oxidant injury restores mitochondrial function. The primary goals of this project were to identify novel pharmacological compounds capable of inducing mitochondrial biogenesis in the renal proximal tubule and evaluate if this induction would promote the recovery of mitochondrial and/or renal function after in vivo AKI. The secondary goal was to employ our mitochondrial approach for drug discovery towards identifying a novel treatment for a different disease state, skeletal muscle atrophy.

Stimulation of the G-protein couple receptor (GPCR) family in response to physiological stress results in the downstream activation of effectors, which up-regulates the expression and activity of PGC-1 α and subsequently activates the mitochondrial biogenic program. Pharmacological agonism of both the stimulatory GPCR (β_2 -AR) and the inhibitory (A_1 AR) GPCR family via full and partial agonists resulted in the stimulation of mitochondrial biogenesis in the renal proximal tubule. The A_1 AR partial agonist CVT-2759 was superior to the full agonist CCPA in stimulating mitochondrial biogenesis in the proximal tubule.

Acute kidney injury (AKI), by induction of ischemia-reperfusion (I/R), in mice produced persistent proximal tubule damage, which resulted in minimal recovery of kidney and mitochondrial function at 144 h post injury. Tubule pathology was characterized histologically by the presence of presence of necrosis. Renal dysfunction and injury was evidence by robust increases in serum creatinine and KIM-1 expression. In addition, mitochondrial OXPHOS proteins were suppressed and dysfunctional.

Treatment with formoterol, a potent, highly specific, and long-acting β_2 -AR agonist, restored renal function, rescued renal tubules from injury, and diminished necrosis after I/R-induced AKI. Concomitantly, formoterol stimulated mitochondrial biogenesis and restored the expression and function of mitochondrial proteins.

Skeletal muscle atrophy remains a clinical problem in numerous pathological conditions. β_2 -AR receptor agonists, such as formoterol, are capable of inducing mitochondrial biogenesis and skeletal muscle hypertrophy. Recently, atomoxetine, an FDA approved norepinephrine reuptake inhibitor, was positive in a cellular assay for mitochondrial biogenesis. Using a mouse model of dexamethasone-induced skeletal muscle atrophy we determined that atomoxetine prevents skeletal muscle atrophy via a non-canonical PGC-1 α signaling mechanism. In addition, we determined that formoterol selectively induces the PGC-1 α 4 splice variant, which initiates a discrete gene program resulting in skeletal muscle hypertrophy.

Taken together, we determined that pharmacological stimulation of mitochondrial biogenesis via formoterol is capable of promoting faster recovery of mitochondrial function, which is associated with accelerated recovery of overall kidney function after maximal kidney dysfunction is established. Overall, we have demonstrated that our drug discovery approach is effective in identifying pharmacological compounds capable of inducing mitochondrial biogenesis and other nuclear regulators of metabolism. This approach proves beneficial in defining novel therapies for disease states that are characterized by dysfunctional mitochondria.

Chapter 1:

ACUTE KIDNEY INJURY AND MITOCHONDRIAL BIOGENESIS

RENAL ANATOMY AND PHYSIOLOGY

Overview

The processes of filtration, secretion, and reabsorption, in addition to, hormonal secretion and metabolism, characterize renal function. The kidney's primary role in the overall maintenance of body homeostasis is the urinary excretion of nitrogenous wastes, xenobiotics, water, and electrolytes from the bloodstream [1]. This is achieved through the combination of filtration, secretion and reabsorption, which takes place in the functional unit of the kidney, the nephron. Autoregulatory mechanisms, the sympathetic nervous system, and hormones control these processes. The kidney is comprised of three distinct zones; from the outer most zone termed the renal cortex, to the renal medulla (divided into the outer medulla, further segmented into the outer stripe and inner stripe, and the inner medulla), and the inner most zone known as the renal papilla.

The nephron

As previously stated, the nephron is the functional unit of the kidney and is responsible for the formation of urine through a combination of filtration, secretion, and reabsorption processes, which maintain the balance of solutes and fluid contributing to body homeostasis. The kidney is composed of approximately 1-1.5 million nephrons, which can reside either completely in the cortex (cortical nephrons) or extend from the cortex into the medulla (juxtaglomerular nephrons) [2]. The nephron consists of five distinct regions, which are the renal corpuscle, the proximal tubule, the loop of Henle, the distal tubule, and the collecting duct. Each of these regions and their role in renal physiology is discussed in further detail below and can be referenced in Fig 1-1.

Micro-anatomical terms	Main Divisions	Segmentation (preferred terms)	Abbreviation	Cell Types	Other Frequently Used Descriptions
Proximal Convolution	Proximal Tubule	Proximal Convoluted Tubule	PCT	S1 Cells	P1 Segment
		Proximal Straight Tubule		PST	S2 Cells
Loop of Henle	Intermediate Tubule	Descending Thin Limb	DTL		DTL Cells
		Ascending Thin Limb		ATL	ATL Cells
	Distal Tubule	Thick Ascending Limb (or Distal Straight Tubule)	MTAL	TAL Cells	MAL mTALH CAL cTALH
		post macular segment	CTAL		MD Cells
Distal Convolution	Distal Convoluted Tubule	DCT 1	DCT	DCT Cells (+ IC Cells)	DCTa
		DCT 2			DCTb
Collecting Duct	Collecting System	Connecting Tubule	CNT	CNT Cells + IC Cells	DCTg CCTg
		Cortical Collecting Duct	CCD	Principal Cells (+IC Cells)	DCT/ CCT/
		Outer Medullary Collecting Duct	OMCD		CCT/
		Inner Medullary Collecting Duct	IMCD	Principal Cells	Inner Medullary Collecting Tubule Papillary Collecting Duct (PCD) (Ducts of Bellini)

Figure 1-1. Segmentation of mammalian nephron. Scheme modified from that proposed by Renal Commission of International Union of Physiological Sciences. Note that definitions used in this review correspond to those listed as “preferred terms” except that the term *distal tubule* (see asterisk) is used to denote nephron segment between region of macula densa and confluence with another tubule to form collecting duct [3].

Renal corpuscle: filtration

The renal corpuscle is composed of an outer epithelial shell called the Bowman's capsule, which encases a capillary network known as the glomerulus. The Bowman's capsule and glomerulus function to filter the blood to produce an ultrafiltrate and are the first steps in the formation of urine. The filtrate must transverse three layers, which are the endothelium of the glomerular capillaries, a negatively charged glomerular basement membrane (GBM), and the porous epithelial cells of the Bowman's capsule known as podocytes [2]. The afferent arteriole supplies the glomerulus with blood, which then diverges through the glomerular capillary network ultimately converging on and exiting through the efferent arteriole. Glomerular filtration is a passive process by which the blood is filtered based on size and charge whereby, ions, small molecular weight molecules and proteins (<60 kDa) can be filtered, but polyanionic molecules are restricted from filtration due to the electronegative charge on the GBM [4]. The glomerular filtration rate (GFR), which flows at approximately 180 ml/min, is mainly determined by renal blood flow pressure, which is regulated by non-simultaneous vaso-constriction and –dilation of the afferent and efferent arterioles. The arterioles respond to stimuli from autoregulation (i.e.-myogenic and tubular feedback mechanisms), sympathetic nervous system (i.e.-adenosine and norepinephrine), and hormones (i.e.-angiotensin II, atrial natriuretic peptide, and antidiuretic hormone) [2, 5, 6]. Despite such a large volume being filtered by the glomerulus, almost all of it is returned to the blood by a process known as reabsorption.

Proximal tubule: reabsorption and secretion

Reabsorption is the movement of water and solutes (i.e.- Na^+ , Cl^- , Ca^{2+} , PO_4^{3-} , HCO_3^- , amino acids, small proteins and carbohydrates) filtered by the glomerulus from the tubular lumen to the blood. In contrast secretion is the movement of filtered solutes (i.e.- H^+ , K^+ , organic anions and cations) from the blood to the tubular lumen. The majority of reabsorption and secretion occurs within the proximal tubule, which is the segment of the nephron distally attached to the Bowman's capsule. The proximal tubule has two distinct morphological regions: the pars convoluta and the pars recta [2].

The pars convoluta resides in the cortex and is composed of cuboidal/columnar cells and has a denser brush border and mitochondrial concentration than the pars recta, which extends into the renal medulla. Each of these two regions can be further subdivided based on reabsorption and secretion physiology into the S1 and S2 segments (pars convoluta) and the S3 segment (pars recta). More specifically, the pars convoluta reabsorbs HCO_3^- , amino acids, small proteins, glucose via the sodium glucose transporter 2 (SGLT-2), and secretes H^+ and organic anions and cations [2]. The S3 segment of the pars recta is similar in reabsorption and secretion capacity previously described for the S1 and S2 segments, but is differentiated by the use of sodium glucose transporter-1 (SGLT-1) and the presence of the glutathione (GSH) transporter [2, 7].

Loop of Henle, distal tubule, and collecting duct: reabsorption and secretion

The loop of Henle is composed of a thin descending limb composed of cuboidal/columnar cells with a brush border and a thick ascending limb, which is void of a brush border. The function of the loop of Henle is to dilute the urine entering from the proximal tubule. Active transport mechanisms for solutes are absent in the thin descending limb and even though it is permeable to water, it is only slightly permeable to NaCl. In contrast, the thick ascending limb is permeable to Na⁺, impermeable to water, and utilizes Na⁺, K⁺-ATPase as the main active transport mechanism [2, 8]. Beyond the loop of Henle exists the distal tubule, which absorbs 5-10% of the filtered Na⁺ and Cl⁻, secretes K⁺, as well as being central in the homeostasis of Ca²⁺ and Mg²⁺ [3]. Finally, the distal tubule connects to the collecting duct. The collecting duct is relatively impermeable to NaCl and water permeability is regulated by the antidiuretic hormone (ADH) and serves as the region in the nephron where urine concentration occurs [2, 9].

ACUTE KIDNEY INJURY

Definition

Acute kidney injury (AKI), formerly known as acute renal failure (ARF), is a syndrome characterized by the rapid loss of the kidney's excretory function, generally hours to days, and is typically diagnosed by the independent or simultaneous accumulation of end products of nitrogen metabolism (urea and creatinine) [10]. Other clinical and laboratory endpoints include decreased urine

output, accumulation of metabolic acids, and increased potassium and phosphate concentrations [10]. Historically, ARF was defined as a decrease in GFR that is associated with an increase in waste products including urea and creatinine and at that time more than 35 definitions existed for diagnosis [1, 11]. Recently, ARF has been replaced by the term AKI in order to highlight that injury to the kidney precedes current quantitative laboratory measures identifying a loss of excretory function [10]. Despite GRF being an excellent diagnostic tool for evaluating kidney function, the lack of standardization for defining AKI has created challenges in determining contributing factors to and the burden of this pathology.

Efforts to standardize definitions of AKI were developed through the Acute Dialysis Quality Initiative (ADQI), which led to the risk, injury, failure, loss, end stage (RIFLE) criteria and the Acute Kidney Injury Network (AKIN) further modified these criteria [12]. In general, the RIFLE and AKIN criteria stratify injury based upon changes in serum creatinine (SCr), GFR, and urine output (UO). The prognostic merits for both the RIFLE and AKIN definitions have been validated in thousands of patients [10, 13]. More recently, the Kidney Disease: Improving Global Outcomes (KDIGO) working group have combined the RIFLE and AKIN criteria to further refine the diagnostic criteria for AKI [10, 14]. Whereby, the KDIGO criteria retain the AKIN time frame of 48 hours for an absolute increase in serum creatinine of ≥ 0.3 mg/dL, the RIFLE criteria time frame of 7 days for a ≥ 50 percent increase in serum creatinine, and do not include GFR for staging criteria [10, 14]. Figure 1-2 outlines the direct comparisons between the RIFLE, AKIN, and KDIGO criteria.

The future challenges in defining AKI include being able to evolve current diagnostic criteria with the emergence of novel biomarkers and the general complexity surrounding renal fluid dynamics. In addition the variability in administrative claims data for identifying AKI has resulted in problematic interpretation of epidemiological parameters. However, standard definitions for evaluating AKI have resulted in a more accurate interpretation of the epidemiology surrounding AKI.

Criteria for acute kidney injury

	Serum creatinine criteria			Urine output criteria
	RIFLE	AKIN	KDIGO	
Definition	Increase in serum creatinine of >50 percent developing over <7 days	Increase in serum creatinine of 0.3 mg/dL or >50 percent developing over <48 hours	Increase in serum creatinine of 0.3 mg/dL developing over 48 hours or >50 percent developing over 7 days	Urine output of <0.5 mL/kg/hr for >6 hours
Staging				
RIFLE-Risk AKIN/KDIGO stage 1	Increase in serum creatinine of >50 percent	Increase in serum creatinine of 0.3 mg/dL or >50 percent	Increase in serum creatinine of 0.3 mg/dL or >50 percent	Urine output of <0.5 mL/kg/hr for >6 hours
RIFLE-Injury AKIN/KDIGO stage 2	Increase in serum creatinine of >100 percent	Increase in serum creatinine of >100 percent	Increase in serum creatinine of >100 percent	Urine output of <0.5 mL/kg/hr for >12 hours
RIFLE-Failure AKIN/KDIGO stage 3	Increase in serum creatinine of >200 percent	Increase in serum creatinine of >200 percent	Increase in serum creatinine of >200 percent	Urine output of <0.3 mL/kg/hr for >12 hours or anuria for >12 hours
RIFLE-Loss	Need for renal replacement therapy for >4 weeks			
RIFLE-End-stage	Need for renal replacement therapy for >3 months			

AKIN: Acute Kidney Injury Network; KDIGO: Kidney Disease/Improving Global Outcomes.

References:

1. Bellomo R, Ronco C, Kellum JA, et al. Acute renal failure-definition, outcome measures, animal models, fluid therapy and information technology needs: the Second International Consensus Conference of the Acute Dialysis Quality Initiative (ADQI) Group. *Crit Care* 2004; 8:B204. Copyright © 2004 BioMed Central Ltd.
2. Mehta RL, Kellum JA, Shah SV, et al. Acute Kidney Injury Network: report of an initiative to improve outcomes in acute kidney injury. *Crit Care* 2007; 11:R31. Copyright © 2007 BioMed Central Ltd.
3. Kidney Disease: Improving Global Outcomes (KDIGO). Acute Kidney Injury Work Group. KDIGO clinical practice guidelines for acute kidney injury. *Kidney Int Suppl* 2012; 2:1.

Figure 1-2. AKIN, RIFLE, AND KDIGO criteria for identifying acute kidney injury diagram originally published in Up-to-date.

Epidemiology, mortality, and economics

Acute kidney injury is a common condition experienced worldwide. In developed countries it affects 1 in 5 adults and 1 in 3 children hospitalized with an acute condition [14, 15]. In the United States between the years 1996-2003 the incidence of community acquired AKI in renal replacement therapy (RRT) and nonRRT populations increased from 19.5 to 29.5 per 100,000 person-years (33%) and 322.7 to 522.4 per 100,000 person-years (38%), respectively [14]. In the past 50 years, mortality rates have remained unchanged, ranging from 50% to 70% and have become a significant financial burden not only for patients, but also the overall healthcare system [10, 16-18]. In general, an increase in the severity of AKI is correlated with a decrease in survival and is highest in those requiring RRT

Fig. 1-3 [14].

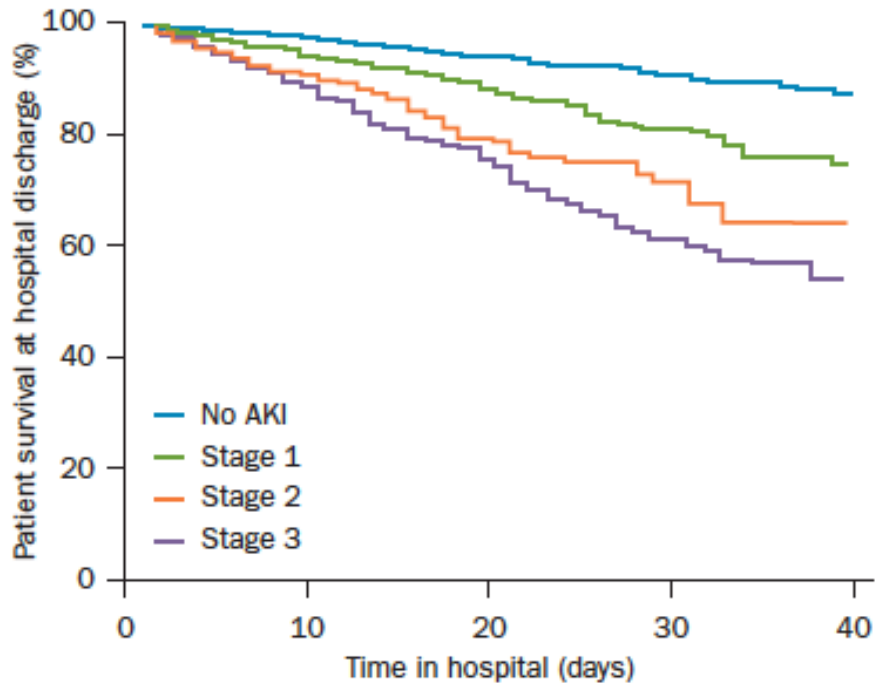


Figure 1-3. Kaplan–Meier graph for hospital survival, stratified by KDIGO stages of acute kidney injury. Reproduced with permission from Oxford University Press © Wang, H. E. et al. Comparison of absolute serum creatinine changes versus Kidney Disease: Improving Global Outcomes consensus definitions for characterizing stages of acute kidney injury. *Nephrol. Dial. Transplant.* 28, 1447–1454 (2013) [14].

More specifically, a study from 2005 evaluated if rates of mortality and hospital costs are correlated with elevations in SCr in hospitalized patients [18]. From this study it was determined that an increase in SCr greater than or equal to 0.5 mg/dl was associated with a 6.5-fold increase in the odds of death (Fig 1-4a), a 3.5 day increase in length of stay, and nearly \$7500 in excess hospital costs (Fig. 1-4b) [18]. When interpreting epidemiological, mortality, and economic studies it is important to note how existing comorbidities in populations suffering from AKI influence a study's outcome. Nonetheless, the results from these studies further emphasize how guidelines from the RIFLE, AKIN, and KDIGO are beneficial in providing a cohesive platform by which to compare various analyses in an effort to provide evidence outlining the impact AKI has on a patient's quality of life and the global healthcare system.

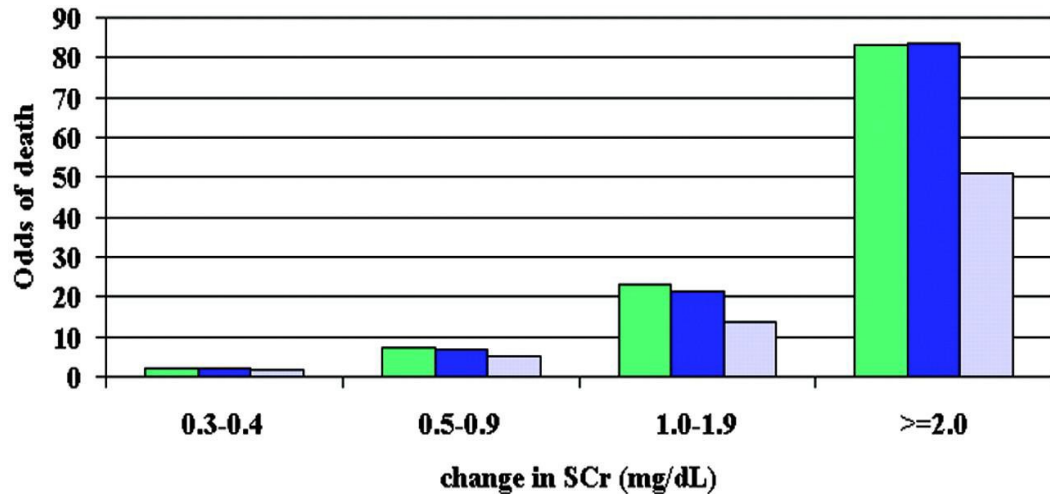


Figure 1-4a. Mortality associated with change in serum creatinine. Green bars are unadjusted, blue bars are age and gender adjusted, and gray bars are multivariable adjusted. Multivariable analyses adjusted for age, gender, diagnosis-related group (DRG) weight, chronic kidney disease (CKD) status, and ICD-9-CM codes for respiratory, gastrointestinal, malignant, and infectious diseases; $n = 1564, 885, 246,$ and 105 for change in SCr 0.3 to $0.4,$ 0.5 to $0.9,$ 1.0 to $1.9,$ and ≥ 2.0 mg/dl [54].

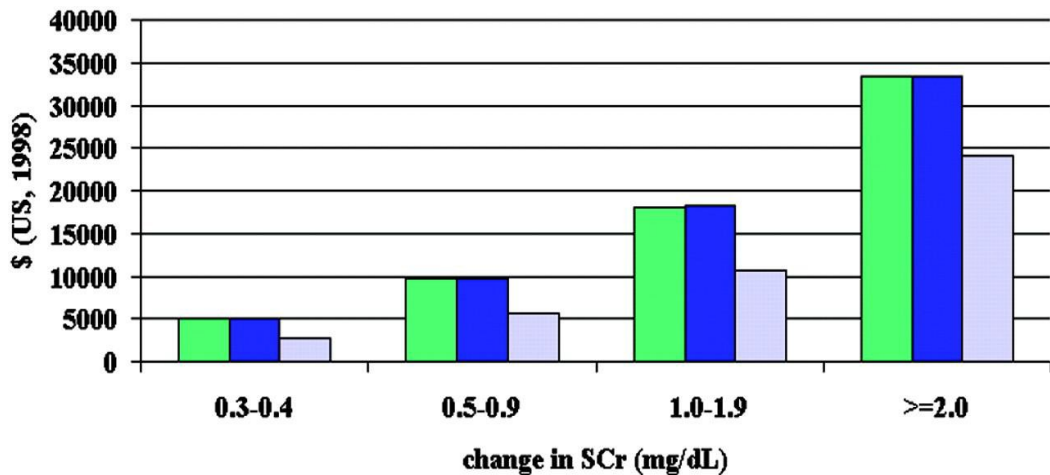


Figure 1-4b. Mean hospital costs associated with changes in SCr. Green bars are unadjusted, blue bars are age and gender adjusted, and gray bars are multivariable adjusted. Multivariable analyses adjusted for age, gender, DRG weight, and ICD-9- CM codes for cardiovascular, respiratory, malignant, and infectious diseases; $n = 1564, 885, 246,$ and 105 for change in SCr 0.3 to $0.4,$ 0.5 to $0.9,$ 1.0 to $1.9,$ and ≥ 2.0 mg/dl [54].

Etiology

The etiology of AKI can be apportioned into the three major pathological categories of injury (i.e.- prerenal, intrinsic, and postrenal) with the associated contributing factors. Major causes of AKI are septic shock, ischemia/reperfusion (IR) injury, cardiogenic shock, hypovolemia, and drug/toxicant exposure. Sepsis (toxic injury) is the most common cause of AKI in hospital inpatients and those in the intensive care unit (ICU) [10]. Ischemic insult (hemodynamic injury) is also a leading cause of AKI and can develop secondary to pathologies reducing renal perfusion (i.e.- sepsis, reduced cardiac output, and/or surgery [1]. Acute kidney injury from general systemic inflammation can manifest, pathologically, similar to either sepsis and/or ischemic injury. Figure 1-5 describes the pathologies associated with the major causes of AKI [10]. Even though this figure portrays a linear progression in cellular injury dependent on the type of insult, it is important to note that the degree of cellular injury (i.e.- sublethal, apoptosis, or necrosis) from sepsis or ischemia is not linear, but rather dependent upon the extent and duration of injury.

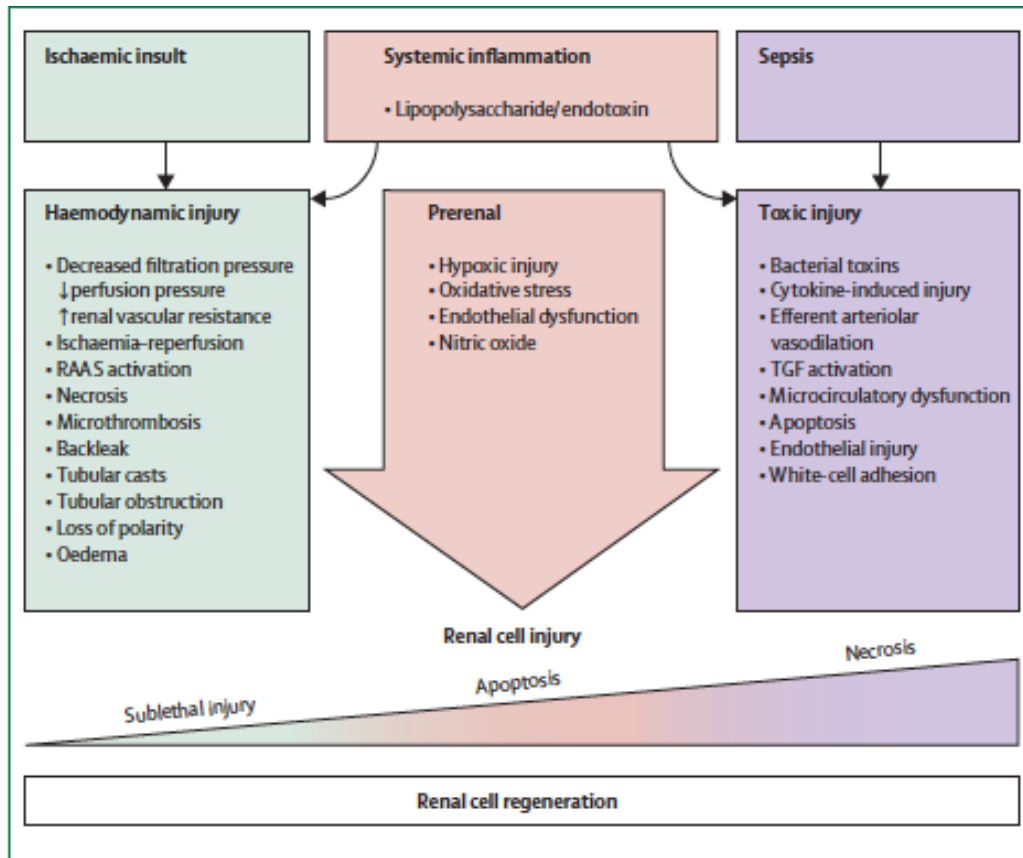


Figure 1-5. Key potential pathways implicated in pathogenesis of acute kidney injury due to ischemia or sepsis. The timing of activation of each pathway, their interaction, and the hierarchy of these pathways remain unknown. RAAS = renin–angiotensin–aldosterone system. TGF = tubuloglomerular feedback [10].

Numerous drugs are established to be nephrotoxic (Table 1-1) and contribute to AKI in roughly 20% of patients, especially in the critically ill patient population [10, 19, 20]. Clinical use of iodinated radiocontrast agents for angiography has been reported as the third most common cause of hospital acquired AKI (behind decreased renal perfusion and nephrotoxic drugs) and responsible for 11% of all hospital acquired AKI cases [21-23].

- Radiocontrast agents
- Aminoglycosides
- Amphotericin
- Non-steroidal anti-inflammatory drugs
- β -lactam antibiotics (specifically contribute to interstitial nephropathy)
- Sulphonamides
- Aciclovir
- Methotrexate
- Cisplatin
- Cyclosporin
- Tacrolimus
- Angiotensin-converting-enzyme inhibitors
- Angiotensin-receptor blockers

Table 1. Drugs that contribute to acute kidney injury [10].

Aminoglycosides are a class of antibiotics known to cause acute tubular necrosis (ATN) via accumulation in the proximal tubule and are reported to induce AKI in 5-15% of prescribed patients [24, 25]. Acute kidney injury can also occur with any class of non-selective or cyclooxygenase -2 (COX-2) selective non-steroidal anti-inflammatory drugs (NSAIDs) due to their inhibition of COX enzymes, which decreases prostaglandin (PG) synthesis; thereby, inhibiting an important afferent arteriole vasodilatory mechanism resulting in a decrease of peritubular blood flow increasing the risk for ischemic ATN [26]. Depending on the type of NSAID being prescribed, with the exclusion of naproxen, the relative risk of developing NSAID induced AKI ranges from 1.5-2.4, compared to NSAID naïve individuals [27]. Cisplatin is a potent chemotherapeutic agent that is highly nephrotoxic. Cisplatin-induced AKI results from direct tubule epithelial cell toxicity, microvascular vasoconstriction, reactive oxygen species (ROS) production from proinflammatory effects, and ATP depletion [28, 29]. Ultimately, cisplatin injures the S3 segment of the proximal tubule causing a decrease in GFR [30].

Pathophysiology: prerenal, intrinsic, and postrenal

The initiation of AKI can broadly be classified into three categories: prerenal, intrinsic, and postrenal. Prerenal AKI results from hypoperfusion of the renal parenchyma with or without systemic arterial hypoperfusion and prerenal azotemia accounts for 55-60% of all AKI incidences [1, 23]. The initial physiological responses to overcome prerenal hypotension are activation of the renin-angiotensin-aldosterone and sympathetic nervous systems and the release of ADH. Activation of these systems and release of hormones results in an increase blood pressure through vasoconstriction, simultaneously with an increase in blood volume via the retention of sodium and water and the stimulation of thirst.

Intrinsic AKI accounts for 35-40% of observed AKI and is categorized based on damage to the following kidney structures: the renal vasculature, glomeruli, tubules, and the interstitium [1, 23]. Occlusion of the renal vasculature can occur when large atheroemboli or thromboemboli block blood flow in bilateral renal arteries leading to a rise in SCr. Glomerular damage accounts for only 5% of intrinsic AKI and arises through similar mechanisms as the renal vasculature, but also can activate the inflammatory response resulting in severe inflammation. Tubular damage that manifests in acute tubular necrosis (ATN) accounts for approximately 85% of intrinsic AKI, of which 50% are the result of renal ischemia, typically arising from prerenal injury [1]. Irrespective of the etiology, tubular damage prevents the kidney from concentrating the urine and ultimately leads to a decrease in GFR [31].

Intrinsic AKI from interstitial damage typically manifests when the interstitium

becomes severely inflamed, which is most commonly caused by medications, bacteria, or viruses; however, up to 30% of cases have no identifiable cause [1, 32]. Finally, postrenal AKI classically develops from an obstruction at any level of the urinary collection system starting with the renal tubule and ending at the urethra [1]. Wherever location of the obstruction, prevention of the outflow of urine will result in an increased pressure upstream; whereby, the ureters, renal pelvis, and calyces all expand, which leads to a decrease in GFR [1].

Pathophysiology of ischemia/reperfusion (I/R) induced AKI

Renal ischemia/reperfusion (I/R) injury is a leading cause of AKI that results from impairment of oxygen and nutrient delivery to, and waste product removal from, cells of the kidney [10, 33-35]. The imbalance between the delivery of oxygen, cellular demand for oxygen, and proper removal of metabolic wastes can lead to cell death via apoptosis or necrosis [35]. The pathophysiology of I/R induced AKI involves complex alterations in the functioning and repair mechanisms of vascular and tubular components, all of which are described in further detail below.

Initiation, extension, maintenance, and recovery phases of I/R injury. The temporal patterns of I/R induced AKI are traditionally divided into four phases: initiation, extension, maintenance, and recovery [36].

The initiation phase is characterized by sublethal injury to the tubule epithelial and endothelial cells, generation of reactive oxygen molecules is initiated, and activation of inflammatory mechanisms commences [36]. An early pathological consequence of the initiation phase is the markedly reduced production of ATP by the proximal tubule, which is less adaptable than the medullary thick ascending limb (MTAL) in converting from oxidative to glycolytic metabolism [35]. During the extension phase blood flow returns to the cortex, but remains severely reduced in the medulla and tubules undergo reperfusion-dependent cell death simultaneously with regeneration processes [36]. Damaged endothelial and epithelial cells, which also cause severe vasoconstriction, intensify inflammatory cascades and GFR continues to decline [36]. Throughout the maintenance phase GFR is at its lowest despite normalization in blood flow, parenchymal injury is established, and concomitant cell injury and regeneration exists [36]. Lastly, in the recovery phase GFR improves and structural tubule integrity is reestablished, with fully differentiated and polarized epithelial cells [36].

Vascular components of injury. Both the endothelial and smooth muscle cells of the microvasculature play critical roles in the pathophysiology of AKI (Fig. 1-6) [35]. The observed decrease in GFR in I/R induced AKI is a byproduct of regional alterations in renal blood flow (RBF) [37]. Data from renal I/R induced AKI animal models have established that following ischemic injury blood flow to the outer medulla is reduced disproportionately to the reduction in total kidney perfusion, which is inferred to be the case in humans [35, 38, 39].

In addition, endothelia of the microvasculature are also injured and vasoconstriction is more prevalent in the postischemic kidney than vessels from a normal kidney in response to increased tissue levels of endothelin-1, angiotensin II, thromboxane A₂, prostaglandin H₂, leukotrienes C₄ and D₄, and adenosine as well as sympathetic nerve stimulation [35, 40-43]. Concomitantly, vasodilatory mechanisms are also compromised in the damaged endothelium due to a reduced production in nitric oxide and other substances that stimulate vasodilation [44]. Beyond the pathologies associated with vaso-constriction and -dilation exists vascular occlusion mechanisms. For example, ischemic injury activates the coagulation cascade resulting in occlusion of small vessels. Furthermore, damaged endothelial cells express cell adhesion molecules, such as ICAM-1, which enhance leukocyte-endothelial adhesion resulting in obstruction of capillaries [45]. Simultaneous vasoconstriction and occlusion mechanisms further propagate injury by compromising microcirculation, preventing the clearance of metabolic wastes, and supplying necessary amounts of oxygen to meet the demands of the injured cells (Fig. 1-6) [35].

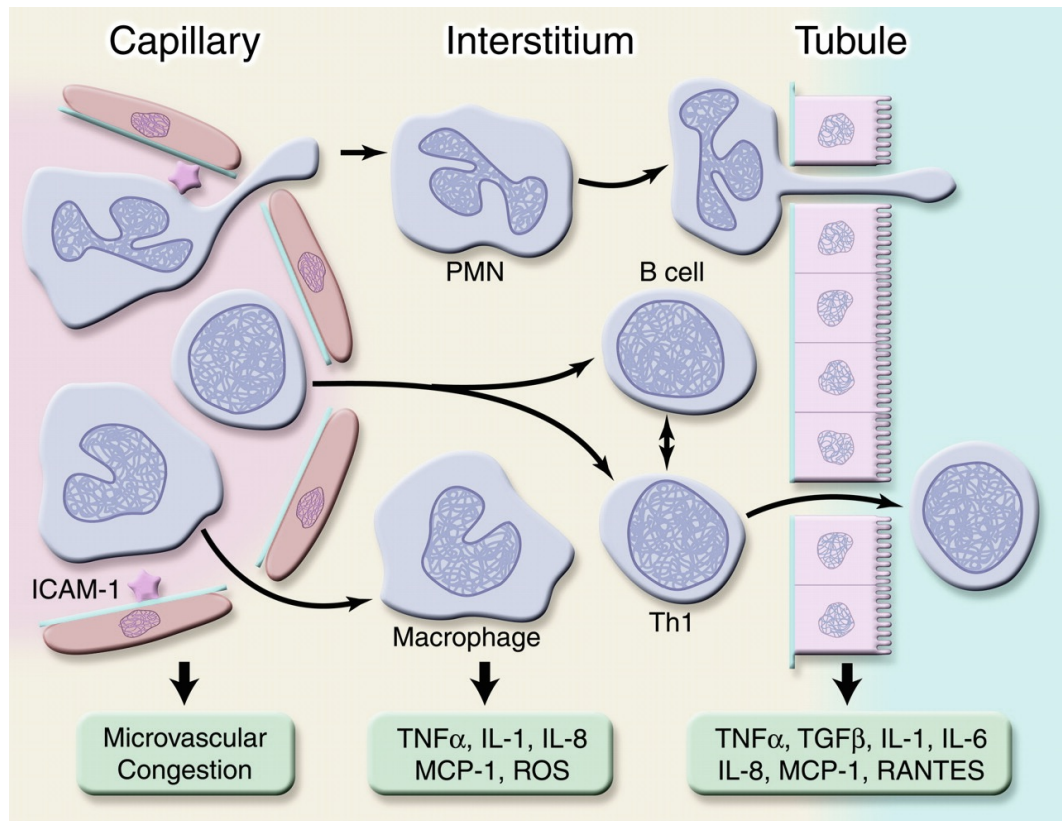


Figure 1-6. Alterations in the microvasculature and inflammation in ischemic AKI. During the extension phase, endothelial injury leads to intense vasoconstriction, microvascular sludging, and microvascular congestion with leukocytes. Activated leukocytes produce a number of inflammatory mediators and reactive oxygen species that potentiate tubule cell damage. In addition, tubule cells exhibit a maladaptive response by generating cytokines and chemokines that further amplify the inflammation. PMN, polymorphonuclear leukocyte; Th1, T-helper 1 cell. Strategies that modulate the inflammatory response may provide significant beneficial effects in ischemic AKI. Illustration by Josh Gramling—Gramling Medical Illustration [36].

Tubular components of injury. The two major tubular components involved with the pathology of AKI are the proximal and distal tubules. Damaged tubular epithelia are not quiescent and respond to I/R injury by triggering an inflammatory response from both the innate and adaptive immune systems. Activation of inflammatory cells by tubule epithelial cells involves the generation of proinflammatory and chemotactic cytokines (i.e.-TNF- α , TGF- β , IL-8, IL-6, IL-1 β) and epithelial neutrophil-activating protein 78 (ENA-78) [46]. In addition, tubular cells express Toll-like receptors (TLRs), complement and complement receptors, and costimulatory molecules, which regulate T lymphocyte activity [35]. It is established in animal models simulating I/R injury that the most evident site of injury is the S3 segment of the proximal tubule [35]. Autophagy is important in proximal tubule cell survival after I/R injury. However, this process can be inhibited during injury, resulting in the cellular accumulation of malformed mitochondria, ubiquitin-positive cytoplasmic inclusions, and, therefore, have an increased propensity to become apoptotic [47]. The straight portion of the distal tubule, the medullary thick ascending limb (MTAL) has a close spatial association with the proximal tubule in the outer stripe of the outer medulla [35]. The cells from the distal nephron are more resistant to oxidative injury than the proximal tubules and, for the most part, remain intact during I/R injury. The MTAL adapt to ischemic conditions by readily switching from oxidative to glycolytic metabolism, as well as producing antiapoptotic Bcl-2 proteins and reparative growth factors, which all work synergistically to minimize cell death [35, 48].

Overall, the tubular component of injury characterized by the breakdown of the cytoskeleton, loss of cell polarity, cell death (i.e.-apoptosis or necrosis), desquamation of viable and nonviable cells, and tubular obstruction [49, 50].

Cellular injury and repair after I/R induced AKI. The typical processes of injury and repair to the kidney epithelium are depicted Fig. 1-7 [35]. Initial ischemic injury results in rapid loss of cytoskeletal integrity. This sets in motion a cascade of morphological changes such as the loss of the apical brush border and redistribution of membrane proteins and a loss in cell polarity [51]. The misappropriated proteins include adhesion molecules and other membrane proteins such as the Na⁺K⁺-ATPase and β -integrins [51]. The inflammatory response (i.e.-cytokine release) disrupts the cell-matrix adhesion dependent on β integrins and disruption of cell-cell interactions at adherent and tight junctions [33, 46, 52]. Actin also re-localizes from the apical to lateral cell membrane [35, 53, 54]. Under normophysiological conditions, epithelial cells communicate with one another via tight and adhesion junctions, which are regulated by the F-actin cytoskeleton [35]. In turn, the cytoskeleton is under control by the Rho family of GTPases, which become activated in response to the ischemic injury [35]. The Rho associated coiled-coil-forming protein kinase (ROCK) is a downstream effector of Rho GTPases and plays a role in increased production of apoptotic cells [35].

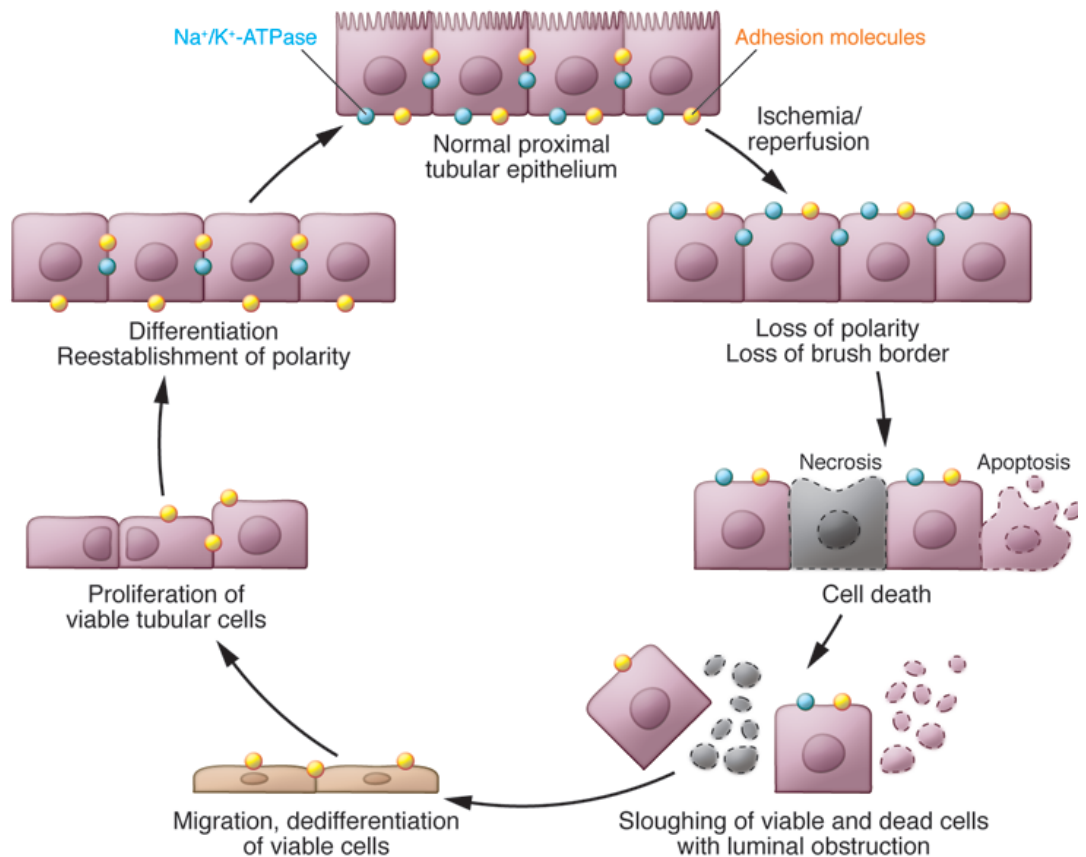


Figure 1-7. Normal repair in ischemic AKI. The current understanding of tubular injury and repair after ischemic AKI. With IRI, the normally highly polar epithelial cell loses its polarity and brush border with proteins mislocated on the cell membrane. With increasing time/severity of ischemia, there is cell death by either necrosis or apoptosis. Some of the necrotic debris is released into the lumen. Viable epithelial cells migrate and cover denuded areas of the basement membrane. These cells undergo division and replace lost cells. Ultimately, the cells go on to differentiate and reestablish the normal polarity of the epithelium [35].

Simulating I/R induced AKI in animal models

The use of animal models to study AKI is a necessity for the elucidation of pathological mechanisms involved at all stages of development and recovery from kidney injury. Inherent limitations exist with any animal model simulating disease or injury observed clinically in humans. With regards to replicating I/R induced AKI in humans, there are validated rodent models that are comparable to the type of injury and recovery observed in humans.

I/R model of AKI. I/R injury can be replicated in a number of animals, but the most common rodents used are mice and rats. Experimentally, renal ischemia can be induced by significantly reducing blood flow via uni- or bi-lateral clamping of the renal artery or pedicle for a specified amount of time. This type of procedure is the most extensively used animal model for AKI studies [55]. Adjustment of ischemic time and choosing to obstruct either one or both kidneys can optimize the degree of injury desired by the researcher. Reperfusion of the kidneys is obtained by simple removal of the arterial or pedicle clamps. It has been reported in rat models mimicking I/R induced kidney injury, that clamping of both kidneys for 60 minutes followed by reperfusion was sufficient to develop AKI [55, 56]. Alternatively, in mice, arterial clamping occurs in the range of 20-60 minutes in followed by reperfusion has also been reported to sufficiently induce kidney injury [55, 57]. During the time frame used for clamping the kidney is anoxic and functional outputs such as GFR and transport activity are completely stopped [55].

Acute tubular necrosis develops upon reperfusion and anatomically is initiated in the S3 segment of the proximal tubule at the corticomedullary junction in the outer stripe of the outer medulla [55, 57]. Endothelial injury, manifested by outer medullary congestion, stasis, and hemorrhage, is accompanied by a substantial inflammatory response with the recruitment of neutrophils [55, 58].

Clinical translational caveats of I/R induced AKI animal models.

The characteristics of I/R induced AKI in animal models are similar to those observed in humans such as the presence of both casts and tubular cells in the urine, matching alterations in biomarkers, and damage to the S3 segment of the proximal tubule. However, the mechanisms by which these characteristics manifest might be achieved differently. Human ischemia can lead to tissue hypoxia or anoxia, but in the previously described animal model only anoxic conditions are generated from the ischemic insult. It is suggested that ROS play a more important role at hypoxic oxygen tensions than at severe anoxic oxygen tensions in protein stabilization and gene regulation [59, 60].

Additionally, tubular damage from I/R induced AKI in humans clinically presents as being focal in nature [55]. In contrast, most experimental models elicit extensive non-focalized injury and therefore the pattern of injury distribution may be misleading in the determination of clinical relevance [55].

AKI Biomarkers: traditional and emerging

As previously discussed, the term acute kidney injury has replaced acute renal failure to emphasize that a continuum of kidney injury exists that begins long before sufficient loss of excretory kidney function can be measured with standard laboratory tests [10]. In the past decade there have been extensive efforts towards the identification of novel biomarkers for detection of AKI that are more specific for the location of injury and sensitive than those currently used clinically. Both traditional and an emerging biomarker for detection of AKI are discussed in further detail below and depicted in Fig. 1-8 [61].

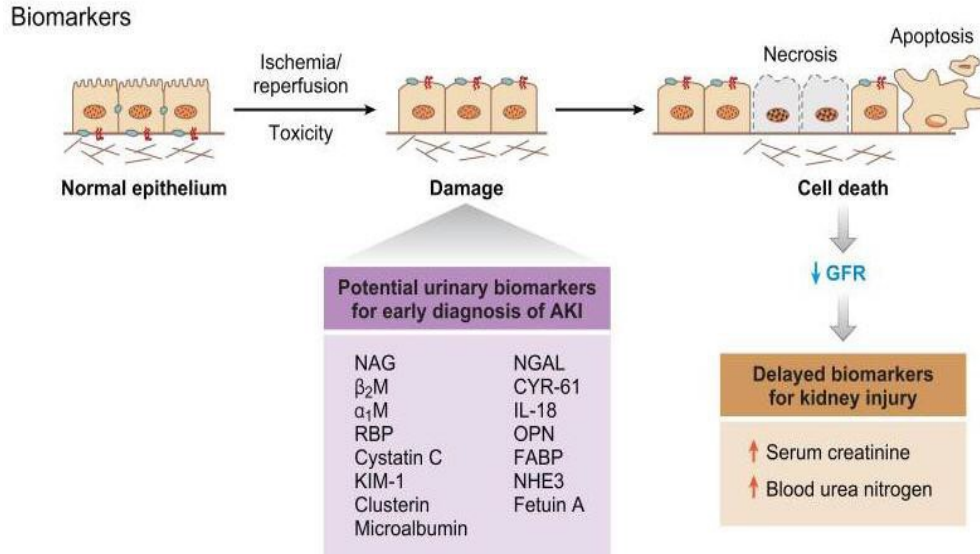


Figure 1-8. Biomarkers of AKI: Traditionally used markers, such as blood urea nitrogen (BUN) and creatinine (CR), are insensitive, nonspecific, and do not adequately differentiate between the different stages of AKI. A delay in diagnosis prevents timely patient management decisions, including administration of putative therapeutic agents. Urinary biomarkers of AKI will facilitate earlier diagnosis and specific preventative and therapeutic strategies, ultimately resulting in fewer complications and improved outcomes [61].

Creatinine. Creatinine is a standard clinical measurement that has been used for over 60 years to diagnose kidney function [62]. It is readily detectable in the urine (UCr) and serum (SCr). For simplicity SCr will be used for the remainder of this section to illustrate benefits and limitations of creatinine as a biomarker for AKI. Creatinine is freely filtered by the glomerulus and trace amounts are secreted into the tubular lumen [63]. During AKI the increase in serum creatinine is a result of decreased GFR and backleaks through damaged proximal tubule cells. Though the initial discovery was a clinical breakthrough for evaluation of kidney function, it has several limitations.

Despite its use in the RIFLE, AKIN, or KDIGO guidelines for determining AKI, SCr is technically a measure of renal function, not injury. Though the two, injury and function, are often correlated, rises in SCr can occur in the absence of kidney injury. In addition, serum creatinine fails to provide accurate diagnostic information with regards to the location of injury, thus it is nonspecific. Furthermore, if injury does exist, there is a lag time between initial insult and observable increases in SCr. Therefore, it is not sensitive to the timing of injury, either. However, when used in conjunction with other functional parameters (i.e.- GFR) or other novel injury biomarkers (KIM-1, cystatin-C, etc.) it is effective in the painting of a prognostic picture for AKI.

Blood urea nitrogen. Blood urea nitrogen (BUN) is a traditional biomarker, like creatinine, which is widely used clinically as a diagnostic parameter for AKI.

Similar to creatinine, BUN is not a specific or sensitive marker for AKI.

Alterations in blood concentrations can be affected by other physiological mechanisms not related to AKI. Overall, its limitations and use as a diagnostic tool closely mirror the benefits and limitations outlined in the previous section about creatinine.

Kidney injury molecule-1. Previous studies, conducted by the laboratory of J.V. Bonventre, that sought the identification of novel biomarkers for AKI led to the discovery of kidney injury molecule-1 (KIM-1). Kidney injury molecule-1 is an emerging biomarker that is both selective for proximal tubule injury and sensitive to the initiation of cell injury [63, 64]. This molecule has been cloned in rats, mice, and humans and is only biochemically expressed after proximal tubule injury [65]. Thus, KIM-1 is an ideal biomarker not only for the diagnosis of AKI, but also clinically translating data obtained from animal models to humans.

Structurally, KIM-1 is a type I membrane glycoprotein that contains both a novel six-cysteine immunoglobulin-like domain and a mucin domain in its extracellular portion [63, 65]. As shown in Fig. 1-9, after injury to the proximal tubule KIM-1 adheres to proximal tubular cells and it is the ectodomain that is cleaved via a metalloproteinase-dependent mechanism [63], which is detectable in the urine by the quantitative micro-bead based KIM-1 ELISA.

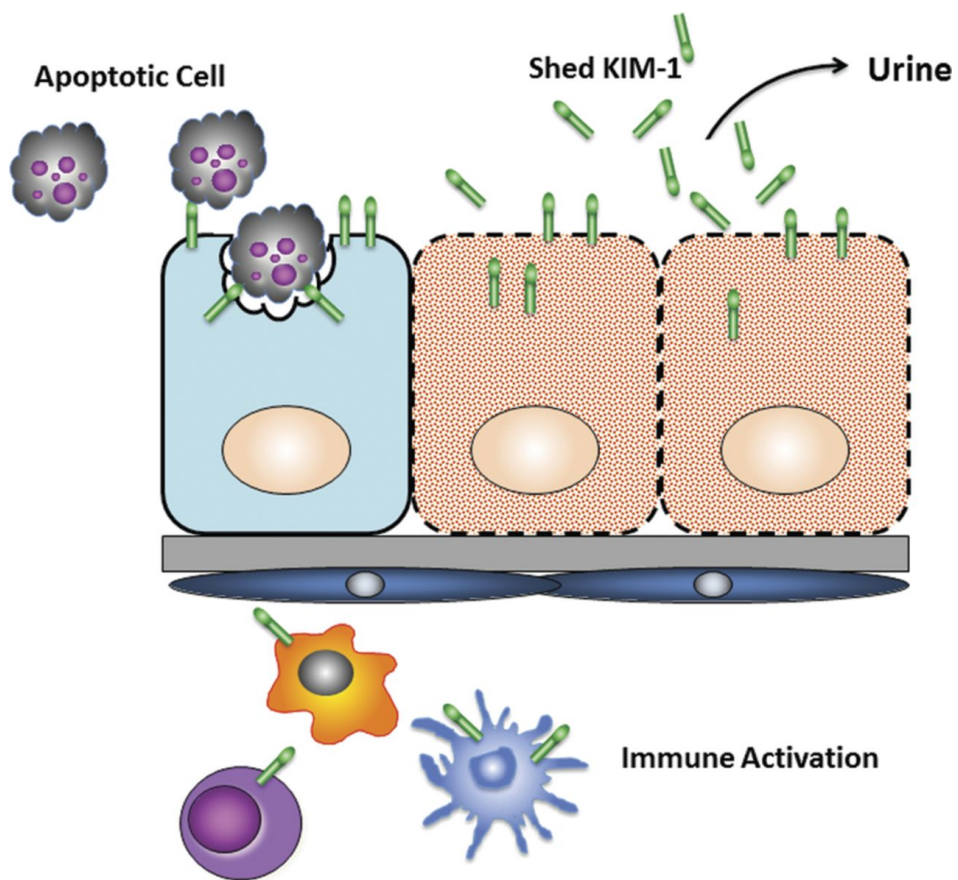


Figure 1-9. KIM-1. It is expressed in proximal tubule cells and is thought to promote apoptotic and necrotic cell clearance. Upon injury, KIM-1 is upregulated and shed into the urine and extracellular space. It is thought to activate immune cells in injury-induced immune response [63].

In addition, KIM-1 is also expressed in immune cells where it is thought to activate T-helper2 (Th2), Th1 and Th17 differentiation as well as activating receptor in B cells, dendritic cells and natural killer cells. The US Food and Drug Administration (FDA) has approved its use as an AKI biomarker for preclinical drug development [66].

MITOCHONDRIA

Mitochondrial structure and function

Mitochondria are cellular organelles that are present in almost all cell types of animals. Intracellular mitochondrial abundance ranges from hundreds to thousands, depending on the type of cell. In healthy cells, the persistent processes of fusion and fission to form tubular networks maintain mitochondrial homeostasis.

Evolutionarily, mitochondria are thought to have previously existed in nature as unicellular organisms of aerobic bacterial origin. The endosymbiotic hypothesis postulates that eukaryotic cellular organisms engulfed mitochondria more than a billion years ago and remain due to a symbiotic relationship based on the exchanging of energy in the form of ATP for intracellular habitation. Supportive evidence for this hypothesis resides in the presence of mitochondrial DNA (mtDNA), the mitochondria's capacity to carry out DNA transcription and RNA translation, and its dependence on the nuclear genome for replication.

Structurally, the mitochondria are composed of four main compartments: (1) the outer membrane, (2) the inner membrane space, (3) the inner membrane, and (4) the matrix. The outer membrane is porous and permeable to certain ions and small molecules in contrast to the inner membrane. The processes of fusion and fission are controlled by: (1) mitofusins (outer mitochondrial membrane fusion), (2) OPA1/Mgm1 (inner mitochondrial membrane fusion), and (3) Drp1/Dnm1 (division of outer and inner mitochondrial membranes) [67]. All three of these molecules are GTP-hydrolyzing proteins (GTPases) that belong to the dynamin superfamily [67].

Functionally, mitochondria are integral in fundamental cellular processes, which include the production of energy in the form of ATP or GTP, biosynthesis, ion homeostasis, oxygen sensing, and apoptosis. The generation of ATP occurs via aerobic metabolism through a process known as oxidative phosphorylation (OXPHOS). Within the inner membrane of the mitochondria exists the electron transport chain (ETC), which is composed of 5 enzyme complexes (Fig. 1-10) [68]. The entire coding capacity of mitochondrial DNA (mtDNA) is devoted to the synthesis of 13 essential subunits of the inner membrane complexes of the respiratory chain whereas the remaining 77 are encoded by the nuclear genome [69]. Complex I, aka nicotinamide adenine dinucleotide (NADH) dehydrogenase-ubiquinone oxidoreductase, and complex II, aka succinate dehydrogenase-ubiquinone oxidoreductase, oxidize reduced forms of nicotinamide adenine dinucleotide (NADH) and flavin adenine dinucleotide (FADH₂), respectively, which are generated in the mitochondrial matrix by the citric acid cycle and beta-oxidation of fatty acids, to initiate the flow of electrons through the ETC.

Electrons are transferred from NADH and FADH₂ to complexes I and II, respectively, to coenzyme Q, which then shuttles electrons to complex III, aka ubiquinone-cytochrome c oxidoreductase, onto cytochrome c, and terminating at complex IV, aka cytochrome c oxidase, with the reduction of molecular oxygen into water. Concurrently, complexes I, III, and IV pump protons across the inner mitochondrial membrane from the matrix to the inner membrane space thereby generating a higher concentration of protons in the inner membrane space relative to the matrix. Protons flow down the concentration gradient through complex V, aka ATP-synthase, triggering its rotary mechanism, which then forms ATP via phosphorylation of ADP (Fig. 1-10) [69, 70].

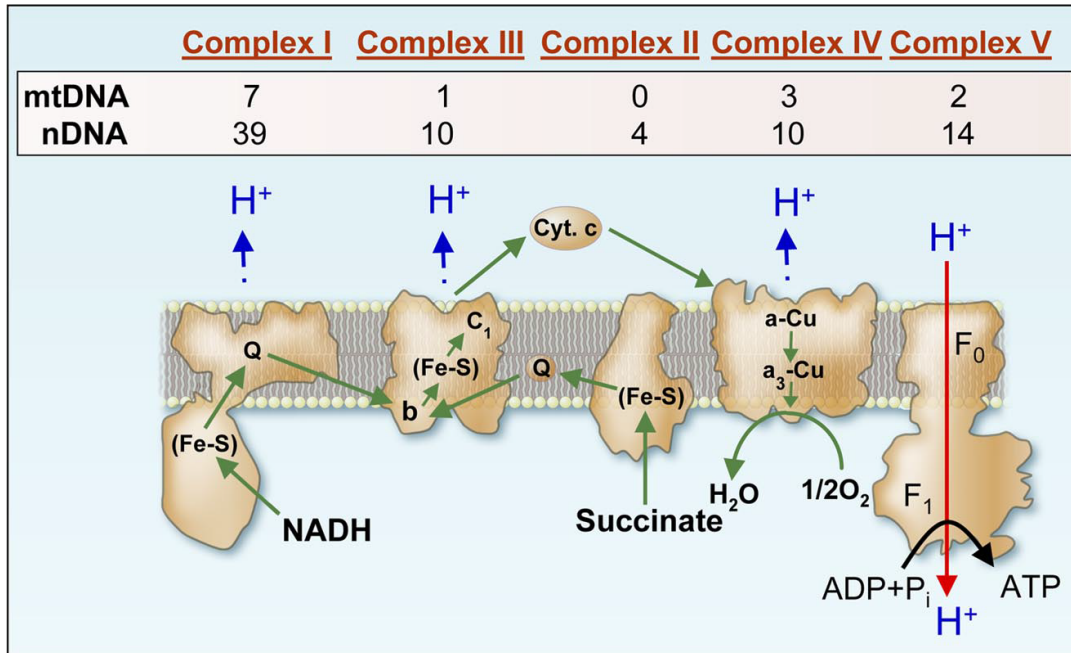


Figure 1-10. Summary of protein subunits of the five respiratory chain complexes encoded by nuclear and mitochondrial genes. Depicted is a schematic of the five respiratory complexes (I–V) embedded in the lipid bilayer of the inner mitochondrial membrane. Dissociable electron carriers cytochrome c (Cyt c) and coenzyme Q (Q) are also shown. Arrows (green) show the pathway of electrons from the various electron donors. Broken arrows (blue) show the sites of proton pumping from the matrix side to the cytosolic side by complexes I, III, and IV. The red arrow shows the flow of protons through complex V from the cytosolic side to the matrix coupled to the synthesis of ATP. Indicated above each complex are the number of protein subunits encoded by nuclear (nDNA) and mitochondrial (mtDNA) genomes [70].

Mitochondrial dysfunction in AKI

A decrease of intracellular mitochondrial abundance and compromised structural integrity manifested as mitochondrial fragmentation is commonly observed in renal cells following AKI [71, 72]. Specifically, the extent of renal injury and the release of apoptotic proteins were attenuated in Drp1 null mice subjected to I/R induced AKI when compared to their wild type littermates [72]. However, elucidation of the precise role of mitochondrial fission and fusion during the initiation, extension, maintenance, and recovery phases has yet to be determined.

Mitochondrial dysfunction contributes to oxidative stress, persistent energy depletion and impairment of energy dependent repair mechanisms, ultimately leading to end organ damage and failure in a variety of tissues including brain, heart, liver, and kidneys [73-76]. Dysfunctional mitochondria are an important component of I/R and sepsis-induced AKI [77-80] and a large number of nephrotoxic xenobiotics target the mitochondria to promote dysfunction [81-90]. Major pathophysiological mechanisms observed in the mitochondria following ischemic injury are characterized by the disruption of mitochondrial respiratory complexes, membrane depolarization and permeabilization, lipid peroxidation, release of apoptotic proteins, and de-energized mitochondria, which result in severe energy deficits within the proximal tubule [49, 50, 74, 85, 91, 92].

Upon reperfusion, dysfunctional mitochondria promote additional damage of injured cells through the production of reactive oxygen and nitrogen species, thus implicating mitochondria as both a target for and a cause of I/R injury [84].

Additionally, elevations in intracellular and mitochondrial Ca^{2+} and Fe^{3+} may contribute to the central role of the mitochondria in the disease process [93, 94].

A sentinel study investigated renal mitochondrial dysfunction in an I/R model of AKI [95]. In mice subjected to I/R insult, injury was evident by a reported spike in serum creatinine at 24 h, which partially recovered, but was persistently elevated through 144 h [95]. Renal mRNA and protein levels of both nuclear and mitochondrial encoded proteins of the electron transport chain (ETC) such as, NADH dehydrogenase ubiquinone 1 beta complex 8 (NDUFB8), ATP synthase subunit β (ATP β), NADH dehydrogenase 6 (ND6), and cytochrome c oxidase subunit I (COX I) were continually suppressed through to 144 h post I/R injury (Fig. 1-11) [95].

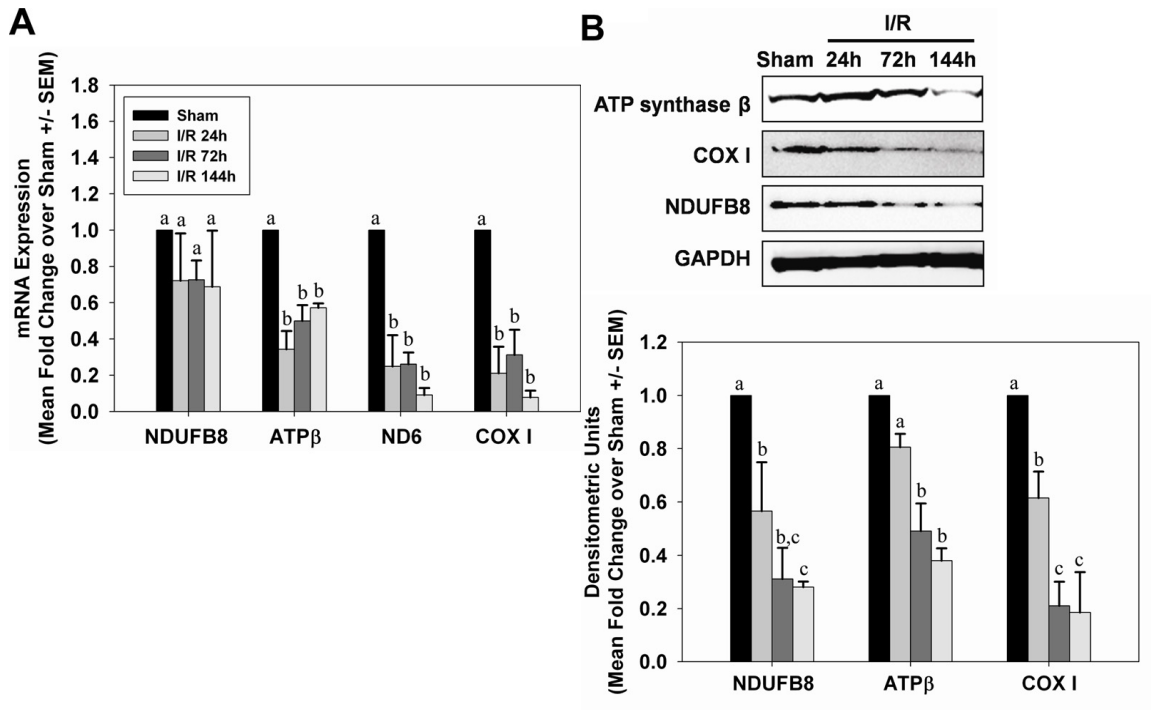


Figure 1-11. Sustained depletion of mitochondrial proteins after I/R AKI. (A) mRNA from sham and I/R mice was analyzed by qPCR for expression of nuclear-encoded respiratory genes NDUFB8 and ATP synthase β and the mitochondrial-encoded genes ND6 and COX I at 24, 72, and 144 h after injury. (B) expression of mitochondrial respiratory proteins from kidneys of sham and I/R mice was examined by immunoblot analysis. Bars with different superscripts are significantly different from one another ($P < 0.05$) [95].

MITOCHONDRIAL BIOGENESIS

Definition of mitochondrial biogenesis

Mitochondrial biogenesis is the physiological process by which the cell forms new mitochondria in response to environmental stimuli or physiological stress [96]. This process serves as the primary mechanism to increase cellular energy, especially under pathologic conditions [97]. The formation of new mitochondria is theorized to occur either through (i) de novo synthesis of mitochondria from submicroscopic precursors present in the cytoplasm; (ii) formation from other membranous structures of the cell; and/or (iii) growth and division of pre-existing mitochondria [98]. To date, the majority of evidence in the literature supports the theory that biogenesis of mitochondria transpires from growth and division of pre-existing mitochondria.

The formation of new mitochondria is a dynamic and complex process involving crosstalk between both the mitochondrial and nuclear genome, which is dependent on transcription factors and their associated coactivators. This process is thought to be under control by the nuclear encoded coactivator protein peroxisome proliferator-activated receptor-gamma coactivator-1 α (PGC-1 α), aka the “master regulator” of mitochondrial biogenesis, which is abundantly expressed in tissues with high metabolic demand (e.g. heart, skeletal muscle, and kidneys) [70, 99-101].

Nuclear control of mitochondrial biogenesis and function

Successful transcription of mtDNA is entirely dependent on a set of nuclear-encoded genes. Briefly, transcription of mtDNA necessitates formation and binding of initiation complexes on a promoter of the of the D-loop region of mtDNA. These complexes contain a mitochondrial RNA polymerase (POLMRT), mitochondrial transcription factors (Tfam, TFB1M, and TFB2M), and ultimately binding of a termination factor (MTERF1). The transcription of the subunits as well as nuclear-encoded subunits of the respiratory complexes, is controlled by nuclear transcription factors and their associated co-activators (Fig. 1-12) [102].

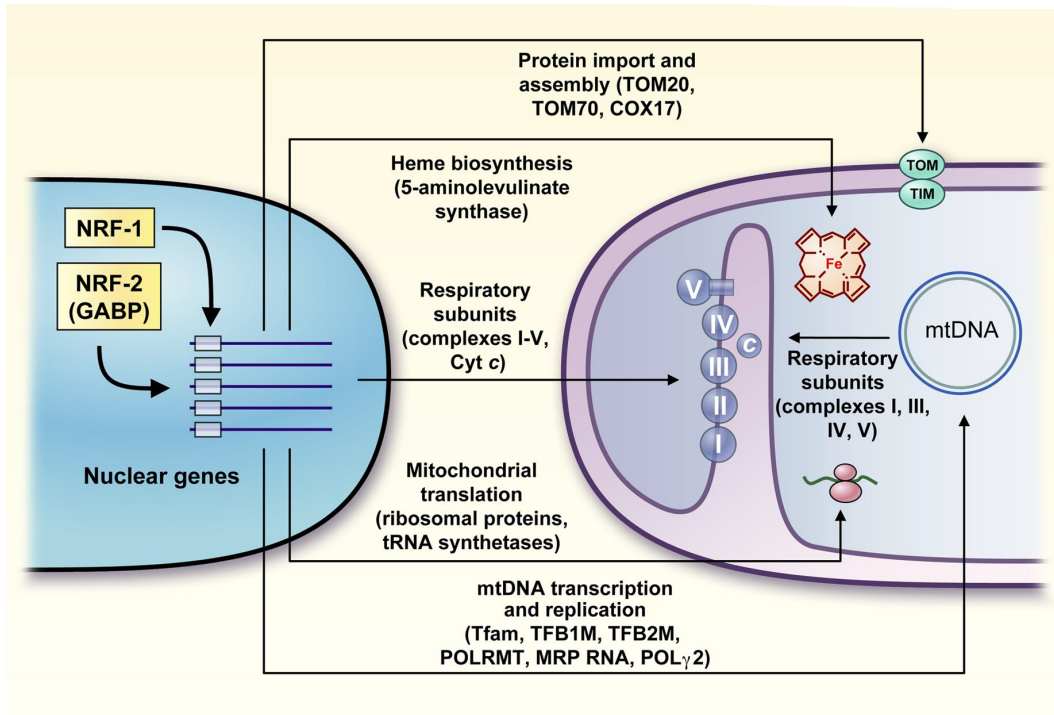


Figure 1-12. Diagrammatic summary of the nuclear control of mitochondrial functions by NRF-1 and NRF-2 (GABP). NRFs contribute both directly and indirectly to the expression of many genes required for the maintenance and function of the mitochondrial respiratory apparatus. NRFs act on genes encoding cytochrome c, the majority of nuclear subunits of respiratory complexes I–V, and the rate-limiting heme biosynthetic enzyme 5-aminolevulinate synthase. In addition, NRFs promote the expression of key components of the mitochondrial transcription and translation machinery that are necessary for the production of respiratory subunits encoded by mtDNA. These include Tfam, TFB1M, and TFB2M as well as a number of mitochondrial ribosomal proteins and tRNA synthetases. Recent findings suggest that NRFs are also involved in the expression of key components of the protein import and assembly machinery [70].

Nuclear respiratory factors 1 and 2. Nuclear respiratory factors-1 and 2 (NRF-1 and NRF-2) are transcription factors that act upon nuclear genes, which activate the transcription of nucleus-encoded subunits for cytochrome c oxidase, respiratory complexes I-V of the respiratory chain, and mitochondrial transcription, translation, and import machinery that are necessary for the expression of genes encoded by the mitochondrial genome [70, 103]. The NRF-1 transcription factor was first discovered from the identification of promoter regions of mammalian cytochrome c [104]. Whereas NRF-2 was identified through its specific binding to essential cis acting elements on the cytochrome oxidase subunit IV (COXIV) promoter region [70, 105]. Both respiratory factors are considered upstream modulators of mitochondrial transcription and ribosome assembly, due to their ability to activate the promoter for the mitochondrial exclusive transcription factors Tfam and Tfb1m, a mitochondrial methyltransferase that dimethylates 12S rRNA and controls the stability or assembly of the mitochondrial ribosome [103]. In addition, NRF-1 is involved with the transcription of TOMM20, a key functional subunit of the TOMM complex [70, 103]. The TOMM complex exists in the outer mitochondrial membrane and is involved with the import of thousands of proteins into the mitochondria that are diverse in function [70]. Thus, providing evidence that NRF-1 and NRF-2 are involved with both the coordination of respiratory chain expression and the biogenesis of mitochondria [103].

Nuclear receptor superfamily. Nuclear-encoded mitochondrial genes are also under control by the nuclear receptor (NR) superfamily.

The peroxisome proliferator-activated receptor (PPAR) family and the estrogen-related receptors (ERR) are both members of the NR superfamily that regulate nuclear genes of the mitochondria involved with fatty acid oxidation [103, 106, 107]. However, the ERR α receptors can regulate the transcription of the PPAR α gene in addition to nucleus-encoded mitochondrial proteins involved in the TCA cycle and the respiratory chain [102]. The cis – containing elements of the cytochrome c promoter recognize transcription factors of the ATF/CREB family [70, 104, 108]. In vitro and in vivo studies revealed that these elements bind CREB directly and the serum induction of cytochrome c in quiescent fibroblasts is associated with the phosphorylation of cAMP response element binding (CREB) and NRF-1 [70, 109, 110]. The Sp1 transcription factor is also involved in the regulation of cytochrome c1 as well as adenine nucleotide translocase 2 genes, both of which lack NRF sites [70, 111]. This is significant as this property illustrates alternative regulation of nucleus-encoded respiratory chain proteins. Another nuclear transcription factor involved in the control of mitochondrial biogenesis is the initiator element YY1, which has been implicated in both positive and negative control of cytochrome oxidase subunit gene expression [70, 112, 113].

Nuclear coactivators in mitochondrial biogenesis: the PGC-1 family. As described above the NRFs, Sp1, and ERR α have the most evidence supporting their role in the coordination of expression of nuclear and mitochondrial respiratory proteins. In addition, other mitochondrial oxidative pathways are controlled by alternative factors such as PPAR α and the fatty acid oxidation pathway [70, 114].

However, this evidence does not provide the answers to how these transcription factors are incorporated into the mitochondrial biogenesis program. The identification of the PGC-1 α family of transcriptional coactivators has provided an explanation for the mechanistic framework, which describes how the regulatory pathways of nuclear transcription factors are coupled to the biogenesis of mitochondria. This family of transcriptional coactivators is composed of PGC-1 α , PGC-1 β , and the PGC-1 related coactivator (PRC).

The first identified member of this family was PGC-1 α , which was described as a cold inducible coactivator of the nuclear receptor, PPAR γ , in brown adipocytes [100]. Canonical coactivation of certain nuclear receptors via PGC-1 α , PGC-1 β , or PRC is dependent on binding of nuclear receptor coactivator signature motifs (LXXLL) adjacent to the activation domain, an RNA recognition domain (RRM), and a host cell factor-1 (HCF) binding domain [70, 103]. The pairing of RNA processing and transcription by these coactivators occurs similarly through COOH-terminal arginine/serine rich (R/S) as well as RNA recognition motifs comparable to those found in RNA splicing factors [70, 115]. In vitro studies that overexpressed PGC-1 α in myoblasts have reported an induction of mRNAs of the respiratory chain, increases in COXIV and cytochrome c protein levels and the steady-state level of mtDNA (Figs. 1-13, 1-14) [70, 101, 116].

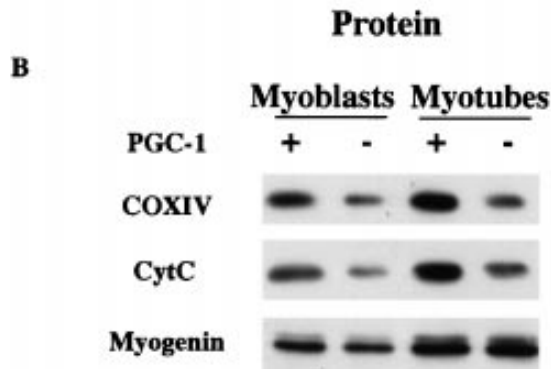
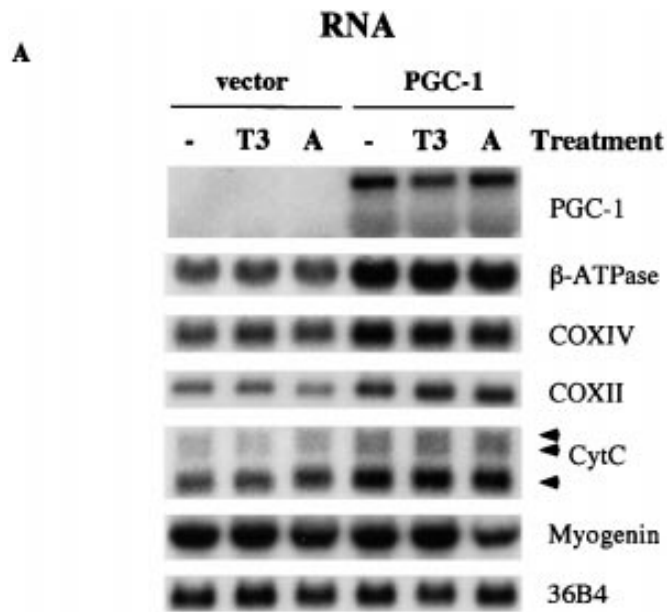


Figure 1-13. PGC-1 Increases Expression of Genes of the Mitochondrial Respiratory Chain. (A) RNA analysis of PGC-1-expressing cells. Myoblasts expressing PGC-1 and the control cells were induced to differentiation and were then treated with various stimuli, including 100 nM T3 (24 hr) and 1 mM 8-bromo-cAMP (A) (6 hr). Total RNA was extracted and subjected to Northern blot analysis. Probes used for hybridization were PGC-1, β -ATP synthetase, COXII and IV, CytC, and myogenin. A cDNA encoding a ribosomal protein, 36B4, was also used as a control for loading equivalence of RNA. (B) Protein analysis of PGC-1-expressing cells. Total proteins were extracted from the cells at confluence (myoblasts) or day 5 postconfluence (myotubes) and were subjected to Western blot analysis [101].

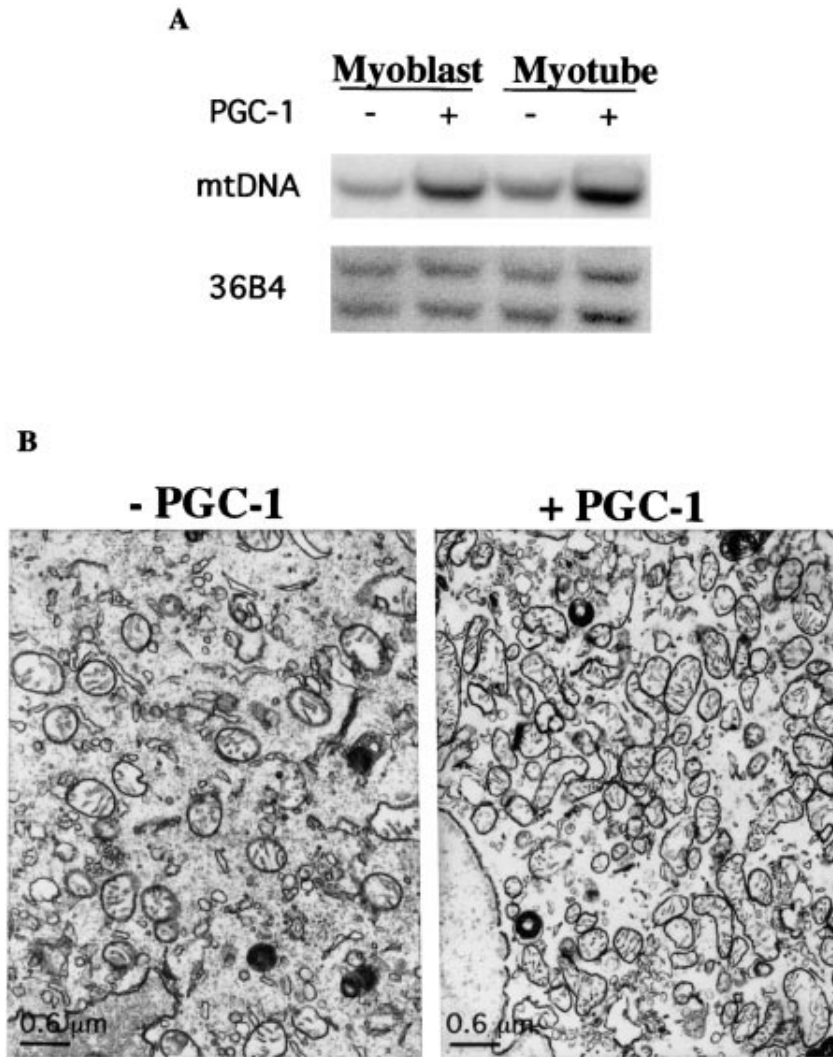


Figure 1-14. PGC-1 Stimulates Mitochondrial DNA Replication and Biogenesis
 (A) Southern blot analysis of mitochondrial and genomic DNA. Total cellular DNA was isolated from C2C12 cells expressing PGC-1 and their controls, in both the myoblast and myotube states. Ten micrograms of DNA was digested with NcoI and subjected to Southern blot analysis using a cDNA for COX II as a probe for mtDNA. The blot was then stripped and hybridized to a cDNA for 36B4, a nuclearly encoded gene. (B) Transmission electron microscopy of PGC-1 expressing myoblasts and control cells. The magnification is 8750 \times [101].

The nuclear transcription factors NRF-1, NRF-2, CREB, ERRs, and PPARs have been identified as important targets for coactivation by PGC-1 α and subsequent induction of mitochondrial biogenesis (Fig. 1-15) [70]. The illustration in figure 1-15, portrays the biological link between PGC-1 α and the mitochondrial transcriptional machinery, which can occur through PGC-1 α induction of NRF-1/2 and coactivation of the NRF-1 and NRF-2 recognition sites within Tfam and TFB1/2M promoters leading to an increase mRNA expression [70, 117]. The PGC-1 α coactivator also stimulates expression of numerous OXPHOS genes, such as cytochrome c and ATP synthase- β , through interactions with conserved ERR α and NRF-2 recognition sites in their promoter regions (Fig. 1-15) [70, 118]. As previously mentioned, other nuclear transcription factors that function in the replication of subunits of the respiratory chain and ribosomes are YY1 and MEF-2, both of which are also coactivated by PGC-1 α (Fig. 1-15) [70].

Physiological mechanisms controlling mitochondrial biogenesis

The PGC-1 family of coactivators is highly inducible by various types of stimuli. Tissue specific expression of PGC-1 α alters in response to the type of external stimuli (Fig. 1-15): cold in brown adipose tissue (BAT), exercise and decreased ATP levels in skeletal muscle, and fasting in liver [70, 119]. Diverse signaling mechanisms have been identified for the regulation of PGC-1 α at the transcriptional level, such cellular pathways include those involved with growth, differentiation, and energy metabolism [70, 103, 120].

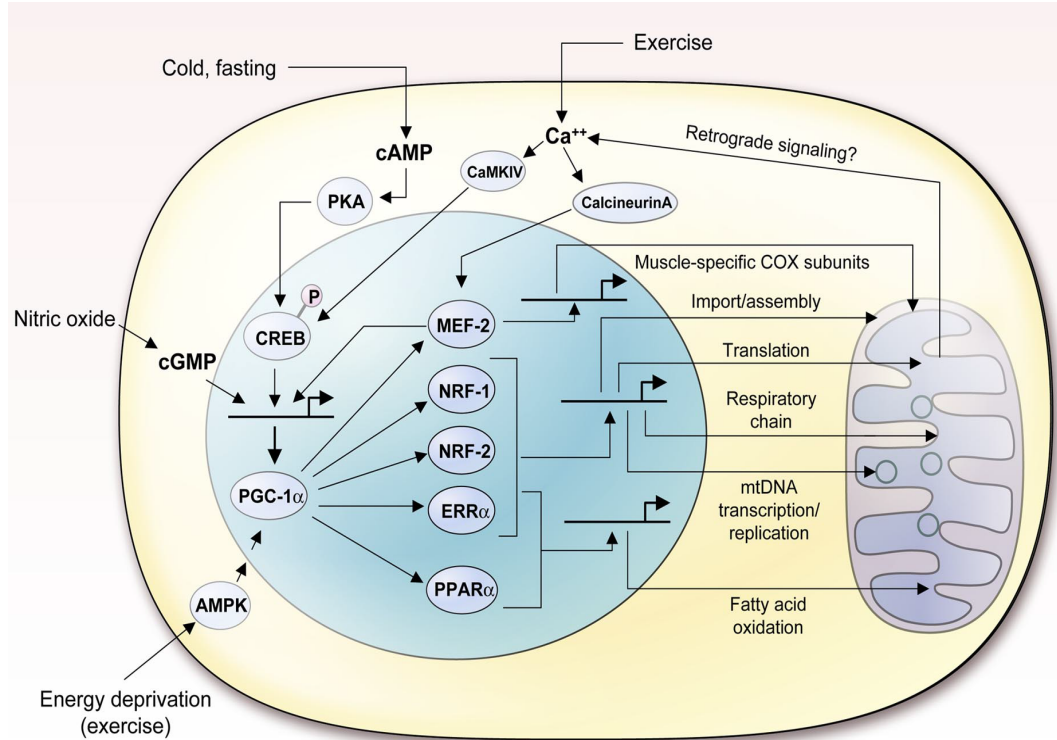


Figure 1-15. Illustration summarizing PGC-1 α -mediated pathways governing mitochondrial biogenesis and function. Depicted in the nucleus (shaded sphere) are the key transcription factors (NRF-1, NRF-2, ERR α , PPAR α , and MEF-2) that are PGC-1 α targets and act on nuclear genes governing the indicated mitochondrial functions. Some of the physiological effector pathways mediating changes in the transcriptional expression or function of PGC-1 α are also shown. The CREB activation of PGC-1 α gene transcription in response to cold (thermogenesis), fasting (gluconeogenesis), and exercise has been well documented. The physiological mechanisms of PGC-1 α induction by nitric oxide are not established but may involve the production of endogenous nitric oxide by eNOS. A potential pathway of retrograde signaling through calcium is also included [70].

More specifically, it is well established that caloric restriction, cold exposure, and other environmental stimuli activate β -adrenergic and cytokine cell surface receptors triggering cascades involving the phosphokinase A (PKA) and p38 mitogen-activated protein kinase (p38 MAPK) pathways [96]. Activation of PKA phosphorylates the CREB transcription factor, which can then directly bind to the promoter region of the PGC-1 α gene and influence expression [96, 121].

Alternatively, the p38 MAPK protein can directly phosphorylate the PGC-1 α protein, resulting in its activation, stabilization, and triggering the expression of the nucleus-encoded subunits of respiratory chain and Tfam through the induction of the expression of NRFs and the coactivation of NRF-1-mediated transcription [96]. In the same fashion previously discussed, Tfam subsequently translocates into the mitochondrion and directly increases the transcription and replication of mtDNA [96].

In addition, regulation of PGC-1 α is also controlled through signaling of the calcium/calmodulin-dependent protein kinase (CaMK-IV) pathway, and post-translational modifications alter its subcellular localization and activation by either phosphorylation (β -adrenergic/cAMP/p38 MAPK) or deacetylation by sirtuin1 (SIRT1) [96, 122-124]. See Table 1-2 for the complete description of biological consequences of post-translation modifications of PGC-1 α [125].

Post-translational modifications	Biological outcome	References
Phosphorylation		
AKT	Inhibition of activity affecting the expression of gluconeogenic and lipid oxidation genes	(Li et al., 2007)
AMPK	Increase in activity and regulation of genes involved in mitochondrial functions and glucose metabolism	(Jäger et al., 2007)
CLK2	Decrease in expression of gluconeogenic genes	(Rodgers et al., 2010)
GSK3B	In combination with phosphorylation of p38 MAPK, GSK3B designates PGC1 α for proteasomal degradation	(Olson et al., 2008)
p38 MAPK	Increase in activity leading to expression of mitochondrial genes	(Puigserver et al., 2001)
S6 kinase	Decrease in the induction of gluconeogenic genes while maintaining the expression of mitochondrial genes	(Lustig et al., 2011)
Acetylation		
GCN5	Inhibition of transcriptional activity	(Lerin et al., 2006)
Deacetylation		
SIRT1	Increase in expression of gluconeogenic genes	(Rodgers et al., 2005)
SUMOylation		
SUMO1	Decrease in transcriptional activity	(Rytinki and Palvimo, 2009)
Methylation		
PRMT1	Increase in activity leading to expression of mitochondrial biogenesis genes	(Teyssier et al., 2005)

Table 1-2. Post-translational modifications of PGC-1 α and their biological consequences [125].

Mitochondrial biogenesis in renal cell injury

Studies simulating sublethal oxidant injury with the model oxidant *tert*-butylhydroperoxide in renal proximal tubule cells (RPTC) have established that within 24 h of injury mitochondrial function, as measured by ATP production and respiration, and expression of OXPHOS components are markedly decrease, which gradually recover over 6 days [126-129]. Previously our laboratory utilized the same in vitro oxidant model to evaluate expression of PGC-1 α throughout the phases of injury and recovery and discovered that PGC-1 α is endogenously upregulated in response to injury; furthermore, overtime expression is inversely correlated with respiratory capacity (Fig. 1-16) [130]. Additionally, this study determined that the upregulation in PGC-1 α was partly mediated through the p38 MAPK pathway, which is an established downstream effector of β -adrenergic/cAMP signaling [130].

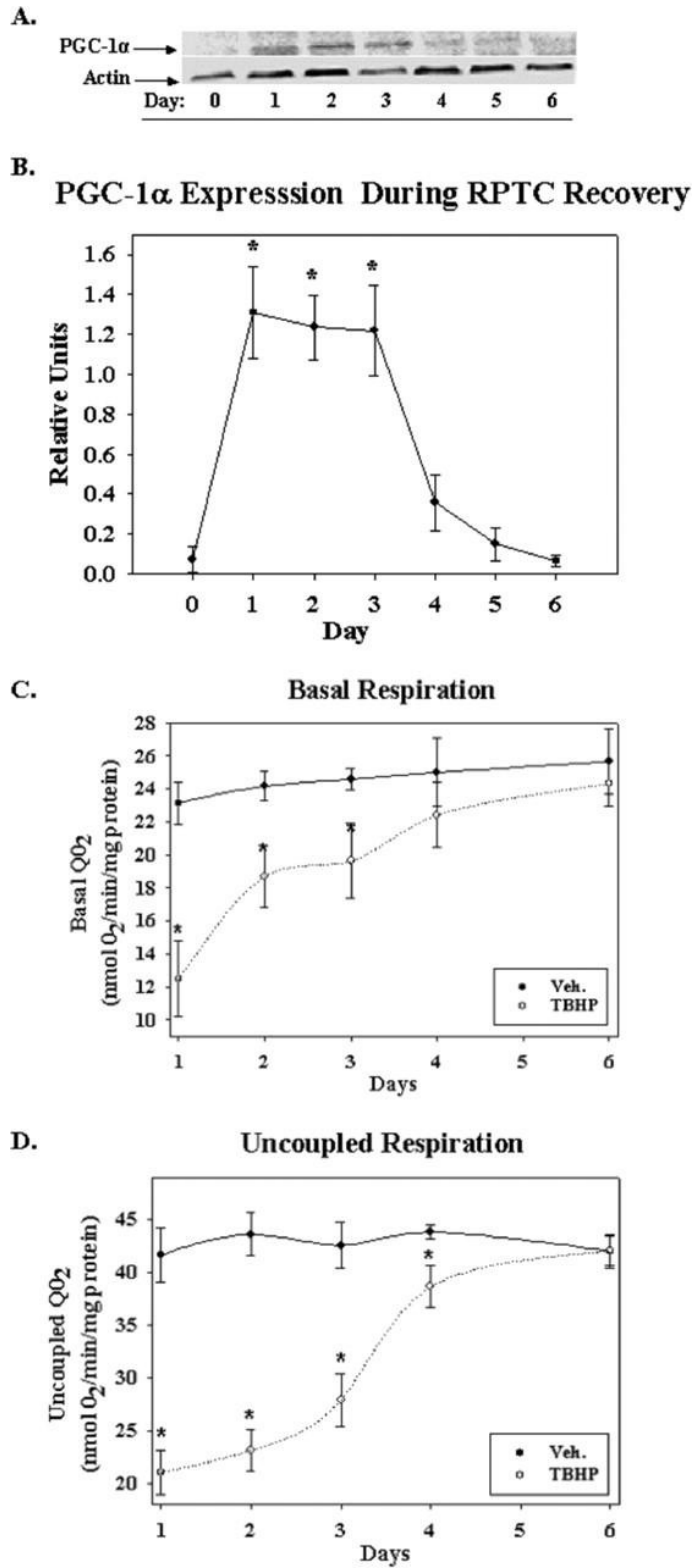


Figure 1-16. Induction of PGC-1 α protein (A, B) correlates with recovery of basal (C) and uncoupled (D) respiration after oxidant injury in RPTC [130].

Since PGC-1 α was associated with the recovery of mitochondrial function, a follow-up study was conducted by Rasbach, et al., which evaluated if the induction of mitochondrial biogenesis via overexpression of PGC-1 α in RPTC either prior to or after oxidant injury affected mitochondrial function [128]. Renal proximal tubular cells overexpressing PGC-1 α resulted in an increase in mitochondrial number/function prior to oxidant exposure, potentiated dysfunction and cell death, but did not preserve mitochondrial function once injured [128]. However, increased mitochondrial biogenesis after oxidant injury accelerated recovery of mitochondrial function [128]. Illustrated in Fig. 1-17A, the mitochondrial proteins ATP synthase β and NDUFB8 were significantly reduced after TBHP exposure, but were almost completely restored in cells overexpressing PGC-1 α after injury [128]. Concomitantly, mitochondrial functional markers, including total cellular ATP (Fig 1-17B), basal respiration (Fig 1-17C) and uncoupled respiration (Fig 1-17D) were significantly suppressed following oxidant injury, but were reported to be fully recovered in RPTC overexpressing PGC-1 α post oxidant exposure [128].

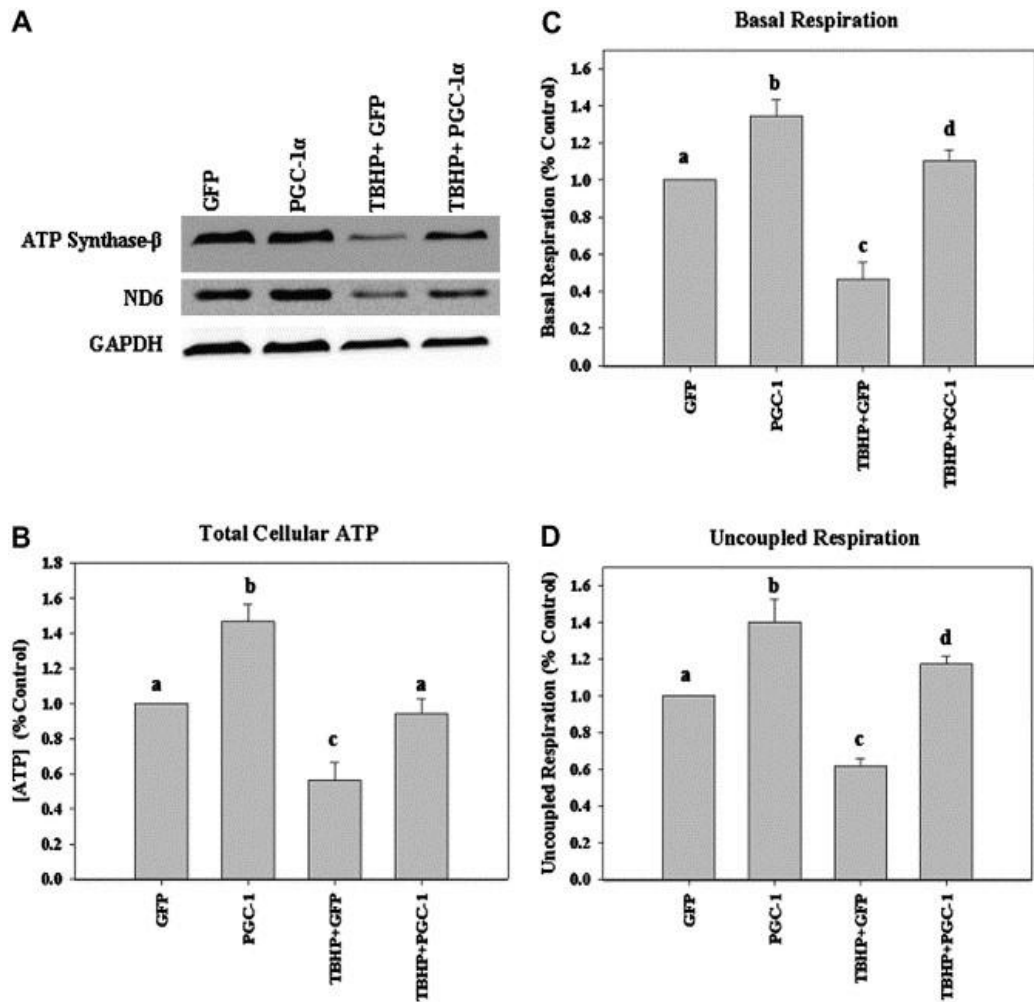


Figure 1-17. Overexpression of PGC-1 α after oxidant injury restored mitochondrial protein expression (A), as well as total cellular ATP (B) and basal (C) and (D) uncoupled oxygen consumption in RPTC exposed to *tert*butylhydroperoxide [128]

Alternative splice variants of PGC-1 α

As previously stated, PGC-1 α is an inducible transcriptional co-activator. In skeletal muscle, PGC-1 α has been reported as a major regulator that allows muscle to adapt to endurance-type exercise, but has no effect on muscle strength or hypertrophy.

Recently, the laboratory of Bruce Spiegelman identified 4 alternatively spliced variants of the PGC-1 α gene [131]. Of the 4 identified, the PGC-1 α isoform (PGC-1 α 4) that results from alternative promoter usage and splicing of the primary transcript was highly expressed in exercised muscle but did not control most known PGC-1 α targets such as the mitochondrial OXPHOS genes [131].

Instead, PGC-1 α 4 specifically induced insulin-like growth factor-1 (IGF1), a stimulator of muscle hypertrophy, and repressed myostatin, a known inducer of muscle atrophy [131]. Moreover, Ruas, et al., reported that mice overexpressing PGC-1 α 4 showed increased muscle mass and strength and resistance to the muscle wasting in an animal model of cancer cachexia [131]. Their studies identify a novel biological target, the PGC-1 α 4 protein, which regulates and coordinates factors involved in skeletal muscle hypertrophy [131]. Finally, discrete pharmacological activation of the PGC-1 α 4 represents a clinically rationale approach to defining a drug therapy that can combat skeletal muscle hypertrophy, a clinical disease void of approved treatment.

BIOTECHNOLOGY: DRUG DISCOVERY AND MITOCHONDRIAL BIOGENESIS

G-protein coupled receptors: biological targets for mitochondrial biogenesis

The previous section described key players involved with the regulation of mitochondrial biogenesis, which includes the nucleus-encoded transcription factors (NRF-1, NRF-2, ERRs, PPARs, MEF-2, and SP-1), and coactivators (PGC-1 α , PGC-1 β , and PRC). These players and their associated upstream regulators are representative of potential targets for pharmacological stimulation of mitochondrial biogenesis. More specifically, it is established that PGC-1 α expression can be induced via β -adrenergic receptor (β -AR) activation intrinsically as part of an adaptive thermogenic response for energy homeostasis [100] or by treatment with exogenous pharmacological agents that are β -AR agonists [132].

Stimulatory G-protein coupled receptors. In general, the family of receptors known as G-protein coupled receptors (GPCR) is a class of cell surface receptors that are composed of a polypeptide chain that weaves through the phospholipid bilayer 7 times forming a transmembrane helix. Approximately 1/3 of all clinically approved drugs target this family of receptors. The β -AR is a classical stimulatory G-protein coupled receptor (G_s) that is characterized by a markedly increase expression of cAMP and exist in three distinct isoforms (β_1 , β_2 , β_3) [133, 134]. More specifically, the β_2 -AR is a heterotrimer composed of G-protein subunits α , β , and γ . After ligand binding on the extracellular surface, this receptor undergoes a conformational change of the intracellular domain that leads to activation of the G-

proteins. The $G\alpha$ subunit releases GDP in exchange for GTP when activated and dissociates from the $G\beta\gamma$ dimer. This subunit then binds and stimulates adenylyl cyclase resulting in the increased production of cAMP from ATP. Cyclic AMP acts as an intracellular messenger capable of initiating a diverse set of signaling cascades, depending on the tissue type, stimulus, and downstream effector(s) involved. With regards to mitochondrial biogenesis, cAMP can phosphorylate PKA initiating CREB mediated increases in PGC-1 α as discussed in the section entitled physiological mechanisms controlling mitochondrial biogenesis (Fig. 1-15). Stimulation of the β_2 -AR also leads to activation of the $G\beta\gamma$ subunit, which in turn regulates its own effectors such as increased intracellular Ca^{2+} . An increase in Ca^{2+} leads to activation of CamKK β and activation of AMPK, which is capable of targeting PGC-1 α [135].

Inhibitory G-protein coupled receptors. In contrast to the G_s receptor family, the inhibitory G-protein coupled receptors ($G_{i/o}$) prevent formation of cAMP. An example of this class of GPCRs includes the A₁ adenosine receptors (A₁ AR). Upon ligand binding and activation of the $G_{i/o}$ receptor, the $G\alpha$ subunit releases GDP in exchange for GTP and dissociates from the $G\beta\gamma$ dimer, as previously described. However, the $G\alpha$ -i protein inhibits adenylyl cyclase activity, which leads to the decrease of cAMP level and attenuation of CREB phosphorylation by PKA. In addition, $G_{i/o}$ receptor activation can also inhibit G-protein-coupled activation of voltage dependent Ca^{2+} channels and is reported to induce phospholipase C activation [136, 137].

Drug discovery: AKI and mitochondrial biogenesis

AKI drug discovery. Currently, there no clinically approved drug therapies for the treatment of AKI. Current treatments are limited to mechanical support by dialysis. Historically, the vast majority of drug research efforts for AKI have focused on pretreatment. However, clinical translation of the outcomes obtained from this approach is limited, as AKI primarily presents with an unpredictable acute onset. Except for a few isolated studies where pretreatment is beneficial for the prevention of AKI [138], the vast majority of animal and clinical studies have yet to demonstrate conclusively the benefit of pharmacologic treatment of AKI and Table 1-3 briefly outlines barriers to successful treatment of AKI [139]. Therefore, an approach that identifies novel and relevant biological targets in the kidney is quintessential for successful drug discovery for the treatment of AKI.

Barriers to Successful Treatment of AKI
Patient and comorbid factors
Complexity of AKI
AKI is a multisystem disease
Design issues clinical trials
biomarkers
definition of AKI
end points in clinical trials
*AKI, acute kidney injury.

Table 1-3. Complexity of human AKI: barriers to successful treatment [139].

Mitochondrial biogenesis as a pharmacological target. Experimental assessment of mitochondrial biogenesis is challenging, as one succinct technique does not exist which can directly count the amount of newly formed mitochondria. Therefore, the technique utilized for determination is dependent on which definition, previously discussed under the section “mitochondrial biogenesis”, is employed by the investigator to define endpoint mitochondrial biogenesis.

As previously discussed, mitochondrial biogenesis is a conserved mechanism to maintain cellular homeostasis in response to cellular stressors, and is stimulated when increased tissue energy demand exceeds mitochondrial ATP-producing capacity [140]. The high inducible nature of mitochondrial biogenesis makes it an ideal target for drug discovery and pharmacological induction of MB might be capable of accelerating recovery of mitochondrial and organ function post acute injury [141]. Activators of SIRT1, a protein deacetylase, including isoflavones, resveratrol and SRT1720, have proven effective at increasing the expression and activity of PGC-1 α and promoting increased mitochondrial number and improved function [142-145]. In addition, our laboratory reported that treatment with SRT1720 promotes recovery from oxidant injury in RPTC [126].

Given the success of these experiments and that there are only a few pharmacological agents reported that are capable of stimulating mitochondrial biogenesis, the need for accurate experimental approaches determining the ability of pharmacologically active compounds to induce mitochondrial biogenesis is a

necessity for this field to reach maturation. Described below are several techniques that are established in the literature as being validated approaches for determination of mitochondrial biogenesis.

Screening: mitochondrial function. Evaluation of functional endpoints for mitochondrial biogenesis is an effective approach for both the screening and/or validation. High throughput assays have been developed, as described Beeson, et al., utilizing the Seahorse Biosciences extracellular flux analyzer (XF96), which uses maximal oxygen consumption rates (uncoupled respiration) as an output to evaluate mitochondrial biogenesis as well as toxicity of pharmacologically active compounds [146]. The XF96 instrument uses fluorescent detectors to measure oxygen consumption rates (OCR) and determine mitochondrial function. Injection of the proton ionophore carbonylcyanide p-trifluoromethoxyphenyl-hydrazone (FCCP) uncouples the mitochondrial membrane potential from the production of ATP, increasing the OCR.

Their realization that maximum respiratory capacity (FCCP-OCR) could be used as a screening tool for the identification of mitochondrial biogenic compounds has revolutionized this field of drug discovery not only because of its adaptability to high throughput screening, but also the flexibility in the type of cell line used, which translates to identification of mitochondrial biogenic compounds for all tissue cells types, theoretically.

There are also assays developed that evaluate mitochondrial function based on intracellular ATP levels, which can also correlate with an increase in mitochondrial numbers. It is important to note either of these measurements may only conclude that the mitochondria are functioning more efficiently in one sample set versus another, or that increases in function may be related to more efficient mitochondria, as opposed to more mitochondria. Therefore, it is imperative to perform validation experiments with the discovered pharmacological “hits” identified from screening.

Mitochondrial DNA (mtDNA) content. As previously described in the section mitochondrial structure and function, mitochondria possess their own genome. Each mitochondrion contains approximately 2 to 10 copies of their genome and each cell can have hundreds to thousands of mitochondria [147]. Since the mitochondrial genome contains genes unique to the mitochondria, primers can be designed for these genes for use in quantitative real-time polymerase chain reactions (qPCR) that measure the abundance of mtDNA. Thus, if there is more mtDNA then one could infer that there are more mitochondria. Given that the ratio between mtDNA and mitochondria is not directly proportional, data from these experiments should be viewed as a precise, but not completely accurate in the measurement of mitochondrial abundance.

Mitochondrial biogenic machinery. Evaluation of the expression of components involved with mitochondrial biogenic machinery can be used as an indicator for the presence of mitochondrial biogenesis. Given that the upregulation of specific

components of the mitochondrial biogenic machinery (see section “entitled nuclear control of mitochondrial biogenesis”) or subunits of the ETC (i.e.- NDUFB8, COX I, ATP β , etc.) is an indication of activation of the mitochondrial biogenic process, their expression can be used as a tool to infer the presence of mitochondrial biogenesis. Experimentally, this can be carried out via qPCR (genes) or immunoblotting (proteins). With both of these techniques the relative expression levels can be compared to a control group to determine if treatment with a specific drug was efficacious in stimulating mitochondrial biogenesis.

Protein synthesis is highlighted because the transcription of DNA to mRNA, which is the first step in this process followed by translation into protein. Therefore, it is important to evaluate both gene and protein expression of the specific target because successful synthesis of necessary proteins can serve as a negative feedback modulator for gene expression, therefore expression can occur non-simultaneously. Meaning, one might observe no change when evaluating just one parameter when in fact a change may exist in the other.

Often a response can be maximized based on exposure to the optimal dose, which can be discovered by treatment with a comprehensive range of doses, aka a dose response. Both qPCR and immunoblotting can be utilized to evaluate expression of key mitochondrial components after exposure to a range of doses. It is also important to consider the time point at which samples are analyzed because a response also depends on the amount of time a drug has had to elicit an effect

(i.e.-receptor occupancy, drug half-life, conversion to the active form in case of prodrugs, etc.). Therefore, it is most beneficial to run in parallel experiments assessing a dose response at relevant time points.

Microscopy. Determination of mitochondria volume/number by microscopy is a commonly used technique that broadly falls into one of two categories: fluorescent microscopy or transmission electron microscopy (TEM). Fluorescent microscopy is the more commonly used of the two methods and utilizes potentiometric dyes such as tetramethylrhodamine methyl ester (TMRM), rhodamine 123 and JC-1 are membrane-potential-dependent dyes incorporated into the mitochondrial membrane and fluoresce in the presence of polarized mitochondria. As described in the previous section “mitochondrial structure and function”, healthy mitochondria are polarized; therefore these dyes are exceptional tools for evaluating mitochondrial health. Visualization of mitochondria can be observed in real-time in either cultured cells or living tissue in situ. These dyes are not accurate tools for the quantification of mitochondria, as it is established that JC-1 and Rhodamine 123 are “washed out” in non-respiring mitochondria [148]. Mito Tracker® (10-N-nonyl acridine) dyes are commercially available dyes, which fluoresce upon entering the mitochondria and are thought to be resistant to washing out due to the linking of thiol groups in the cardiolipin of the mitochondrial membrane [149]. However, Gohil, et al., reported this may not be correct when using stains of yeast [150]. Nevertheless, it is also beneficial for use in experiments in which multiple labeling diminishes mitochondrial function

[149]. Fluorescent techniques are beneficial in drug discovery as they can be adapted for high throughput screens identifying pharmacological agents that are mitochondrial toxic.

Transmission electron microscopy is an established method for the quantitation of mitochondria. The preparation of samples for TEM is more laborious than the aforementioned techniques as it requires fixation, dehydration, sectioning, and staining of sections [148]. Furthermore, TEM is limited to small intracellular fields of view and does not allow for entire cell imaging, which would be optimal in post-hoc analysis evaluating mitochondrial biogenesis. Taken together, the arduous sample preparation and inability to comprehensively identify the existence of new mitochondria prevents TEM from being an effective drug screening tool.

Chapter 2:

Renal Mitochondrial Biogenesis Via A₁ Adenosine Receptor Activation

ABSTRACT

Mitochondria remodel via autophagy, fission/fusion, and biogenesis. Dysfunctional mitochondria are removed and replaced via biogenesis under control of peroxisome proliferator-activated receptor gamma coactivator-1 α (PGC-1 α), a “master regulator” of mitochondrial biogenesis most tissues. In an effort to identify small molecules that induce mitochondrial biogenesis, we screened a compound library using an established, phenotypic mitochondrial biogenesis assay based on respiration of RPTC. Positive “hits” from the library were clustered according to chemical similarity and pharmacophores were defined. One of the pharmacophores corresponds to adenosine receptor (AR) agonists. Several specific A₁ AR agonists were subsequently shown to induce mitochondrial biogenesis in RPTC and mice as measured by increased PGC-1 α , respiratory function, mitochondrial protein expression, and mitochondrial DNA content. Metabolic stress in the kidney increases extracellular adenosine and subsequent signaling via adenosine receptors (AR). Activation of the AR (A₁, A_{2A}, A_{2B}, and A₃) tunes metabolic load via modulation of filtration and transport rates, the major ATP-demanding processes. There have been no reports suggesting that AR signaling also affects mitochondrial biogenesis but adenosine is ideally suited to be a biogenic trigger.

Our preliminary studies demonstrate that A₁ AR signaling converges on PGC-1 α activation in the kidney to drive mitochondrial biogenesis suggesting a possible therapeutic strategy for treatment of acute kidney injury (AKI).

INTRODUCTION

Cells replace old and dysfunctional mitochondria through fission, fusion and mitochondrial biogenesis. Cells and tissues that experience increased energy demand respond via production of new mitochondria. Therefore, the maintenance of mitochondrial number and functions are indispensable for cellular homeostasis during different environmental conditions. Because the mitochondrial genome only encodes 13 proteins, the biogenesis of mitochondria requires the coordinated expression of nuclear and mitochondrial genes. The nuclear encoded 92 kDa protein, PGC-1 α is considered a major regulator of mitochondrial biogenesis; during various physiological conditions it targets genes involved in the maintenance of mitochondrial architecture and function [151]. Originally, PGC-1 α was identified as a transcriptional co-activator of the nuclear receptor PPAR γ , a key component of several transcription factors (SP1, YY1, CREB, MEF-2/E-box, mtTFA) and nuclear respiratory factors (NRF-1, -2, REBOX/OXBOX, MT-1 to -4) involved in the activation and regulation of mitochondrial biogenesis [152].

Several groups have developed strategies designed to increase the expression and activity of PGC-1 α [142, 145]. For example, Spiegelman and colleagues demonstrated that microtubule and protein synthesis inhibitors alter PGC-1 α expression [153]. We reported that a number of differentially substituted isoflavone derivatives promote mitochondrial

biogenesis through a SIRT1-mediated pathway leading to PGC-1 α activation [126, 145]. However, such responses only occurred with high concentrations or long exposure times, and these compounds have low bioavailability. Although it has been reported that SRT1720 induces mitochondrial biogenesis, a recent report suggests that SRT1720 has numerous “off-target” effects [126, 154]. While these compounds do not harbor significant therapeutic potential, they illustrate the potential for pharmacological-induced mitochondrial biogenesis.

Immortalized cell lines have been used extensively to study mitochondrial physiology and biogenesis. Two severe limitations of these cells are the loss of differentiated functions and high rates of glycolysis with limited respiration. A number of years ago we modified the culture conditions of primary cultures of RPTC to provide polarized cells with a greater retention of differentiated functions; and the cells exhibited respiration and gluconeogenesis rates comparable to the rates measured *in vivo* [155, 156]. We recently published results to demonstrate that several classes of compounds produce mitochondrial biogenesis in RPTCs using multiple endpoints such as basal and uncoupled oxygen consumption rates (OCR), ATP levels, PGC-1 α activation, mtDNA content and mitochondrial protein levels [126, 145]. Using the XF instrument, these validated compounds and other compounds known to produce mitochondrial biogenesis (e.g., AICAR, metformin), were used to demonstrate that FCCP-uncoupled respiration is a sensitive marker of mitochondrial biogenesis in these cells [146]. It is important to note that the FCCP uncoupled rate is not increased by addition of additional metabolic substrates and, thus, the uncoupled rate is limited only by the capacity of the electron

transport chain. Under these conditions, increases in the uncoupled rate reflect increased mitochondrial capacity, which is usually only achieved via biogenesis. The use of these uniquely optimized primary RPTC with the XF96 respirometry platform represents the first high-through-put assay to measure phenotypic mitochondrial biogenesis [146].

Using respirometry assay, we subsequently screened a chemical library for inducers of mitochondrial biogenesis using the FCCP uncoupled OCR as the endpoint. A number of molecules were identified as hits and these were subsequently validated as biogenic agents using secondary assays for PGC-1 α activation, mitochondrial protein message & expression, and mtDNA content. One of the pharmacophores identified overlaps with adenosine and several known AR ligands. We tested AR-specific ligands and determined that A₁ AR-specific agonists, and in particular, partial agonists induce mitochondrial biogenesis both *in vitro* and *in vivo*. Given that recent reports have demonstrated improved recovery from AKI in mice treated with the mitochondrial biogenesis inducer formoterol [157], these results provide an intriguing new approach to development of a new class of therapeutic treatments for AKI.

EXPERIMENTAL PROCEDURES

Animal Dosing

Eight-week-old male C57BL/6 mice weighing 25–30 g were dosed via intraperitoneal (i.p.) injections every 8 hours for a total of 24hrs with CCPA (Tocris) (0.1mg/kg), vehicle (n.s.), or CVT-2759 per dosing regimen outlined in table 2. After 24hrs animals were euthanized and tissue was flash frozen.

All procedures involving animals were performed with approval from the Institutional Animal Care and Use Committee (IACUC) in accordance with the NIH Guide for the Care and Use of Laboratory Animals.

Immunoblot analysis

Renal cortical tissue from flash frozen kidneys was lysed in RIPA buffer containing cocktail protease and phosphatase inhibitors. Forty micrograms of total protein were loaded into SDS-PAGE gels and immunoblots were performed as previously described.[130] Antibodies used for immunoblot studies were obtained from the following vendors: GAPDH (Fitzgerald Antibodies), COX I and NDUFB8 (Invitrogen), PGC-1 α (Calbiochem), and KIM-1 (R&D Systems).

Quantitative Real-Time Polymerase Chain Reaction (qPCR)

Total RNA was extracted from renal cortex tissue and RPTC samples using TRIzol reagent (Invitrogen, Grand Island, NY) according to the manufacturer's protocol. cDNA was synthesized via reverse transcription using the iScript Advanced cDNA synthesis kit (Bio-Rad, Hercules, CA) with 5 μ g of RNA. qPCR analysis was performed with cDNA. qPCR was carried out using 5 μ l of cDNA template combined with Brilliant II SYBR Green master mix (Stratagene, La Jolla, CA) at a final concentration of 1 \times and primers (Integrated DNA Technologies, Inc., Coralville, IA) at a concentration of 400 nM. mRNA expression of all genes was calculated using the 2- $\Delta\Delta$ CT method normalized to β -actin. Primer sequences are as follows:

PGC-1 α (EX2) (FW: TGA TGT GAA TGA CTT GGA TAC AGA CA, REV: GCT CAT

TGT TGT ACT GGT TGG ATA TG)

COX I (FW: TAA TGT AAT CGT CAC CGC ACA, REV: ATG TCA GGA GCC CCA ATT
ATC)

NDUFB8 (FW: GGC GAT CCC AAC AAA GAA CC, REV: TTT CTA GGA TTG AAG
GAG TC)

β -actin (FW: GGG ATG TTT GCT CCA ACC AA, REV: GCG CTT TTG ACT CAG GAT
TTA)

Respirometry Assay

The oxygen consumption rate (OCR) measurements were performed by using a Seahorse Bioscience XF-96 instrument according to the protocol outlined in Beeson et al., (2010) [146]. Each experimental plate was treated with vehicle controls (DMSO <0.5%), a positive control (Cilostamide, 10 μ M), blank controls, and the appropriate concentration of the compound of interest. The XF-96 protocol consists of five measurements of basal OCR (1 measurement/1.5 min), injection of p-trifluoromethoxyphenylhydrazine (FCCP) (0.5 μ M), and three measurements of uncoupled OCR (1 measurement/1.5 min). The consumption rates were calculated from the continuous average slope of the O₂ partitioning among plastic, atmosphere, and cellular uptake [158].

Quality-control evaluations considered the basal and uncoupled rates of the vehicle control, positive control, and variances between duplicate treatment wells.

Pharmacophore modeling

Three of the most chemically similar hits from the screen as defined via closeness on a Tanimoto coefficient-based cladogram were selected to develop a pharmacophore. The three hit molecules were aligned manually to give maximal overlap of physicochemical features in which the smaller size of the meshed spheres indicates tightness of spatial overlap.

Statistical Analysis.

Data are presented as means \pm S.E.M. and were tested for normality. Data that were confirmed to have a normal distribution were subjected to one-way analysis of variance. In the absence of normally distributed data with a sample size greater than $n=5$, a Kruskal-Wallis one-way analysis of variance on ranks was conducted. Multiple means were compared to the vehicle at each concentration and a Dunn's post hoc test was used to evaluate statistical significance. Data points were considered statistically different at $P < 0.05$. RPTC isolated from a single animal represented an individual experiment ($n = 1$) and were repeated until $n \geq 4$ was obtained. Rodent studies were repeated until $n \geq 3$ was obtained.

RESULTS

The previously validated respirometric mitochondrial biogenesis assay [146] was used to screen a diverse chemical library for inducers of mitochondrial biogenesis using FCCP-uncoupled OCR as the endpoint. As the first phenotypic screen for mitochondrial biogenesis inducers using a platform that is only moderately high-throughput, we chose

to use the “classic” LOPAC 1280 compound library available from Sigma-Aldrich that has been used as a test case for many other screens. Because of our own internal success with the ChembridgeTM DIVERset library that contains 50K structurally diverse, ‘drug-like’ small molecules, we randomly chose 476 compounds to give a total of 1746 molecules for the first screen. The RPTC were treated with 10 μ M compound for 24 h and then were assayed for basal and FCCP-uncoupled OCR (1 μ M). As shown in Fig. 2-1 PGC-1 α , the rank order distribution of FCCP-uncoupled OCR (normalized to vehicle control) demonstrated that a surprising number of compounds had little effect. Although not shown, the basal rates and cell counts assessed from automated microscopic counting of Hoechst 33342 stained nuclei were largely unaffected.

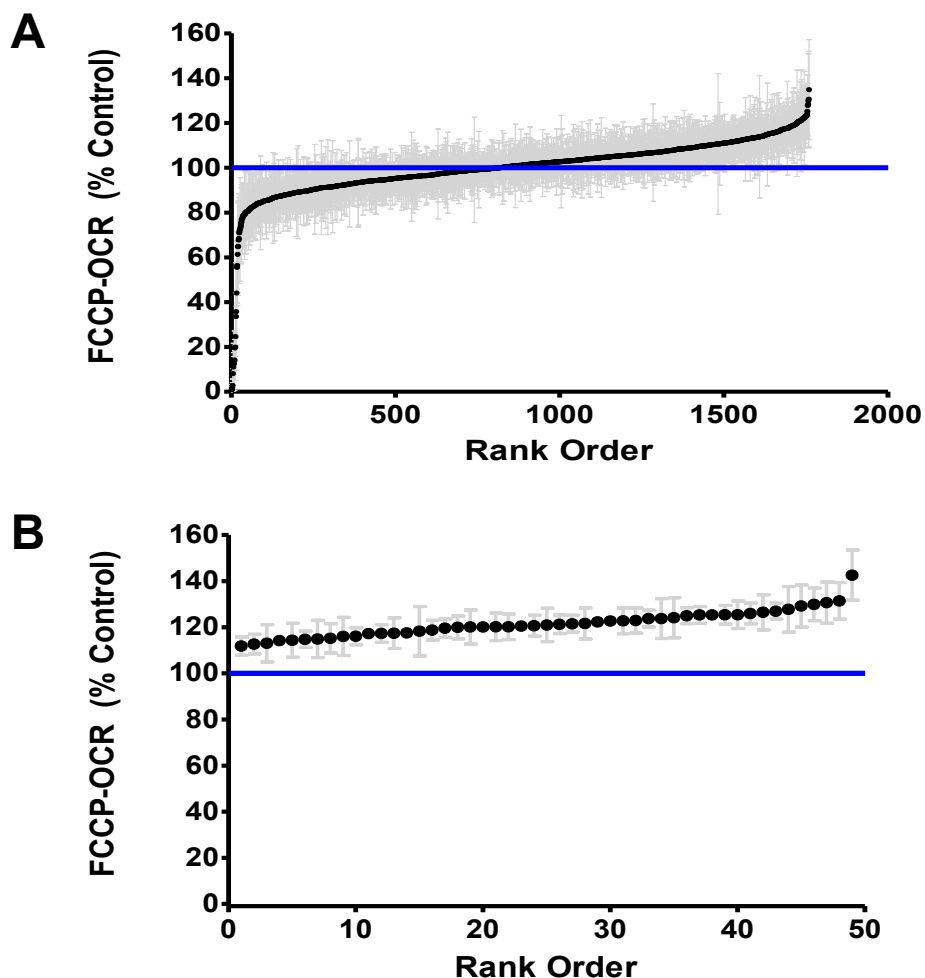
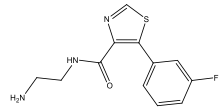
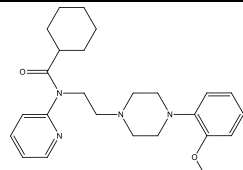
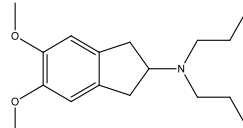
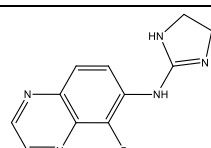
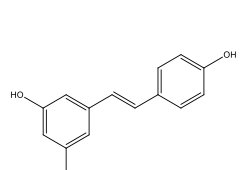
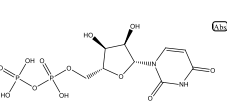
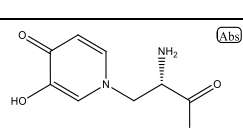
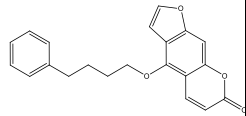
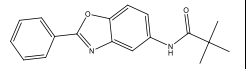
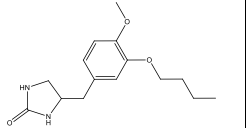
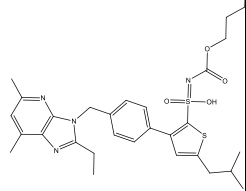
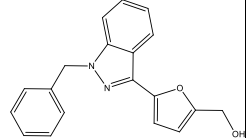
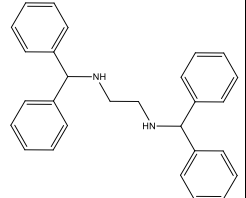


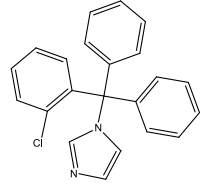
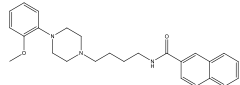
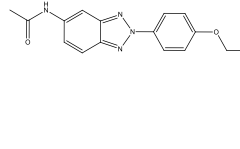
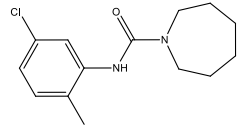
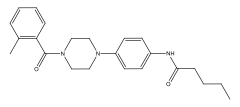
Figure 2-1. A respirometric screen of 1756 structurally diverse molecules identifies mitochondrial biogenesis inducers and mitochondrial toxicants. RPTC were treated with 10 μ M of library compound or vehicle control (0.05% dms0) for 24 h after which a Seahorse Biosciences XF96 instrument was used to measure basal and FCCP-uncoupled OCR (1 μ M). Numbers of live versus dead cells were measured separately via automated microscopy (not shown). **A.** Shown are the FCCP uncoupled rates normalized to vehicle control where error bars are s.e.m. for $n = 5$ where n is defined as testing on a separate rabbit preparation of RPTC. Subsequent statistical analyses indicated that compounds that produce uncoupled rates ≥ 1.15 are possible mitochondrial biogenesis inducers and that compounds producing uncoupled rates ≤ 0.85 are likely to be mitochondrial toxicants. **B.** Shown are the rates for potential mitochondrial biogenesis inducers based on the OCR ≥ 1.15 of vehicle control. The specific molecules and their rates are listed in **Table 1**.

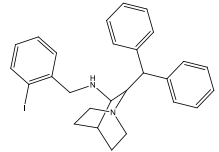
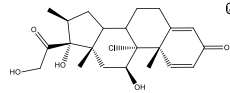
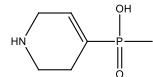
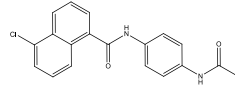
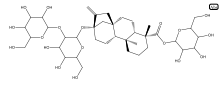
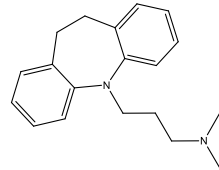
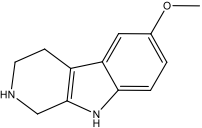
A small number of treatments caused either increases or decreases in FCCP-uncoupled rates not associated with changes in cell number or hypertrophy. Based on prior statistical analyses, we have shown that mitochondrial biogenesis is linked to increases in treated OCR relative to vehicle control of ≥ 1.15 [146]. Indeed, in a related screen we found that the best hits were adrenergic ligands and we subsequently demonstrated that β_2 -adrenergic ligands induce potent and efficacious mitochondrial biogenesis *in vitro* and *in vivo* [132, 159]. Perhaps not surprisingly, the molecules that induced losses in FCCP-uncoupled OCR of ≤ 0.85 (with no cytotoxicity) are mitochondrial toxicants and it was shown that these molecules can be integrated via structural similarities to define ‘toxicophores’ that are conceptually related to pharmacophores but describe molecular features of molecules that disrupt mitochondrial function [160].

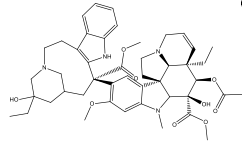
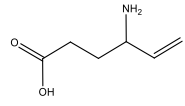
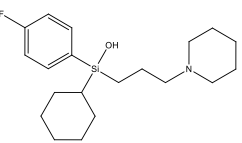
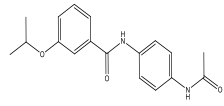
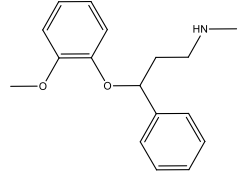
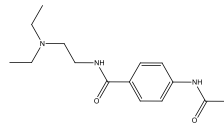
Upon examination of the data, illustrated in Fig. 2-1A, 49 molecules were identified as putative inducers of mitochondrial biogenesis (Fig. 2-1B and Table 2-1).

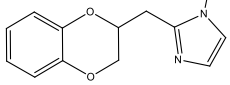
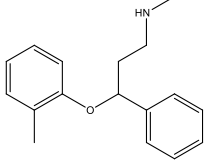
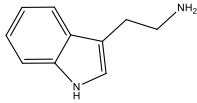
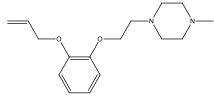
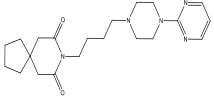
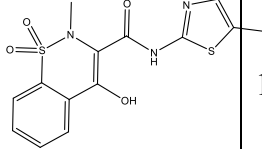
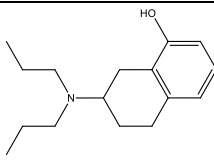
Structure	Average % Control	Standard Error	CAS	Name (CAS)
	142.62	10.88	2750 0-84	Ro 41-1049 Hydrochloride
	131.44	7.96	1627 60- 96-5	WAY-100635 Maleate
	130.67	8.96	8266 8- 33-5	U-99194A maleate
	129.90	7.07	5980 3- 98-4	UK 14,304
	129.22	9.20	501- 36-0	Resveratrol
	127.77	9.91	58- 98-0	Uridine 5'- diphosphate sodium
	126.99	3.46	500- 44-7	L-Mimosine from Koa hoale seeds

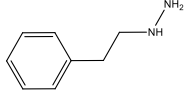
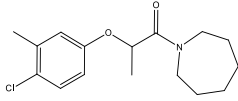
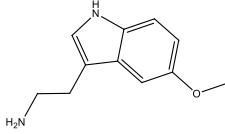
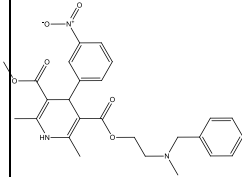
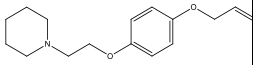
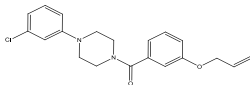
	126.47	7.64	7247 09- 68-6	Psora-4
	125.98	4.50	8396 89- 71-3	Propanamide, 2,2- dimethyl-N-(2- phenyl-5- benzoxazolyl)-
	125.45	6.02	2992 5- 17-5	Ro 20-1724
	125.43	4.05	1514 88- 11-8	L-162,313
	125.40	0.82	1706 32- 47-0	YC-1
	125.35	3.68	8302 7- 13-8	AMN082

	124.99	3.45	2359 3- 75-1	Clotrimazole
	124.14	8.69	3147 76- 92-6	BP 897
	123.78	8.66	8396 95- 65-7	Acetamide, N-[2-(4-ethoxyphenyl)-2H-benzotriazol-5-yl]-
	123.77	3.66	8906 02- 33-2	1H-Azepine-1-carboxamide, N-(5-chloro-2-methylphenyl)hexahydro-
	122.95	5.47	6897 41- 80-8	Pentanamide, N-[4-[4-(2-methylbenzoyl)-1-piperazinyl]phenyl]-

	122.75	5.59	1444 25- 84-3	L-703,606 oxalate salt hydrate
	122.68	1.81	4419 -39- 0	Beclomethasone
	122.35	0.31	1824 85- 36-5	TPMPA
	121.65	6.76	8396 96- 52-5	1- Naphthalenecarbo xamide, N-[4- (acetylamino)phen yl]-5-chloro-
	121.52	3.71	5781 7- 89-7	Stevioside
	121.27	4.00	50- 49-7	Imipramine hydrochloride
	120.98	7.25	2031 5- 68-8	6-Methoxy- 1,2,3,4-tetrahydro- 9H-pyrido[3,4b]

				indole
	120.66	4.54	865-21-4	Vinblastine sulfate salt
	120.51	2.17	68506-86-5	Vigabatrin
	120.22	5.54	116679-83-5	Hexahydro-siladifenidol hydrochloride, p-fluoro analog
	120.17	5.94	899299-77-5	Benzamide, N-[4-(acetylamino)phenyl]-3-(1-methylethoxy)-
	120.15	1.95	53179-07-0	Nisoxetine hydrochloride
	120.10	7.38	32795-44-1	N-Acetylprocainamide hydrochloride

	119.95	4.98	8116 7- 16-0	Imiloxan hydrochloride
	119.62	4.04	8301 5- 26-3	Tomoxetine
	118.73	4.29	61- 54-1	Tryptamine hydrochloride
	118.28	10.71	1004 717- 09-2	Piperazine, 1- methyl-4-[2-[2-(2- propen-1- yloxy)phenoxy]eth yl]-
	117.54	0.71	3650 5- 84-7	Buspirone hydrochloride
	117.42	6.66	7112 5- 38-7	Meloxicam sodium
	117.30	3.83	7895 0- 78-4	S(-)-8-Hydroxy- DPAT hydrobromide

	117.23	1.57	51-71-8	Phenelzine sulfate
	116.07	3.66	9034-37-90-1	1-Propanone, 2-(4-chloro-3-methylphenoxy)-1-(hexahydro-1H-azepin-1-yl)-
	116.04	8.26	608-07-1	O-Methylserotonin hydrochloride
	115.20	6.40	5598-5-32-5	Nicardipine hydrochloride
	114.91	8.07	8396-96-09-2	Piperidine, 1-[2-[4-(2-propen-1-yloxy)phenoxy]ethyl]-
	114.75	3.53	8396-97-58-4	Methanone, [4-(3-chlorophenyl)-1-piperazinyl][3-(2-propen-1-yloxy)phenyl]-

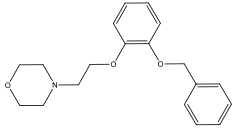
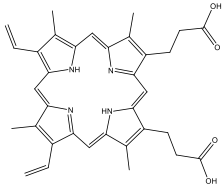
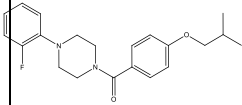
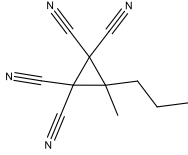
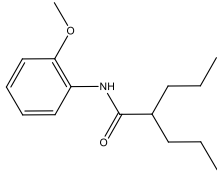
	114.36	7.38	1001 605- 77-1	Morpholine, 4-[2-(2-(phenylmethoxy)phenoxy)ethyl]-
	114.20	0.67	553- 12-8	Protoporphyrin IX disodium
	113.05	8.07	9034 70- 16-6	Methanone, [4-(2-fluorophenyl)-1-piperazinyl][4-(2-methylpropoxy)phenyl]-
	112.70	4.23	1301 7- 69-1	CCG-2046
	111.84	4.00	1619 0- 55-9	Pentanamide, N-(2-methoxyphenyl)-2-propyl-

Table 2-1. Structures, nomenclature, and rates for potential mitochondrial biogenesis inducers based oxygen consumption rate (OCR).

The molecules were examined for structural similarity and it was found that three in particular had close structural and biochemical similarity (Fig. 2-2A). Alignment of the chemical structures for these three structures defined an A₁ AR ligand pharmacophore (Fig. 2-2B).

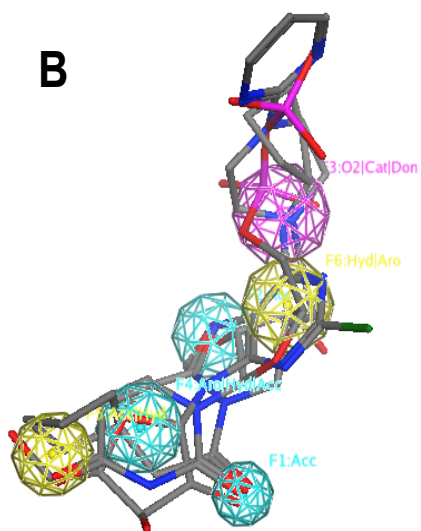
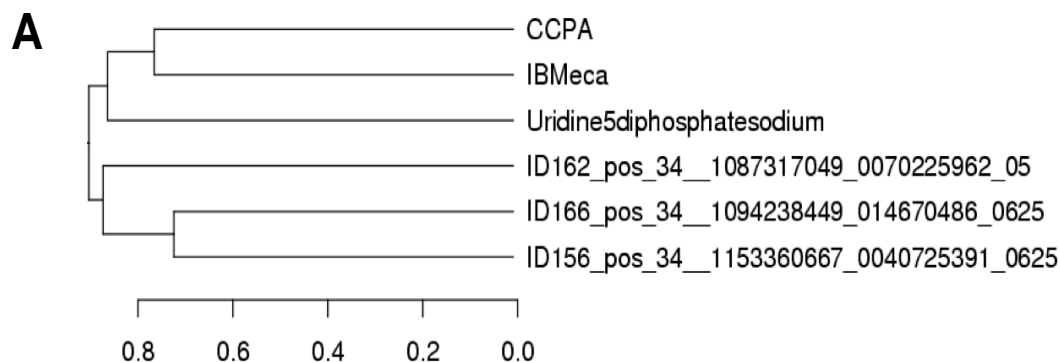


Figure 2-2. Alignment of chemically similar hits in the mitochondrial biogenesis screen produces an adenosine receptor pharmacophore. A. Three of the most chemically similar hits as defined via closeness on a Tanimoto coefficient-based cladogram were selected to develop a pharmacophore. **B.** The three hit molecules were aligned manually to give maximal overlap of physicochemical features in which the smaller size of the meshed spheres indicates tightness of spatial overlap. Key: yellow = hydrophobic, cyan = acceptor, magenta = donor.

To identify a role for AR signaling in RPTC mitochondrial biogenesis, and the specific AR involved, RPTC were treated with a number of AR-selective agonists for 24 h and respirometric analysis determined. The kidney expresses all four AR isoforms (A_1 , A_{2A} , A_{2B} , and A_3) [161], but none have been evaluated for having a role in mitochondrial biogenesis. Also, it is well known that there are significant inter-species structural differences between the AR as measured by the affinities and K_i values of agonist and antagonist ligands, respectively [162, 163]. Thus, we chose AR agonists with highly selective affinities for both human and rodent A_1 and A_3 AR. CCPA is a A_1 AR agonist with an A_1 AR $K_D/EC_{50} = 1$ nM, and it is 40-fold more selective for A_1 than A_3 . There are no A_2 -selective agonists. 2-Cl-IB-Meca, IB-Meca, and Hemado are A_3 AR agonists with K_D/EC_{50} of 0.3 nM and 1 nM, and are 2,500- and 327-fold selective for A_3 compared to A_1 .

Treatment with escalating doses of CCPA (3, 5, 10, and 20 nM) resulted in increased primary RPTC FCCP-uncoupled rates indicative of mitochondrial biogenesis, whereas 2Cl-IB-MECA, IB-MECA and Hemado had no measurable effects (Fig. 2-3A).

Importantly, the biogenesis induced via CCPA was blocked by low concentrations of the A_1 AR-specific antagonist DPCPX (Fig. 2-3B). These results suggest that A_1 AR activation selectively induces mitochondrial biogenesis in RPTC.

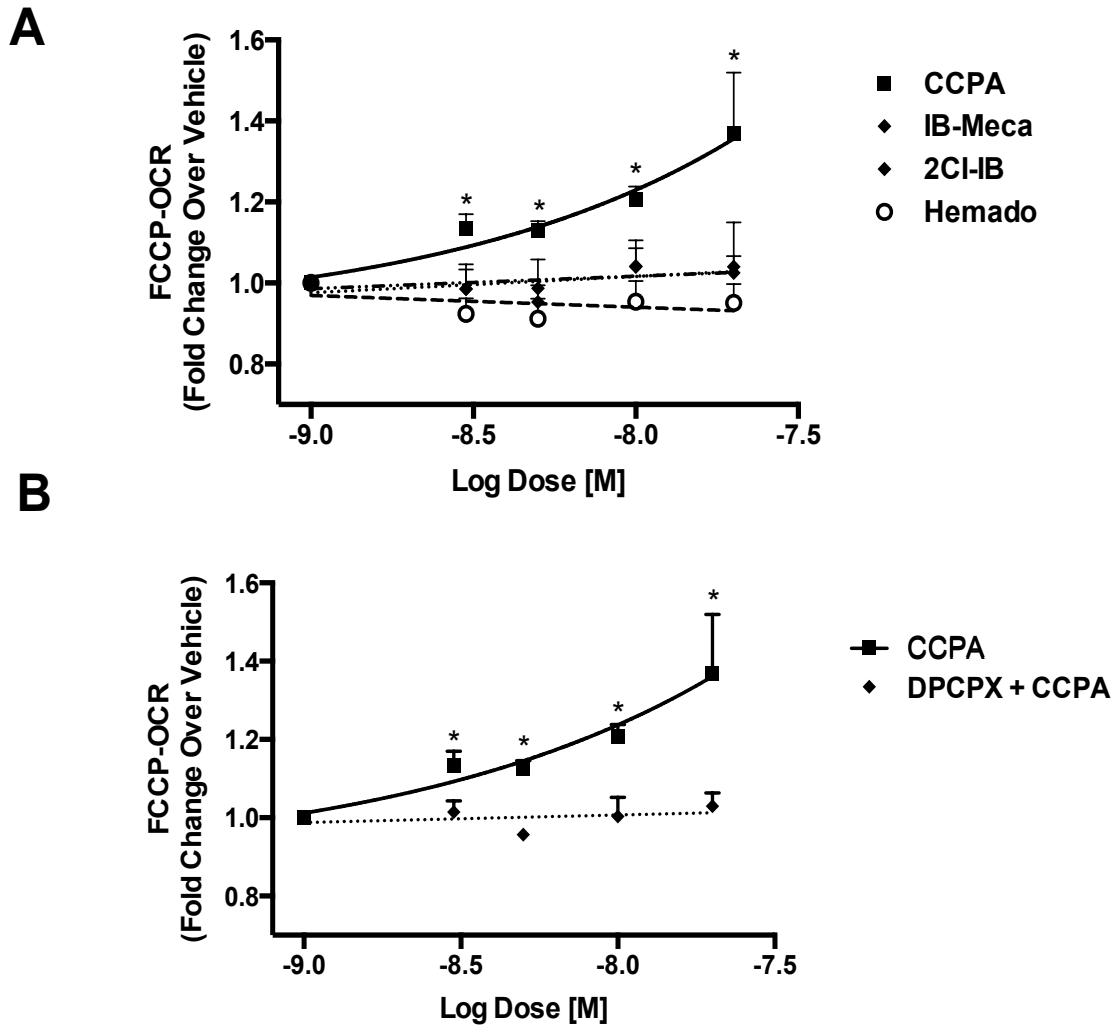


Figure 2-3. CCPA specifically induces functional mitochondrial biogenesis in RPTC. FCCP-uncoupled oxygen consumption rate (OCR) was measured in RPTCs exposed to 3, 5, 10, and 20nM concentrations of the ADOR agonists, CCPA, IB-Meca, 2CI-IB, Hermado (**A**), and co-treatment of A₁R antagonist, DPCPX, with CCPA (**B**) for 24 hours using the Seahorse Extracellular Flux (XF) Analyzer. Rates are expressed as a percentage change relative to vehicle (DMSO) treatment. Data points are mean \pm sem; $N \geq 6$; * $p < 0.05$.

To characterize mitochondrial biogenesis at the molecular level, the expression of nuclear- and mitochondrial-encoded genes and proteins (nuclear = ATP synthase b, NDUF8; mitochondrial = COX1, ND6) were determined by qPCR and immunoblots, respectively, as previously described [126, 128]. It was found that treatment of primary RPTC with 3 nM CCPA for 24 h promoted significant increases of the message for PGC-1 α (Fig 2-4).

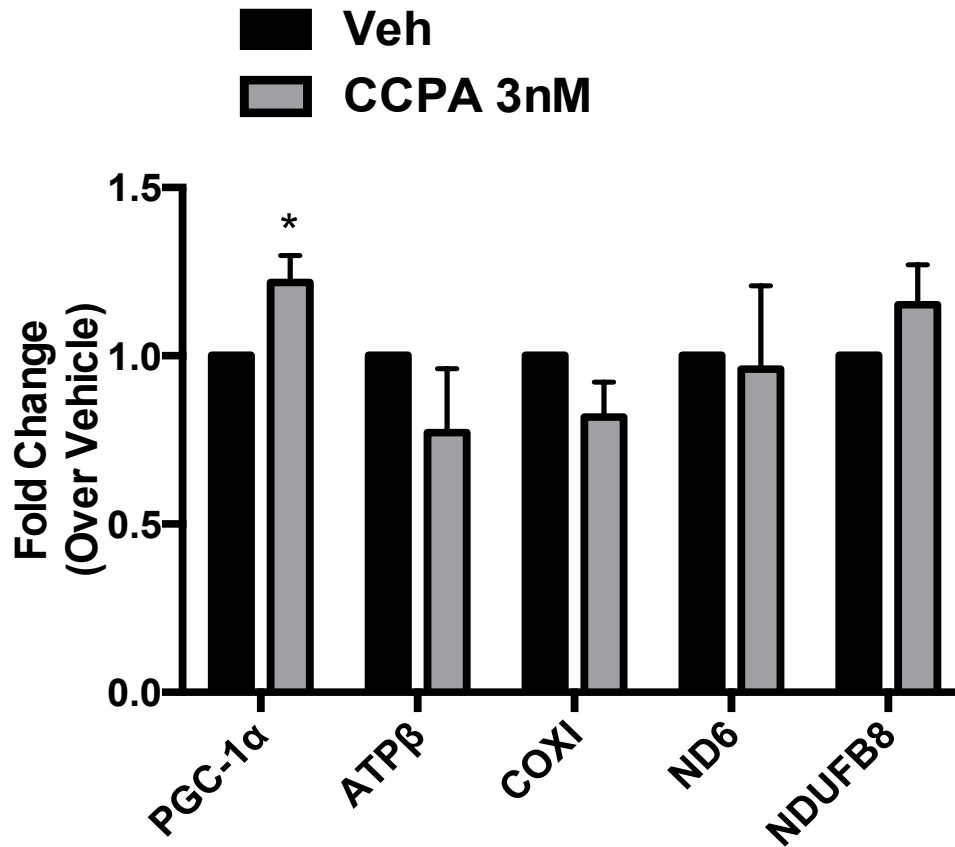


Figure 2-4. CCPA treatment induces increased expression of mitochondrial biogenetic markers in renal proximal tubular cells. CCPA was dosed in RPTC (3nM) for 24hrs. After 24 expressions of mitochondrial and nuclear encoded genes were analyzed via real-time PCR. Relative mRNA expression levels of the genes PGC-1 α , NDUFB8, COX I, ATP β , and ND6 was measured in RPTC. Data points are mean \pm sem; N \geq 4; *p<0.05.

To demonstrate A₁ AR mediated mitochondrial biogenesis *in vivo*, C57BL/6 mice were treated with 0.1 mg/kg CCPA intraperitoneally (5%DMSO in 0.9% saline) every 8 h for 24 h. An exhaustive literature search found that the range of CCPA used in mice is 0.05 – 0.5 mg/kg [164, 165]. In our studies we used 0.1 mg/kg CCPA, a commonly used dose in the literature. The kidneys of treated animals were removed and the cortex was homogenized, solubilized, and lysed for qPCR analyses (Fig 2-5). Gene expression of PGC-1 α was increased 1.5 fold, ND6 nearly 2-fold, and NDUFB8 was increased above 2.5 fold. In addition, evaluation of protein expression for OXPHOS components revealed COX I (mitochondrial-encoded) was increased approximately 1.5 fold with only a minor increase in NDUFB8 (nuclear-encoded) (Fig. 2-6).

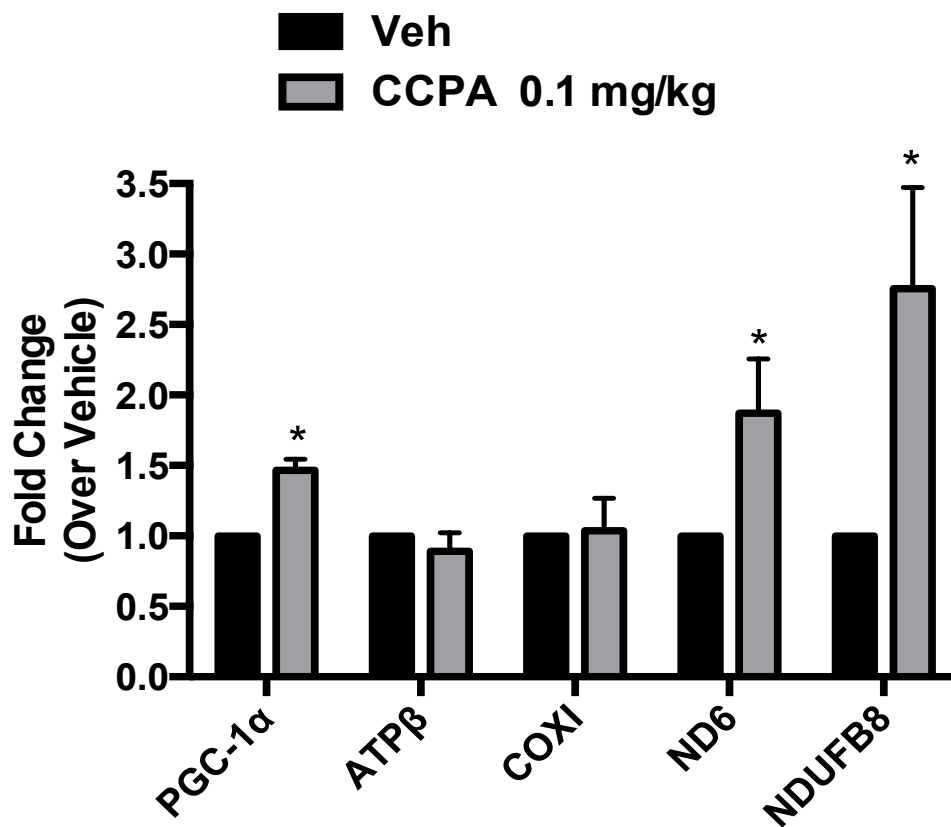


Figure 2-5. CCPA treatment induces increased expression of mitochondrial biogenetic markers in renal cortical tissue. CCPA was dosed in naïve C57BL/6 mice (0.1mg/kg) every 8 hours for 24hrs. After 24 h expressions of mitochondrial and nuclear encoded genes were analyzed via real-time PCR. Relative mRNA expression levels of the genes PGC-1 α , NDUFB8, COX I, ATP β , and ND6 was measured in RPTC. Data points are mean +/- sem; N=6; *p<0.05.

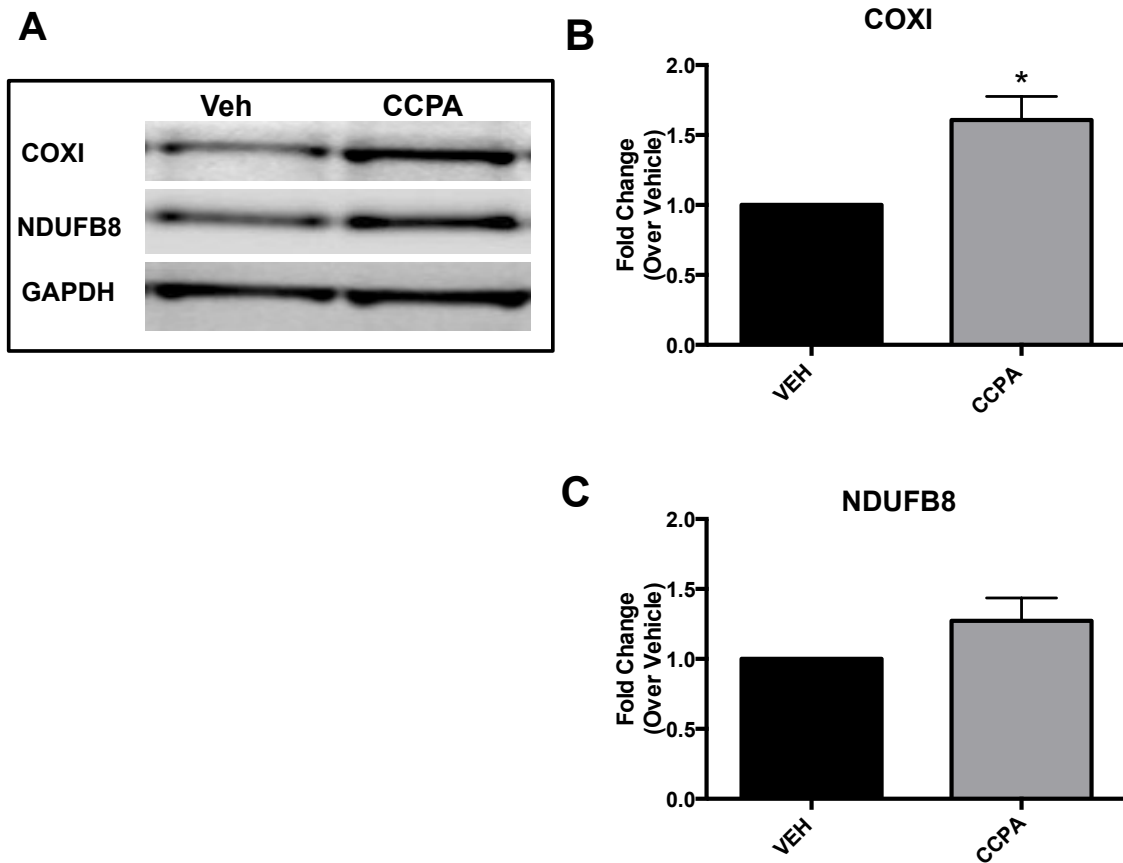


Figure 2-6. CCPA treatment induces increased protein expression of mitochondrial biogenetic markers in the renal cortical tissue of mice. C57BL/6 mice were subjected to either CCPA (0.1mg/kg) or vehicle (n.s.) via i.p. injections every 8 hours for a total of 24hrs. After 24 hours the kidneys were harvested, the renal cortical tissue was removed, and subjected to protein isolation. Representative immunoblots for COXI, NDUFB8, and GAPDH from the renal cortices of both vehicle and CCPA treated mice (A), Relative densitometry units COX I (B) and NDUFB8 (C). Data points are mean +/- sem; N=6; *p<0.05.

Furthermore, since CCPA acts as a global A₁AR agonist and the role of receptor agonism has been evaluated as a potential therapy in type 2 diabetes [166], Alzheimer's disease [167], and, overall, is arguably the most potent and widespread presynaptic modulator in the CNS [168-170]; we therefore also evaluated the liver, frontal cortex, and hippocampus for alterations in gene expression of PGC-1 α , COX I, and NDUFB8 as described above. These genes were increased in all tissues with COX I expression being the most robust in liver and hippocampus, while the frontal cortex showed an increased in PGC-1 α of 1.5 fold, approximately (Fig. 2-7).

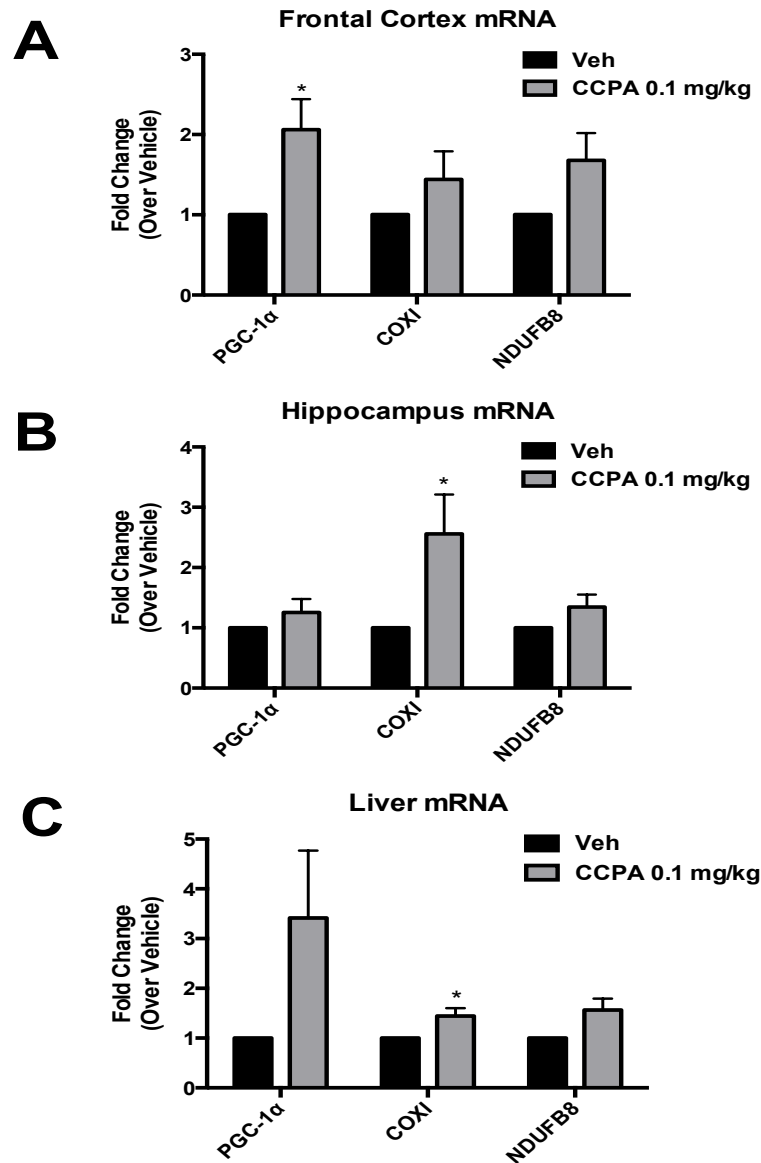


Figure 2-7. CCPA treatment induces mitochondrial biogenesis various tissues of mice. C57BL/6 mice were dosed via intraperitoneal (i.p.) injections every 8 hours for a total of 24hrs with either CCPA (0.1mg/kg) or vehicle (n.s.). After 24hrs the frontal cortex, hippocampus, and liver were removed, subjected to RNA and isolation, and relative expression of mitochondrial and nuclear genes were analyzed via real-time PCR. Rates are expressed as a percentage change relative to vehicle treatment. Relative mRNA expression levels of the genes PGC-1 α , NDUF8, and COX I in frontal cortex (A), Hippocampus (B), and Liver (C). Data points are mean +/- sem; N=3; *p<0.05.

Highly specific A₁ AR antagonists have been evaluated in the clinic for management of heart failure patients with renal impairment. However, three clinical trials of the A₁ AR antagonists KW3902 (rolofylline) and BG9928 (tonapofylline) have been terminated because of side effects [171-173]. Agonism of A₁ AR has also been evaluated for therapeutic treatment of arrhythmias, type-2 diabetes, and angina [166]. The most advanced A₁ AR agonist therapeutics, selodenoson, and tecadenoson, are administered via IV bolus infusion to control ventricular rates [174]. A₁ AR agonists also reduce triglyceride and non-esterified fatty acid levels in models of type-2 diabetes [175]. The A₁ AR agonist ARA was evaluated as a potential anti-diabetic agent in humans, but there was a rapid onset of tolerance [176, 177]. The potential for cardiovascular effects, and agonist-mediated tolerance, has stimulated the development of A₁ AR partial agonists. For example, the partial agonists CVT-3619 and CVT-2759 are devoid of cardiovascular effects and do not exhibit tolerance induction [175, 178].

We chose to evaluate the CVT-2759 partial agonist for mitochondrial biogenesis induction given that it is the more characterized and developed of the two. In vivo, treatment with CVT-2579 exhibited a good dose response for mitochondrial biogenesis activity (see Table 2-2 for dosing schedule) (Fig. 2-8A). Evaluation of CVT-2579 in vivo demonstrated that it is extremely potent and efficacious in inducing mitochondrial biogenesis the kidney of C57BL/6 mice and, thus, partial agonism of the A₁ AR appears to be an appealing approach to treatment of AKI (Fig. 2-8B).

Total Daily Dose (mg/kg)	Frequency (over 24 hours)	Sample size
0.02	bid	3
0.03	tid	6
0.09	bid	6
0.15	qd	3
0.3	tid	3

Table 2-2. CVT-2759 dosing concentrations and frequencies used to define optimal dose for stimulating mitochondrial biogenesis. C57BL/6 mice were subjected to CVT-2759 via i.p. injections as described in the above table for a total of 24hrs at which time they were euthanized. Once daily (qd), twice daily (bid), and three times daily (tid). Total daily dose (single injection concentrations) are as follows: 0.02 (0.01) mg/kg, 0.03 (0.01) mg/kg, 0.09 (0.045) mg/kg, 0.15 (0.15) mg/kg, 0.3 (0.3) mg/kg.

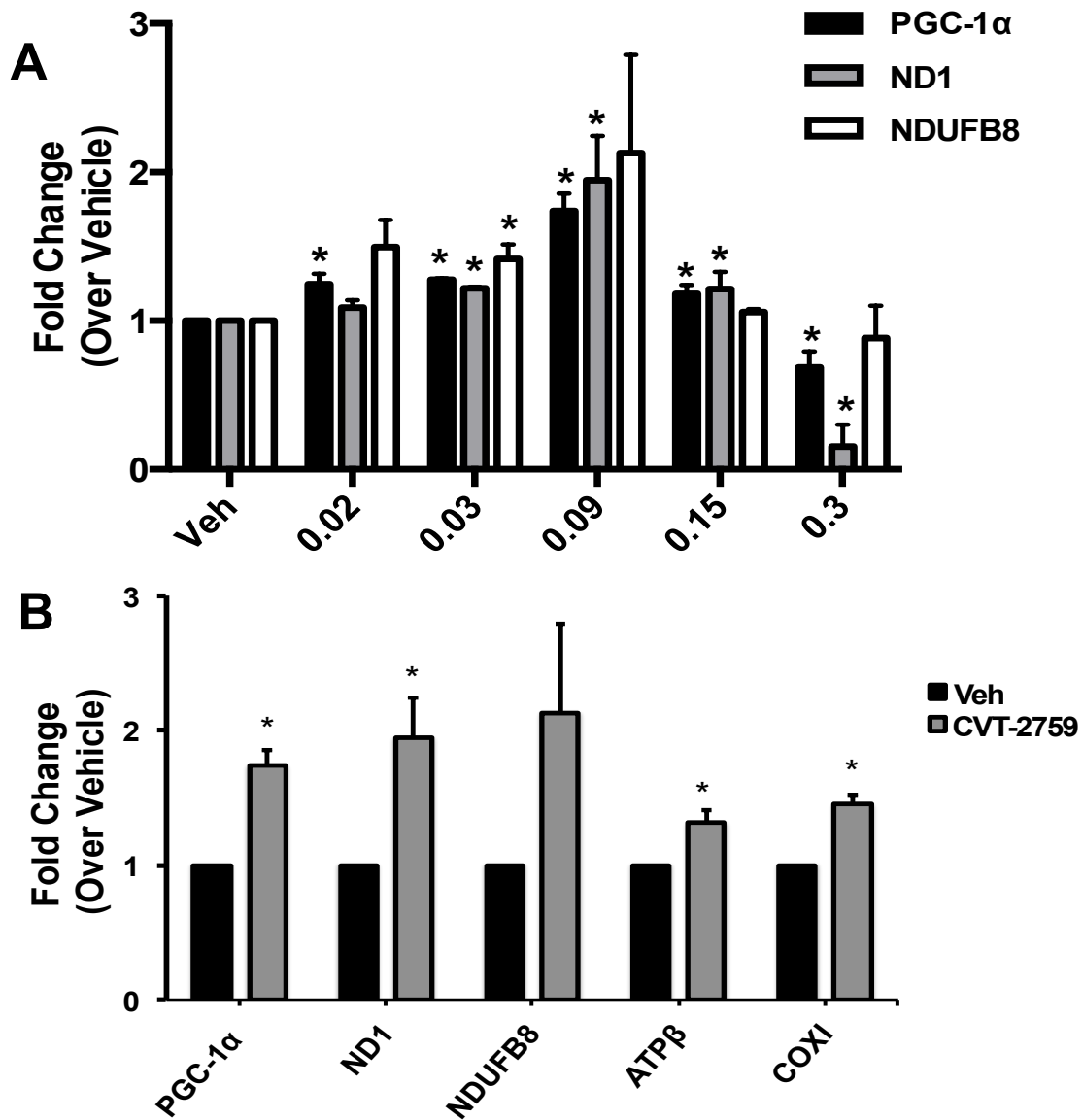


Figure 2-8. CVT2759 treatment induces mitochondrial biogenesis in renal cortical tissue of mice. Dose response for CVT-2759 in C57BL/6 mice (A). Animals were dosed via i.p. injections with the dosing regimen defined in table 1 for a total of 24hrs. C57BL/6 mice were dosed via i.p. injections every 12 h for a total of 24 h with either 0.045mg/kg (total daily dose= 0.09) of CVT2759 or vehicle (n.s.) (B). After 24 hrs the kidneys were harvested, the renal cortical tissue was removed, subjected to RNA isolation, and relative expression of mitochondrial and nuclear genes were analyzed via real-time PCR. Relative mRNA expression levels of the genes PGC-1 α , NDUFB8, COX I, ATP β , and ND6. Data points are mean \pm sem; N=6; *p<0.05.

In particular, a pharmacophore developed on CCPA, and the two CVT compounds creates a much clearer image of the needed structural features to best achieve mitochondrial biogenesis via activation of the A₁ AR in kidney (Fig. 2-9).

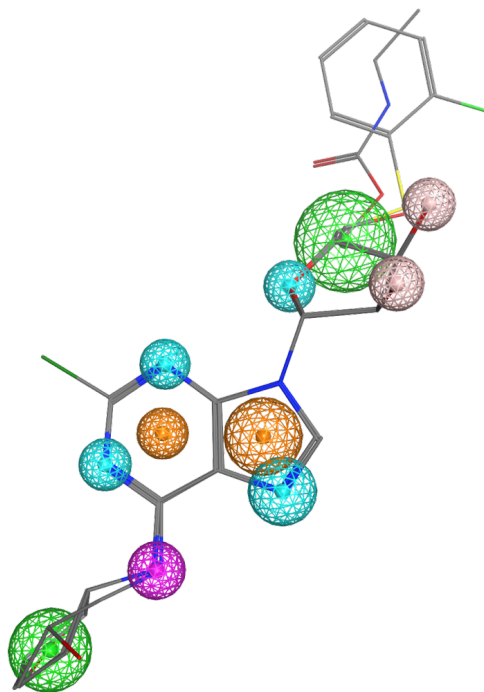


Figure 2-9. Alignment of CCPA, CVT2579 and CVT3619 produces a well-defined A1AR agonist/partial-agonist pharmacophore. The three A1AR ligands were aligned manually to give maximal overlap of physicochemical features in which the smaller size of the meshed spheres indicates tight, spatial overlap. Key: green = hydrophobic, cyan = acceptor, magenta = donor, brown = acceptor/donor.

DISCUSSION

Adenosine is a tissue hormone normally present in the extracellular milieu, in the cytoplasm and within intracellular organelles. It is generated from intracellular and extracellular nucleotidases and its concentration reflects the balance between ATP utilization and production. Its primary role in most tissues is to regulate hemodynamics and thereby match local blood flow with energy demand. The differential adenosine-mediated functional responses are achieved, in part, via the existence of the four AR (A_1 , A_{2A} , A_{2B} , A_3) that vary in their distribution, ligand affinities and utilization of small G-protein coupling partners. For example, the A_{2A} and A_{2B} AR are G_s coupled and mediate cAMP formation whereas the A_1 AR are $G_{i/o}$ coupled and inhibit cAMP formation. The A_1 AR regulates tubular absorption while the A_2 AR regulates medullary vasodilation to balance GFR to metabolic load.

The rich pharmacology of renal AR has resulted in the generation of varied therapeutic approaches to modulate renal dysfunction. The general lack of highly selective A_{2A}/A_{2B} AR agonists and antagonists, and their pleiotropic action in different tissues, has limited their use as therapeutic targets. In contrast, studies with A_1 AR knockout mice suggest that modulation of A_1 AR signaling has therapeutic potential in treating renal injury. I/R-induced renal injury was potentiated in the A_1 AR knock-out mice, or in wild type mice treated with the A_1 AR-selective antagonist DPCPX [179]. Treatment with the A_1 AR-selective agonist attenuated I/R-induced renal injury in WT mice. Renal injury due to hepatic I/R and septic peritonitis was also potentiated in the A_1 AR knock-out mice [165]. In all of these cases the oxidant mediated renal injury is primarily at the level of tubular

epithelial cell death and the protective effect of A₁ AR has been attributed to enhanced Akt activation, p38/AP2 MAPK signaling, and/or increased expression of HSP27 [180-182]. Although the A₁ AR knock-out mice used in these studies have confounding non-renal deficits, it has been shown that kidney-selective delivery of A₁ AR-expressing lentivirus in the knock-out mice reduces renal injury due to either renal or hepatic I/R [183, 184]. Finally, it has also been reported that A₁ AR agonism can produce a preconditioning phenotype that is protective from hypoxia [185, 186]. None of these studies have attempted to discriminate the role of A₁ AR on prevention of AKI injury versus recovery.

Metabolic stress in the kidney increases extracellular adenosine and subsequent signaling via adenosine receptors. Activation of the AR (A₁, A_{2A}, A_{2B}, and A₃) tunes metabolic load via modulation of filtration and transport rates, the major ATP-demanding processes. There have been no reports suggesting that AR signaling also affects mitochondrial biogenesis but adenosine is ideally suited to be a biogenic trigger. Our studies demonstrate that A₁ AR signaling converges on PGC-1 α activation in the kidney to drive mitochondrial biogenesis.

Mitochondrial dysfunction observed *in vivo* can be reproduced in cellular models subjected to diverse stresses [187-189]. For example, RPTC mitochondrial dysfunction is easily measured in response to cisplatin and oxidants such as hydrogen peroxide and *t*-butylhydroperoxide [129, 190]. In these studies, the injured RPTC exhibit mitochondrial dysfunction with decreased respiration and ATP levels that recover over the course of six

days. The recovery is temporally associated with the return of RPTC confluence suggesting that mitochondrial function is central to the overall restoration of cellular ultrastructure and function [129]. Although, the mechanisms mediating recovery of mitochondrial function have not been fully established, we have shown that mitochondrial biogenesis inducers can improve recovery from AKI in mice suggesting that mitochondrial function could be key to functional recovery [157].

AKI is a serious disease state associated with many complications and co-morbidities, and nearly half of those who develop the disease do not survive. Despite a growing body of knowledge concerning the causes and effects of AKI, treatment strategies remain largely supportive, and survival rates have remained unchanged for several decades. Mitochondrial dysfunction is a significant contributing factor to this disease state, and reversal of this dysfunction via mitochondrial biogenesis post-injury may be a potent therapy strategy for the treatment of severe organ injury. We have shown that A₁ AR agonists induce renal mitochondrial biogenesis in primary RPTC and mice. Elucidation of a partial agonist A₁ AR pharmacophore and the downstream signaling pathway responsible for this phenomenon will reveal additional targets for pharmacological intervention and treatment of AKI.

Chapter 3:

FORMOTEROL RESTORES MITOCHONDRIAL AND RENAL FUNCTION AFTER ISCHEMIC/REPERFUSION INJURY

ABSTRACT

Mitochondrial biogenesis may be an adaptive response necessary for meeting the increased metabolic and energy demands during organ recovery after acute injury and renal mitochondrial dysfunction has been implicated in the pathogenesis of AKI.

We proposed that stimulation of mitochondrial biogenesis 24 hours after ischemia/reperfusion (I/R)-induced AKI, when renal dysfunction is maximal, would accelerate recovery of mitochondrial and renal function in mice. We recently showed that formoterol, a potent, highly specific, and long-acting β_2 -adrenergic agonist, induces renal mitochondrial biogenesis in naïve mice. Animals were subjected to sham or I/R induced AKI, followed by once-daily intraperitoneal injection with vehicle or formoterol beginning 24 hours after surgery and continuing through 144 hours after surgery.

Treatment with formoterol restored renal function, rescued renal tubules from injury, and diminished necrosis after I/R-induced AKI. Concomitantly, formoterol stimulated mitochondrial biogenesis and restored the expression and function of mitochondrial proteins.

*Data from this work is published under: Jesinkey, S.R., et al., *Formoterol restores mitochondrial and renal function after ischemia-reperfusion injury*. J Am Soc Nephrol, 2014.

25(6): p. 1157-62.

Taken together, these results provide proof of principle that a novel drug therapy to treat AKI, and potentially other acute organ failures, works by restoring mitochondrial function and accelerating the recovery of renal function after injury has occurred.

Introduction

Acute kidney injury (AKI) is a clinical disorder characterized by a rapid decrease in kidney excretory function and subsequent retention of nitrogenous waste products, metabolic acids, and increased potassium and phosphate concentrations [191]. Acute kidney injury AKI incidence is increasing with prevalence of approximately 60% in patients during intensive care admission and in the past 50 years mortality rates have remained unchanged ranging from 50%-70% [17, 191, 192]. In addition, AKI is costly to treat and is a significant financial burden on the healthcare system [18]. Current treatments are limited to mechanical support by dialysis. Historically, the vast majority of drug research efforts for AKI have focused on pretreatment. However, clinical translation of the outcomes obtained from this approach is limited, as AKI primarily presents with an unpredictable acute onset. Taken together the high mortality rates, financial burden, and limitations in treatment demonstrate a significant clinical need for discovery of novel approaches to therapeutics that promote recovery of renal function following AKI.

A common etiology of AKI is ischemia reperfusion (I/R) injury and it is now recognized that tubular mitochondrial dysfunction contributes to oxidative stress, persistent energy depletion, impairment of energy dependent repair mechanisms, and cell death in AKI [129, 191, 193-197]. Investigation into renal mitochondrial dysfunction in glycerol, sepsis, and I/R models of AKI in rodents revealed a persistent elevation in serum creatinine concomitant with continual suppression of mitochondrial- and nuclear-encoded genes and proteins of the electron transport chain (ETC) and mitochondrial function [194, 198, 199].

Mitochondrial biogenesis (mitochondrial biogenesis) is a complex physiological process by which cells form new mitochondria to increase energy production in response to environmental stimuli or physiological stress [96]. Peroxisome proliferator-activated receptor-gamma coactivator 1 alpha (PGC-1 α) is referred to as the master regulator of mitochondrial biogenesis and is abundantly expressed in those tissues with high metabolic demand (e.g. heart, skeletal muscle, and kidneys) [70, 100, 101, 200]. It is highly inducible by physiological and pathological stimuli, including exercise, caloric restriction, sepsis, and hypoxia [201-204]. The ability of PGC-1 α to respond to numerous stimuli and alter the metabolic profile of the cell makes it a target for pharmacological intervention in a variety of disease states.

Our laboratory previously demonstrated in oxidant-induced renal proximal tubular cell (RPTC) injury that PGC-1 α is up-regulated after injury and that over-expression of PGC-1 α post injury promotes the recovery of mitochondrial and cellular functions [128, 130].

Tran, et al reported that renal specific PGC-1 α null mice subjected to sepsis-induced AKI were unable to recover from injury in contrast to their wild-type littermates [198]. Other evidence from in vivo studies supports the hypothesis that induction of PGC-1 α and subsequent mitochondrial biogenesis is a crucial adaptive response aimed at sustaining metabolic and energy demands required for recovery from acute organ injury [205, 206].

A recent high throughput screen performed by our laboratory revealed that the specific and long-acting beta-2 adrenergic receptor (β_2 -AR) agonist formoterol was a potent inducer of mitochondrial biogenesis in RPTC and in the kidneys of mice [207].

Subsequently, using RPTC, the ability a structurally diverse panel of β_2 -adrenoceptor agonists to stimulate mitochondrial biogenesis was assayed and cheminformatic profiling elucidated four essential chemical moieties to stimulate mitochondrial biogenesis, which was shared by formoterol [208]. Here, we carried out experiments evaluating the efficacy of formoterol to restore mitochondrial and kidney function after an ischemic insult in a mouse model of I/R-induced AKI.

Experimental procedures

Ischemia/reperfusion model of AKI

Eight-week-old male C57BL/6 mice weighing 25–30 g were subjected to bilateral renal pedicle ligation for 20 min as described previously [194]. Dosing was initiated 24 h after reperfusion and mice were given either a daily injection of 0.3 mg/kg of formoterol fumarate dihydrate (Sigma F9952) or vehicle (0.3% DMSO in n.s.) via i.p. injection.

All procedures involving animals were performed with approval from the Institutional Animal Care and Use Committee (IACUC) in accordance with the NIH Guide for the Care and Use of Laboratory Animals.

Assessing renal function

Blood was collected by retro-orbital eye bleed. Serum was isolated from each blood sample and serum creatinine levels were measured using a Quantichrom Creatinine Assay Kit (BioAssay Systems, Hayward, CA) according to the manufacturer's protocol.

Immunoblot analysis

Renal cortical tissue from flash frozen kidneys was lysed in RIPA buffer containing cocktail protease and phosphatase inhibitors. Forty micrograms of total protein were loaded into SDS-PAGE gels and immunoblots were performed as previously described.[130] Antibodies used for immunoblot studies were obtained from the following vendors: GAPDH (Fitzgerald Antibodies), COX I and NDUFB8 (Invitrogen), PGC-1 α (Calbiochem), and KIM-1 (R&D Systems).

Immunohistochemistry

Kidney sections approximately 5-6 microns from animals at 144 h after I/R or sham surgery were stained with H&E and PAS, and the degree of morphological changes was determined by light microscopy in a blinded fashion. The following parameters were chosen as an indication of morphological damage to the kidney after treatment with either vehicle or formoterol: proximal tubule dilation, brush border damage, proteinaceous

casts, interstitial widening, and necrosis. These parameters were evaluated on a scale from 0 to 4, which ranged from not present (0), mild (1), moderate (2), severe (3), and very severe (4).

Mitochondrial isolation and oxygen consumption

Kidney mitochondria were isolated from male C57BL/6 mice. The whole kidney was minced and homogenized in ice-cold isolation buffer (250 mM sucrose, 1 mM EGTA, 10 mM HEPES, 1 mg/ml fatty acid-free BSA, pH 7.4, 300 mOsm/kg H₂O). Nuclei and cellular debris were pelleted by centrifugation at 1,000 x g for 10 min. The supernatant was centrifuged at 10,000 x g for 5 min, resulting in a crude mitochondrial pellet. The pellet was washed once in ice-cold isolation buffer and resuspended in assay buffer (220 mM mannitol, 70 mM sucrose, 5 mM MgCl₂, 5 mM KH₂PO₄, 10 mM HEPES, 1 mg/ml fatty acid-free BSA, pH 7.4, 330 mOsm/kg H₂O). Crude mitochondria were then diluted 1/10 to 1/100 in buffer B (137 mM KCl, 2 mM KH₂PO₄, 2.5 mM MgCl₂, 20 mM HEPES, 0.5 mM EGTA, 0.2% FA-free BSA, pH 7.4, 330 mOsm/kg H₂O) and 180 µl diluted mitochondria were added to triplicate wells of a Seahorse XF96 assay plate on ice. The plate was spun down at 3,000 xg for 7 min at 4°C and immediately loaded into the XF96 Bioanalyzer. Oxygen consumption rate was normalized to mitochondrial protein per well.

Statistical Analysis

Results were expressed as means +/-SEM, N=3-7.

Data were analyzed by using a one-way ANOVA and post hoc tests (Student-Newman-Keuls or Fisher's least-significant difference where noted in the figure legend) were used to compare I/R untreated and sham and I/R compound-treated groups to vehicle. The level of significance was set at $P < 0.05$.

RESULTS

C57BL/6 mice were divided into four groups that were subjected to either sham or I/R surgery followed by once daily intraperitoneal (i.p.) administration with either formoterol (0.3 mg/kg) or vehicle (0.3% DMSO in n.s.) between 24 h and 144 h post-reperfusion. Prior to injury, serum creatinine (SCr) was approximately 0.2 mg/dL in all animals and increased to approximately 1.3 mg/dL 24 h after I/R (Fig 1A). Treatment was randomly initiated 24 h post-reperfusion when SCr was maximally elevated; therefore, intervention was not initiated until after there was established AKI. Following I/R, there was partial recovery of SCr in mice receiving vehicle treatment (IR+Veh); however, SCr was persistently elevated compared to pre-injury levels at approximately 0.7 mg/dL at 144 h post-reperfusion indicating persistent injury. In contrast, after five daily doses of formoterol following I/R (IR+Form), there was complete recovery of SCr by 144 h (Fig. 3-1A). SCr did not change following sham operation in either vehicle (Sham+Veh)- or formoterol (Sham+Form)-treated animals.

Kidney injury molecule-1 (KIM-1) is a highly sensitive and specific biomarker of renal tubular injury, which is minimally detected in healthy kidneys [209].

In cortical lysates from IR+Veh kidneys, KIM-1 protein was elevated compared to sham animals at 144 h and formoterol treatment attenuated KIM-1 protein expression to levels of the control animals (Fig 3-1B).

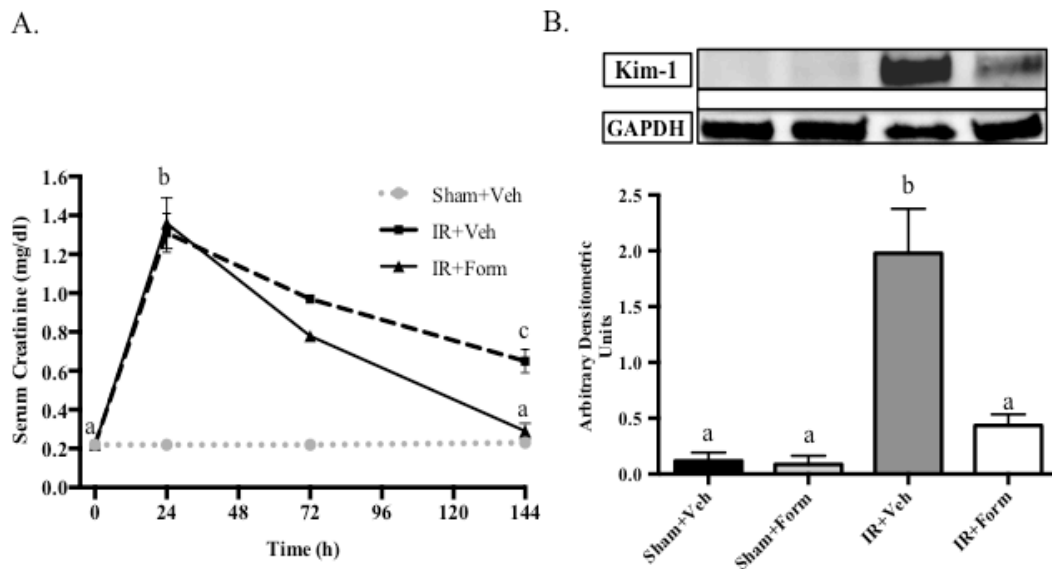


Fig 3-1. Treatment with formoterol restored kidney function and mitigated proximal tubule injury. Mice were subjected to either sham or I/R surgery and subsequent treatment with vehicle or formoterol. Kidney function was assessed via serum creatinine (A) and tubular injury via KIM-1 immunoblot analysis. (B) Kim-1 protein was measured in kidneys from mice 144 h after injury and quantified by densitometry. Samples were analyzed via one-way analysis of variance (ANOVA) followed by a Student-Newman-Keuls post hoc test to evaluate differences between groups. Data points are bars with different superscripts are significantly different from one another, mean (\pm SEM), $N=5$, $P<0.01$.

Renal histopathology was assessed using Periodic acid-Schiff (PAS) and hematoxylin and eosin (H&E) staining. Kidneys from IR+Veh and IR+Form mice displayed proximal tubule dilation, brush border damage, and the presence of proteinaceous casts. Kidneys from IR+Veh mice displayed evidence of persistent tubular necrosis at 144 h, which was attenuated with formoterol treatment (Fig 3-2B). Additionally, there was evidence of interstitial widening, an early sign of renal fibrosis, in IR+Veh kidneys which was not as prevalent in IR+Form mice (Fig 3-2C).

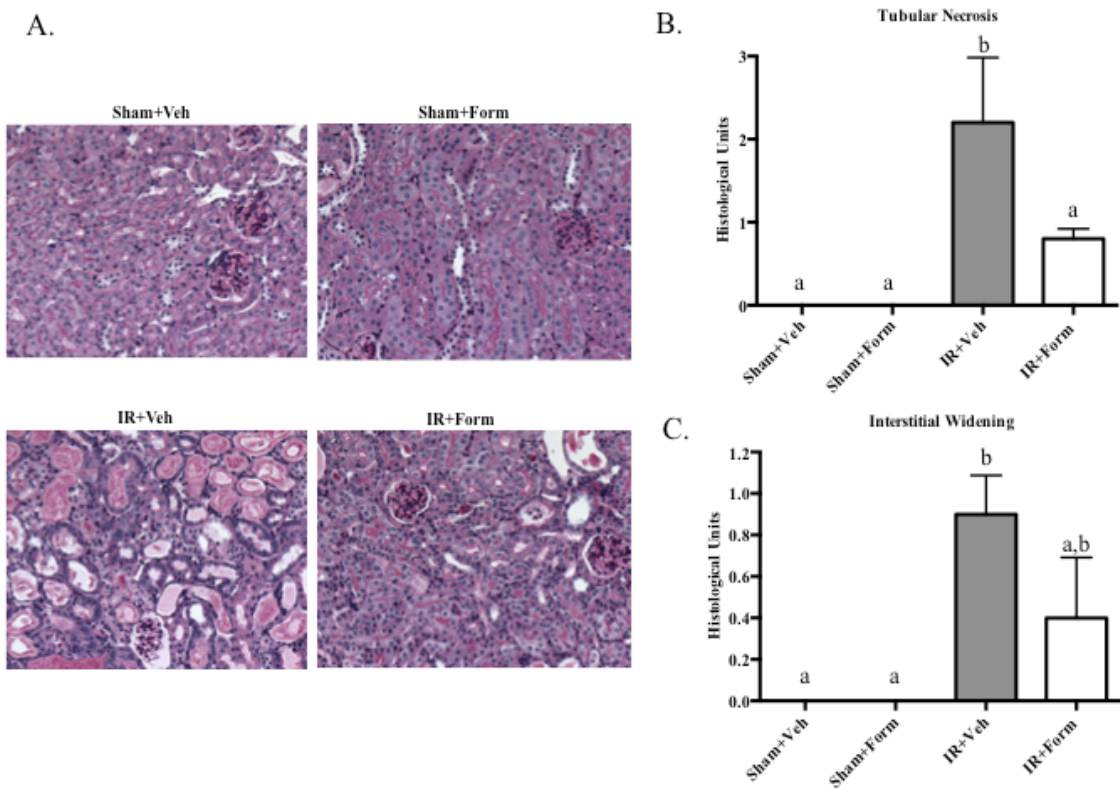


Fig 3-2. Treatment with formoterol (Form) improved tubule histology. Mice were subjected to either sham or I/R surgery, treated with vehicle or formoterol 24 h after and euthanized 144 h after surgery. (A) PAS stain at X10 magnification of representative slides of renal cortical tissue. Scoring of (B) tubular necrosis and (C) interstitial widening. Samples were analyzed via one-way analysis of variance (ANOVA) followed by a Student-Newman-Keuls post hoc test to evaluate differences between groups. Bars with different superscripts are significantly different from one another, mean (+/- SEM), $N=5$, $P<0.05$.

Using our I/R model, we have previously shown that essential components of the ETC, NADH dehydrogenase (ubiquinone) 1 beta subcomplex, 8 (NDUFB8) and mitochondrial cytochrome c oxidase subunit I (COX I), decreased within 24 h of I/R and remain decreased through 144 h [194]. If the improved renal function and decreased tissue injury stimulated by formoterol is the result of renal mitochondrial biogenesis, then renal mitochondrial proteins should be restored and mitochondrial function improved compared to I/R mice. At 144 h, there was no change in PGC-1 α protein expression with treatment or after injury (Fig 3-3A); however, nuclear-encoded NDUFB8 and mitochondrial-encoded COX I ETC proteins were decreased 144 h after reperfusion in IR+Veh kidneys (Fig 3B). Treatment with formoterol after I/R restored NDUFB8 and COX I protein abundance to levels of the control animals (Fig. 3-3B).

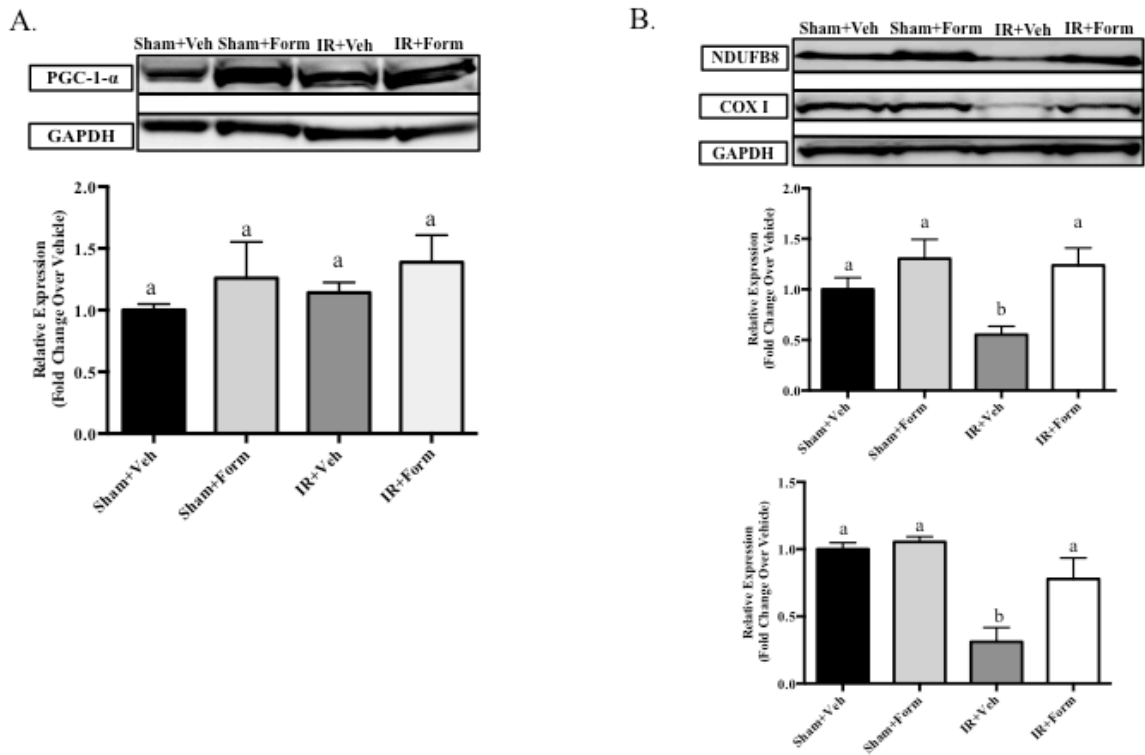
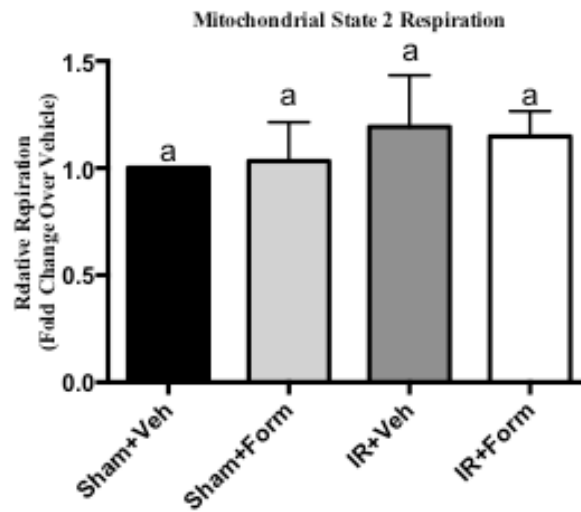


Fig 3-3. Formoterol restored mitochondrial protein expression after I/R-induced AKI. Mice were subjected to either sham or I/R surgery and subsequent treatment with vehicle or formoterol. Markers for mitochondrial biogenesis were evaluated via immunoblot 144 h after surgery. Renal cortical lysate PGC-1 α (**A**) and mitochondrial ETC proteins (**B**) NDUF8 (middle graph) and COX I (bottom graph). Densitometric semi-quantification is shown below the representative blots. Samples were analyzed via one-way analysis of variance (ANOVA) followed by a Student-Newman-Keuls post hoc test to evaluate differences between groups. Bars with different superscripts are significantly different from one another. Data are presented as mean (\pm SEM) and are relative values compared to control, $N=6$, $P<0.05$.

Previous *in vivo* and *in vitro* research in hypoxic and I/R induced models of AKI identified dysfunctional mitochondria, in the presence of suppressed ETC protein expression, in reduced kidney function [194]. Renal mitochondria were isolated from mice at 144 h and mitochondrial function determined. State 2 (basal respiratory rate) was not altered under any conditions (Fig 4A). State 3 (ADP-stimulated respiratory rate) respiration was reduced in mitochondria from IR+Veh kidneys, which indicated sustained mitochondrial dysfunction (Fig 4B), and was restored in IR+Form kidneys (Fig 4B). These results demonstrate that formoterol induced mitochondrial biogenesis and restored mitochondrial function following I/R in concert with the return of renal function.

A.



B.

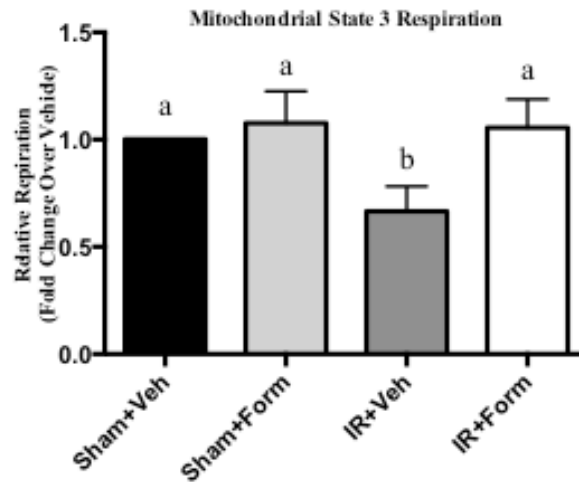


Fig 3-4. Formoterol restored mitochondrial function in the kidney after I/R-induced AKI. Kidneys were excised followed by isolation of mitochondria. Relative state 2 respiration (non-ADP stimulated respiration) (A) and relative state 3 respiration (ADP-stimulated respiration) (B). These results of respiration are expressed as the mean (\pm SEM) and are relative values compared to control). Bars with different superscripts are significantly different from one another, $N=7$, $P < 0.05$.

DISCUSSION

Currently, there are no pharmacological therapies approved for AKI, and the majority of drug discovery research for AKI has historically focused on prevention. Therefore, an animal model in which treatment is initiated after AKI is established is more relevant clinically [191, 192]. In the current study, we sought to discover a pharmacotherapeutic approach focused on accelerating recovery of kidney function in a mouse model of AKI.

A number of studies have demonstrated that mitochondrial dysfunction is a key component of AKI [129, 195-197] and more recent studies have shown persistent mitochondrial dysfunction after injury [194, 198]. Previous proof-of-principal studies were conducted using oxidant injury in RPTC and demonstrated that over-expression or pharmacological activation of PGC-1 α after oxidant injury accelerated recovery of mitochondrial and cellular function [128, 193]. Furthermore, formoterol, a FDA-approved, long-acting, specific β_2 -AR agonist, was shown to induce mitochondrial biogenesis in RPTC and mice [207].

Treatment with formoterol after I/R-induced AKI completely restored kidney function, attenuated tubule injury, and reduced renal cell necrosis. Concurrently, formoterol induced mitochondrial biogenesis and restored mitochondrial proteins and function after injury. These data define formoterol as a first-in-class agent, which successfully promotes full recovery of renal function after maximal injury. Furthermore, since mitochondrial dysfunction is common in many acute organ injuries/failures, our approach may extrapolate to other tissues.

In this model and others, renal function, as measured by serum creatinine, improves over several days following I/R [194], but does not fully recover by 6 days. Interestingly, formoterol treatment resulted in the complete return of renal function and recovery of renal proximal tubular injury as measured by KIM-1, which was associated with the recovery of mitochondrial function. Thus, we speculate recovery of mitochondrial function is critical for complete recovery of the proximal tubule and kidney function. In addition, because the extent of AKI and subsequent prolonged injury to the proximal tubules have been linked to the development of chronic kidney disease (CKD) [210, 211], assuagement of proximal tubule injury by formoterol after AKI may not be limited to short-term benefits by restoring kidney function, but may also have long-term benefits by modulating the progression to CKD due to a reduction in both extent and duration of proximal tubule damage.

Chapter 4:

ATOMOXETINE PREVENTS DEXAMETHASONE-INDUCED SKELETAL MUSCLE ATROPHY IN MICE

ABSTRACT

Skeletal muscle atrophy remains a clinical problem in numerous pathological conditions. β_2 -adrenergic receptor agonists, such as formoterol, are capable of inducing mitochondrial biogenesis (mitochondrial biogenesis) and preventing skeletal muscle atrophy. Recently, atomoxetine, an FDA-approved norepinephrine reuptake inhibitor, was positive in a cellular assay for mitochondrial biogenesis. We used a mouse model of dexamethasone-induced skeletal muscle atrophy to investigate the efficacy of atomoxetine to prevent the loss muscle mass and resolve the signaling pathways of formoterol and atomoxetine. Mice were administered dexamethasone once daily in the presence and absence of 0.3 mg/kg of formoterol, 0.1mg/kg of atomoxetine or sterile saline. Animals were euthanized at 8, 16, 24 h and 7 days later. Gastrocnemius muscle weights; changes in mRNA and protein expression of PGC-1 α 1/4 isoforms, ATP synthase β , Cox 1, NDUFB8, ND1 (mitochondria), IGF, myostatin, MuRF-1 (muscle atrophy), phosphorylated (p)-FoxO3a, Akt, mTOR, and rp S6 (muscle hypertrophy) in naïve and muscle atrophy mice were determined. Atomoxetine had no effect on any of the above biomarkers except for an acute increase in p-mTOR at 24 h after treatment in naïve mice. In contrast, formoterol robustly activated PGC-1 α 4-IGF1-Akt-mTOR-rp S6 pathway and increased p-FoxO3a as early as 8 h and repressed myostatin at 16 h. Chronic treatment of atomoxetine increased p-Akt, p-FoxO3a, and sustained PGC-1 α and muscle

mass in skeletal muscle of dexamethasone-treated mice, comparable to formoterol. In conclusion, chronic treatment with a low dose of atomoxetine prevented the loss of skeletal muscle mass by activating non-canonical mechanisms and supports its potential use in muscle atrophy conditions.

INTRODUCTION

Skeletal muscle is remarkably malleable, allowing phenotypic adaptations to functional demands. Exercise training is known to induce muscle hypertrophy and is characterized by growth of existing myofibrils [212]. Skeletal muscle atrophy is defined as a decrease in muscle mass and occurs when rates of protein degradation exceed those of synthesis [213]. Glucocorticoids (GC) are well-established inducers of catabolism and numerous pathological conditions characterized by muscle atrophy (cachexia, chronic kidney disease, metabolic acidosis, sepsis, diabetes, etc.) are associated with increases in circulating glucocorticoid levels, suggesting a potential role in the development of atrophy [214, 215]. Clinically, severe muscle atrophy, especially when concomitant with other chronic disease states, is associated with increased rates of morbidity and mortality [216-218]. Currently, there is no FDA approved drug to treat muscle atrophy, highlighting the importance of not only identifying novel drug entities capable of preventing skeletal muscle atrophy, but also elucidating the associated signaling pathways.

Several recent reports describe an intricate network of signaling pathways that operate in muscle cells to regulate the size of myofibers and muscle performance [219]. These different pathways crosstalk and modulate one another at different levels, coordinating

protein synthesis and degradation simultaneously. Major pathways that lead to atrophy are activation of forkhead box protein O (FoxO3a), myostatin, and nuclear factor kappa B (NFκB), which result in accelerated protein degradation primarily through activation of muscle atrophy F-box/muscle-specific ubiquitin E3-ligases atrophy gene-1 (MAFbx/atrogen-1) and muscle RING-finger protein-1 (MuRF1) [219-224]. On the other hand, a major signaling pathway that regulates skeletal muscle growth is the insulin-like growth factor 1 (IGF-1)-Akt-mammalian target of rapamycin (IGF-1-Akt-mTOR) [225-228]. Akt stimulates protein synthesis by activating mTOR and its downstream effector ribosomal protein S6 (rp-S6) [219, 226, 227]. In addition, Akt can also prevent muscle protein degradation by phosphorylating the FoxO3a protein; thereby, preventing entry into the nucleus and activating transcription of MuRF-1 [229, 230].

Previous *in vivo* and *in vitro* models have established interactions between these atrophy and hypertrophy-related modulators with peroxisome-proliferator activated receptor-gamma coactivator 1 alpha (PGC-1α) [219]. Recently, alternative splice variants of the PGC-1α gene have been identified [131]. Each of the characterized PGC-1α isoforms elicits discrete gene programs; whereby, induction of the PGC-1α (now called PGC-1α1) isoform promotes mitochondrial biogenesis (mitochondrial biogenesis), regulates mitochondrial OXPHOS genes, and inhibits activation of the FoxO3a and NFκB proteins [101, 118, 231-233]. However, the PGC-1α4 isoform specifically activates the expression of IGF-1 and represses myostatin, which was demonstrated to increase muscle mass, strength, and resistance to muscle wasting in a model of cancer cachexia [131].

Several studies have established the benefits of therapeutic intervention by β_2 -adrenergic receptor (β_2 -AR) agonists in animal models of muscle atrophy [234]. The IGF-1-Akt pathway controls protein synthesis and β_2 -AR agonists such as clenbuterol and formoterol are considered pro-growth and anti-atrophic drugs [235]. In this regard, formoterol has been recently shown to induce skeletal muscle hypertrophy through activation of Akt-mTOR-rp S6 pathway and prevent protein degradation [236]. However, chronic administration of high doses of these drugs resulted in adverse cardiovascular effects in several animal models of muscle atrophy [234]. Therefore development of drugs that prevent muscle atrophy with fewer adverse cardiovascular effects is desirable.

Atomoxetine, also known as atomoxetine, is a FDA-approved drug to treat attention deficit hyperactivity disorder (ADHD) and the mechanism of action of atomoxetine is thought to be norepinephrine re-uptake inhibition (NRI) [237]. As part of our drug discovery program in mitochondrial biogenesis, we initiated a high throughput screen, which revealed atomoxetine and β_2 -adrenergic receptor agonists as potent inducers of mitochondrial biogenesis [132]. Therefore, the goal of this study was to examine the efficacy of atomoxetine to prevent skeletal muscle atrophy in a commonly used mouse model and identify the associated signaling pathways. Furthermore, formoterol was included in this study since it has been used in this model and its actions have been well characterized.

EXPERIMENTAL PROCEDURES

Dexamethasone induced model of skeletal atrophy

Male C57BL/6 (Jackson Laboratories, Bar Harbor ME), 6-8 weeks of age (25-30 g), were housed in temperature-controlled conditions under a light/dark photocycle with food and water supplied *ad libitum*.

Acute treatment details: Groups of naive mice were injected intraperitoneally with a single dose of sterile saline, 0.3 mg/kg of formoterol fumarate dihydrate (Sigma, St. Louis, MO) or 0.1 mg/kg atomoxetine (Tocris Bioscience, Bristol, UK). Animals were euthanized at 8, 16, and 24 h after treatments.

Chronic treatment details: Three groups of naive mice were injected intraperitoneally with sterile saline, 0.3 mg/kg of formoterol and 0.1 mg/kg atomoxetine, respectively, daily for 7 days. Animals were euthanized on the 8th day.

Assessing skeletal muscle atrophy

One group of mice was co-injected intraperitoneally with sterile saline daily for 7 days. Three groups of mice were co-injected intraperitoneally with 25 mg/kg water-soluble dexamethasone (Sigma, St. Louis, MO) followed by a second injection of sterile saline (second), 0.3 mg/kg of formoterol (third), or 0.1 mg/kg atomoxetine (fourth), respectively, daily for 7 days. Animals were euthanized on the 8th day.

Gastrocnemius and body weights were determined and gastrocnemius muscle was flash frozen for further mRNA and protein analysis.

All animal and treatment protocols were in compliance with the Guide for Care and Use of Laboratory Animals as adopted and promulgated by the US National Institutes of Health and were approved by our Institutional Animal Care and Use Committee (IACUC).

mRNA analysis

Total RNA was extracted from mouse gastrocnemius tissue samples using TRIzol reagent (Invitrogen, Grand Island, NY) according to the manufacturer's protocol. cDNA was synthesized via reverse transcription using the iScript Advanced cDNA synthesis kit (Bio-Rad, Hercules, CA) with 5 µg of RNA. qPCR analysis was performed with cDNA. qPCR was carried out using 5 µl of cDNA template combined with Brilliant II SYBR Green master mix (Stratagene, La Jolla, CA) at a final concentration of 1× and primers (Integrated DNA Technologies, Inc., Coralville, IA) at a concentration of 400 nM. mRNA expression of all genes was calculated using the 2- $\Delta\Delta$ CT method normalized to β -actin. Primer sequences are as follows:

Total *PGC-1 α* (EX2) (FW: 5'-TGA TGT GAA TGA CTT GGA TAC AGA CA-3', REV: 5'-GCT CAT TGT TGT ACT GGT TGG ATA TG-3'),

PGC-1 α 1 (FW: 5'-GGA CAT GTG CAG CCA AGA CTC T-3', REV: 5'-CAC TTC AAT CCA CCC AGA AAG CT-3'),

PGC-1 α 4 (FW: 5'-TCA CAC CAA ACC CAC AGA AA-3', REV: 5'-CTG GAA GAT

ATG GCA CAT-3'),

Myostatin (FW: 5'-AGT GGA TCT AAA TGA GGG CAG T-3', REV: 5'-GTT TCC AGG CGC AGC TTA-3'),

IGF-1 (FW: 5'-TGC TCT TCA GTT CGT GTG-3', REV: 5'-ACA TCT CCA GTC TCC TCA G-3'),

β -actin (FW: 5'- GGG ATG TTT GCT CCA ACC AA-3', REV: 5'-GCG CTT TTG ACT CAG GAT TTA-3').

Mitochondrial DNA Content.

The qPCR method was used to determine the relative quantity of mtDNA in mouse gastrocnemius tissue samples. After treatment, DNA was extracted from tissue using the DNeasy Blood and Tissue Kit (QIAGEN, Valencia, CA) and 5 ng of DNA was used for qPCR. ND1 (FW: 5'-TAG AAC GCA AAA TCT TAG GG-3', REV: 5'-TGC TAG TGT GAG TGA TAG GG-3') was used as the mitochondrial gene and expression was normalized to nuclear-encoded β -actin expression.

Immunoblot analysis. Mouse gastrocnemius skeletal muscle tissue was homogenized in 5 volumes of protein lysis buffer (1% Triton X-100, 150 mM NaCl, 10 mM Tris-HCl, pH 7.4; 1 mM EDTA; 1 mM EGTA; 2 mM sodium orthovanadate; 0.2 mM phenylmethylsulfonyl fluoride; 1 mM HEPES, pH 7.6; 1 μ g/ml leupeptin; and 1 μ g/ml aprotinin) using a Polytron homogenizer. The homogenate was stored on ice for 10 min and then centrifuged at 7500g for 5 min at 4°C. The supernatant was collected and protein was determined using a bicinchoninic acid kit (Sigma, St. Louis, MO) with

bovine serum albumin as the standard. Proteins (50–75 µg) were separated on 4 to 20% gradient SDS-polyacrylamide gels and transferred to nitrocellulose membranes.

Membranes were blocked either in 5% dried milk or BSA in TBST (0.1% Tween 20 in 1× Tris-buffered saline) and incubated with 1:1000 antibody dilutions of MuRF1 (ECM Biosciences, Versailles, KY); anti-PGC-1α (EMD, Billerica, MA); anti-ATP synthase β, COX-1 (Abcam, Cambridge, MA); anti-NDUFB8 (Invitrogen, Grand Island, NY); total and phosphorylated anti-FoxO3a, Akt, mTOR, rp S6 (Cell Signaling Technologies, Danvers, MA); and anti-GAPDH (Fitzgerald, Acton, MA) overnight at 4°C. After incubation for 2 h at room temperature with secondary antibodies (1:2000) conjugated with horseradish peroxidase, membranes were detected by chemiluminescence.

Statistical Analysis.

Data are expressed as means ± S.E.M. ($n = 4-5$) for all experiments. Multiple comparisons of normally distributed data were analyzed by one-way analysis of variance, as appropriate, and group means were compared using the Student-Newman-Keuls post hoc test. Single comparisons were analyzed by Student's t test where appropriate. The criterion for statistical differences was $p \leq 0.05$ for all comparisons.

RESULTS

Acute treatment with formoterol, but not atomoxetine, differentially modulates PGC-1α isoform expression in skeletal muscle of naïve mice. The canonical role of the PGC-1α protein, now called PGC-1α1, is to function as the “master regulator” of mitochondrial biogenesis and target mitochondrial OXPHOS genes; formoterol is a potent inducer of

PGC-1 α gene expression [238-240]. In contrast, PGC-1 α 4, a recently discovered PGC-1 α splice variant, induces a discrete gene program resulting in muscle hypertrophy and not mitochondrial biogenesis [131]. It is important to note that all alternatively spliced variants of the PGC-1 α gene identified by Ruas, et al contain the exon 2 (EX2) region. Therefore, primer sequences, which contain this region, are to be interpreted as total PGC-1 α marker for total PGC-1 α expression. Since identification of the specific PGC-1 α isoform induced by formoterol or atomoxetine, has yet to be determined, we evaluated the effects of acute treatment with formoterol or atomoxetine on the PGC-1 α isoforms mRNA in skeletal muscle of naïve mice. Formoterol caused a 12-fold induction of total PGC-1 α (EX2, representative of both PGC-1 α isoforms) at 8 h post treatment, which decreased and returned to baseline at 24 h (Fig. 4-1A). We then evaluated the expression of PGC-1 α 1 and PGC-1 α 4. PGC-1 α 1 gene expression was maximally suppressed at 8 h post treatment with formoterol and returned to control levels by 24 h (Fig. 4-1B). Formoterol induced PGC-1 α 4 gene expression maximally at 8 h after treatment (6-fold increase over vehicle) and returned to control levels by 24 h (Fig. 4-1C). In contrast, atomoxetine had no effect on EX2 or PGC-1 α 1 and expression of PGC-1 α 4 was decreased 20-25% at 16 and 24 h after treatment (Figs. 4-1D-F).

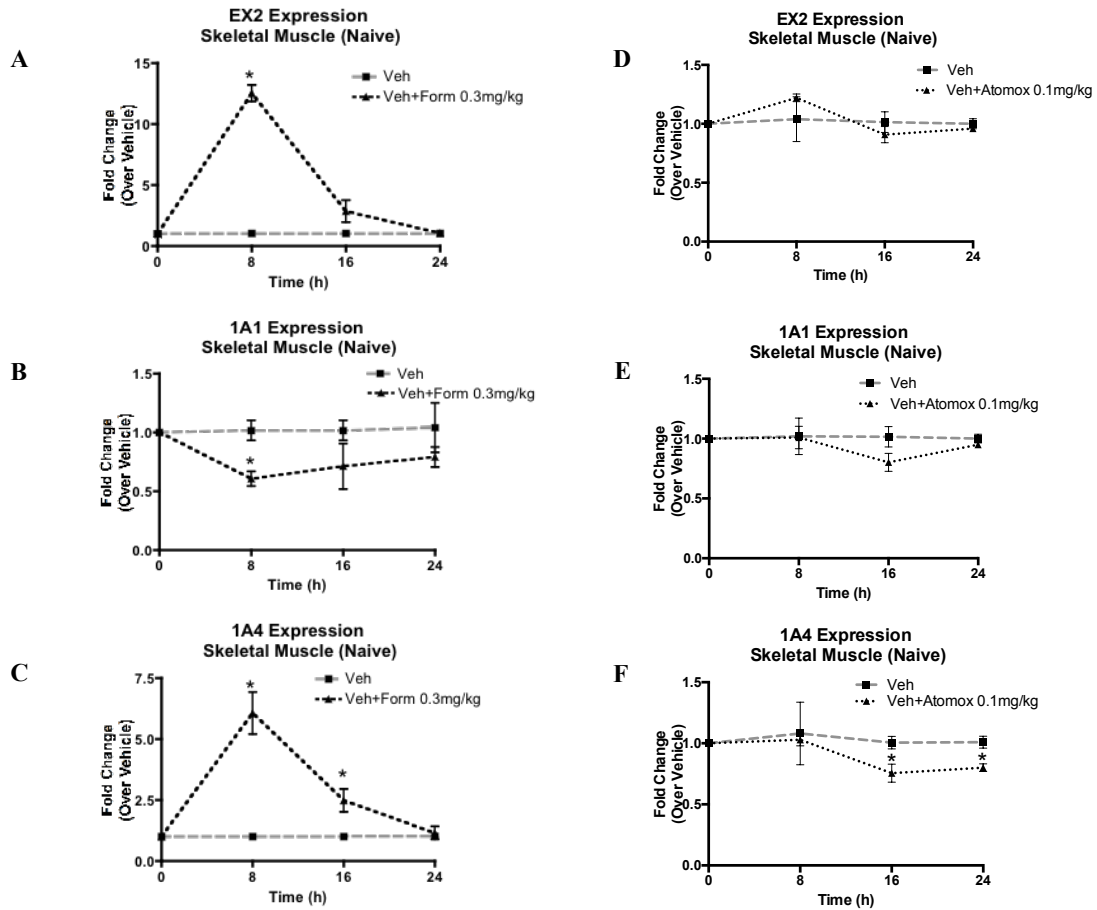


Fig. 4-1. PGC-1 α isoform gene expression in skeletal muscle of naive mice following formoterol and atomoxetine treatment. Naïve mice were subjected to a single intraperitoneal (i.p.) dose of either formoterol (0.3 mg/kg), atomoxetine (0.1 mg/kg), or sterile saline (veh) and euthanized at 8, 16, and 24 h. Gastrocnemius muscle was excised from animals at each time point and RNA was isolated for qPCR analysis. Total PGC1 α (EX2), PGC1 α 1, and PGC1-1 α 4 at 0, 8, 16, and 24 h after treatment with formoterol (A, B, C) or atomoxetine (D, E, F). Data were normalized to vehicle and represented as a relative fold change. Data are expressed as mean \pm SE (n = 5). * Significantly different from untreated mice ($p \leq 0.05$).

Formoterol but not atomoxetine treatment acutely increases IGF-1 gene expression and suppresses myostatin in skeletal muscle of naïve mice. PGC-1 α 4 regulates a discrete gene program responsible for inducing skeletal muscle hypertrophy via induction of IGF-1 and suppression of myostatin [131]. Formoterol increased IGF-1 gene expression by 2-fold at 8 h post treatment, which returned to baseline at 24 h (Fig. 4-2A). In addition, formoterol suppressed myostatin gene expression by 50% at 16 h post treatment (Fig. 4-2B). In contrast, atomoxetine did not alter IGF-1 or myostatin (Figs. 4-2C, D).

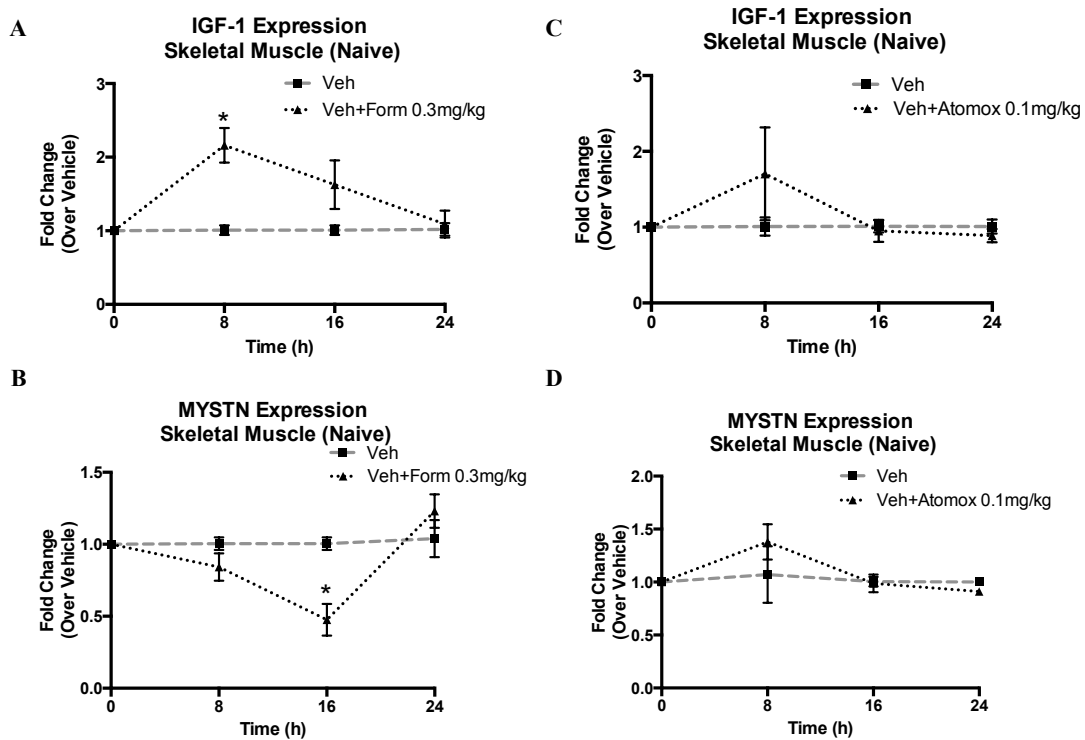


Fig. 4-2. IGF-1 and myostatin gene expression in skeletal muscle of naïve mice following formoterol and atomoxetine treatment. Mice were treated as described in Figure 1. Expression of IGF-1 and myostatin at 0, 8, 16, and 24 h after treatment with formoterol (**A, B**) or atomoxetine (**C, D**). Data were normalized to vehicle and represented as a relative fold change. Data are expressed as mean \pm SE (n = 5). * Significantly different from untreated mice ($p \leq 0.05$).

Atomoxetine acutely increases p-mTOR protein expression in the naïve mouse.

The mechanism by which formoterol induces skeletal muscle hypertrophy has been well characterized as signaling through the phosphorylation of all components of the AKT-mTOR-rp S6 pathway [236, 241]. In addition it prevents muscle atrophy via phosphorylation of FoxO3a [230, 233]. Formoterol increased protein expression of p-FoxO3a, p-Akt, p-mTOR and p-rp S6 8 h after treatment (Figs. 4-3A-E). Atomoxetine increased p-mTOR protein expression 24 h after treatment without altering rp S6 phosphorylation (Figs. 4-3F-J).

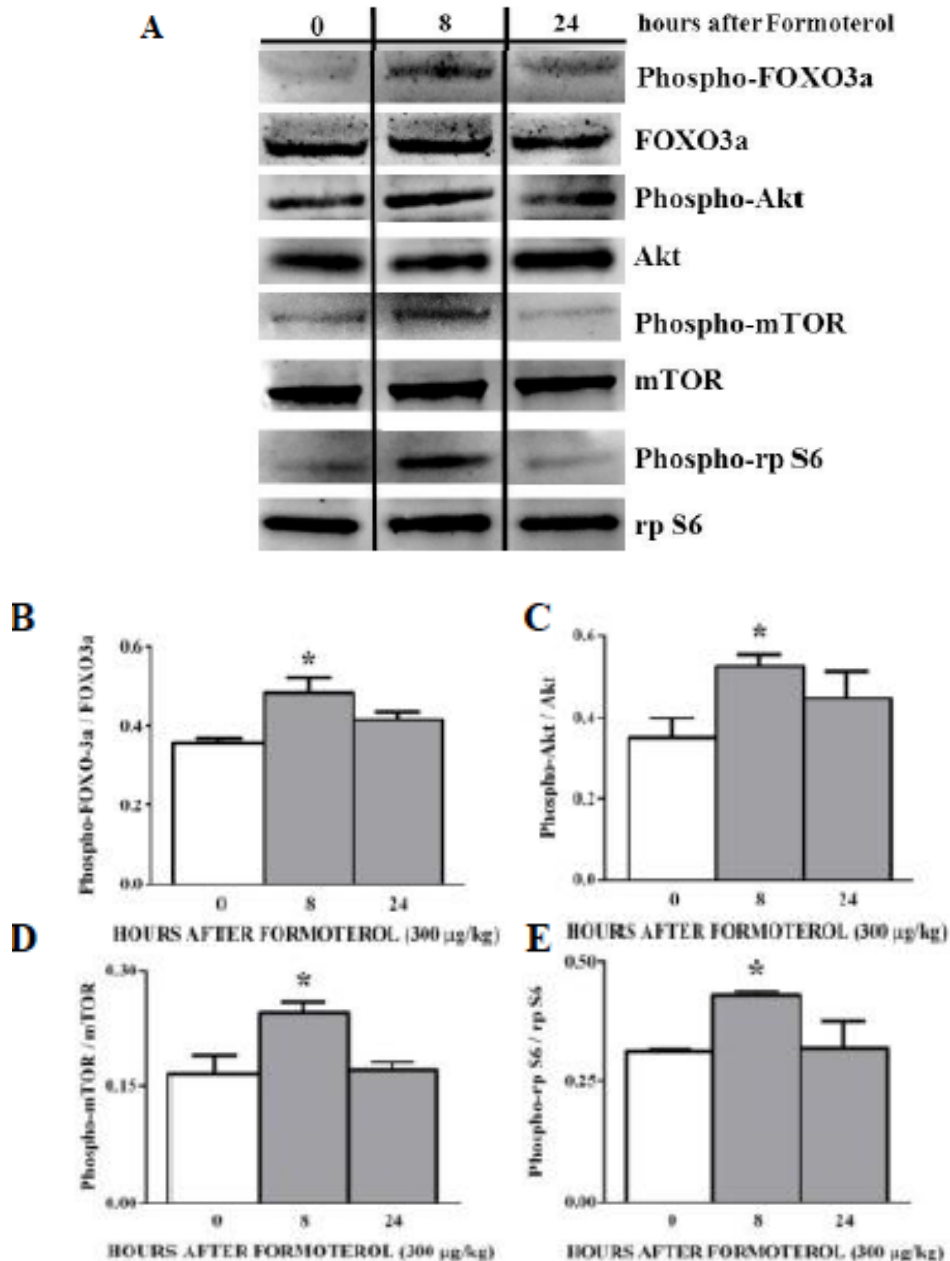


Fig. 4-3A-E. Acute effects of atomoxetine and formoterol on protein synthesis signaling mechanisms in skeletal muscle of naïve mice. Mice were treated as described in Figure 1. Representative immunoblots for markers of muscle protein homeostasis: Total and phosphorylated forms of Akt-mTOR-rp S6 axis and FoxO3a at 0, 8 and 24 h after formoterol (A); densitometric analysis of FoxO3a (B), Akt (C), mTOR (D) and ribosomal protein rp S6 (E) ± formoterol. Data were normalized to vehicle and represented as relative fold change. Data are expressed as mean ± SE (n = 4). * Significantly different from untreated mice ($p \leq 0.05$).

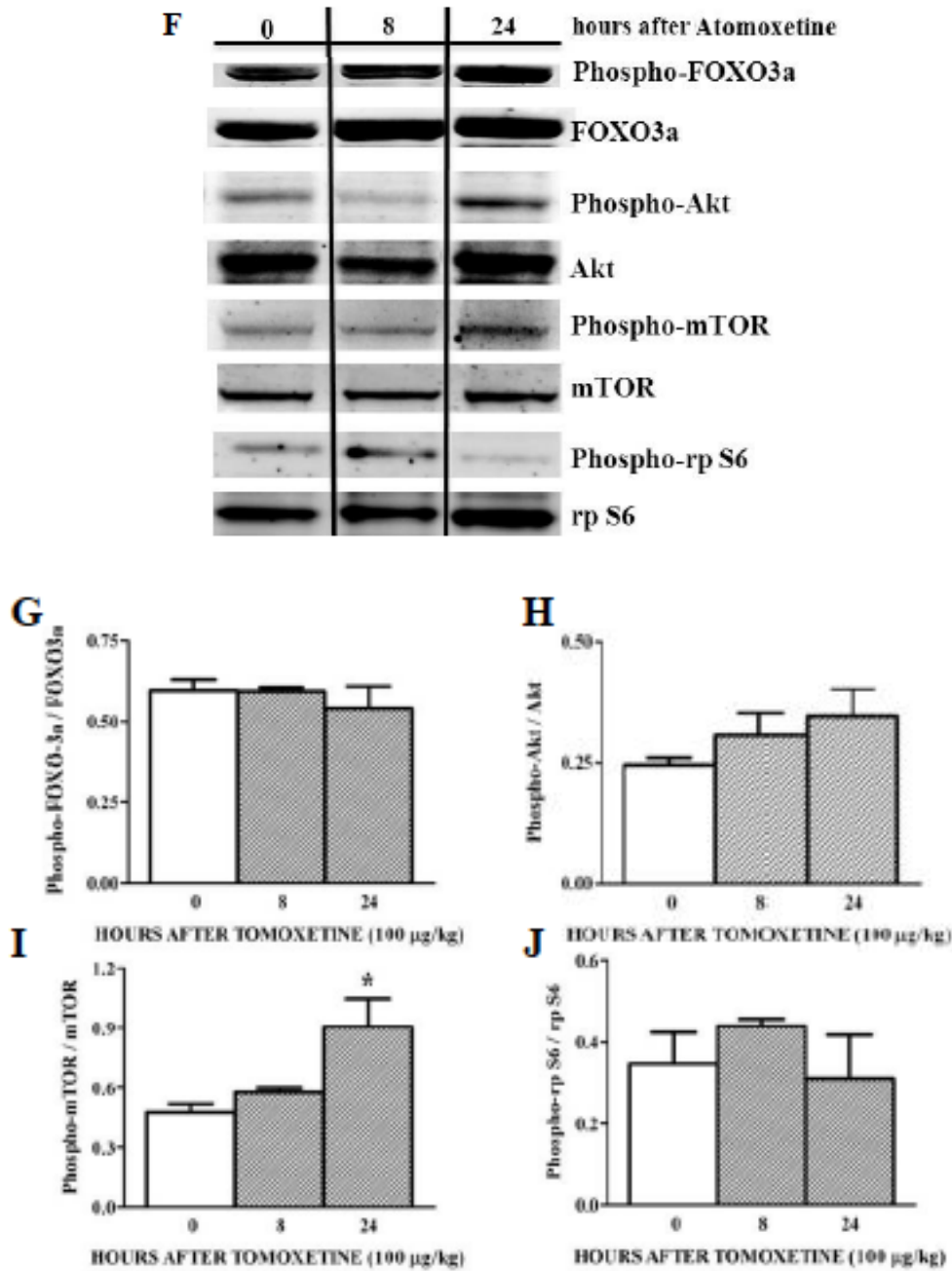


Fig. 4-3F-J. Acute effects of atomoxetine and formoterol on protein synthesis signaling mechanisms in skeletal muscle of naïve mice. Mice were treated as described in Figure 1. Representative immunoblots for markers of muscle protein homeostasis: Total and phosphorylated forms of Akt-mTOR-rp S6 axis and FoxO3a at 0, 8 and 24 h after atomoxetine (**F**). Densitometric analysis of FoxO3a (**G**), Akt (**H**), mTOR (**I**) and ribosomal protein rp S6 (**J**) \pm atomoxetine. Data were normalized to vehicle and represented as relative fold change. Data are expressed as mean \pm SE (n = 4). * Significantly different from untreated mice ($p \leq 0.05$).

These results demonstrate that acute formoterol treatment initiates the hypertrophy pathway by increasing PGC-1 α 4, suppressing PGC-1 α 1, increasing IGF-1 expression, decreasing myostatin (MYSTN) expression, and increasing p-FoxO3a, p-Akt, p-mTOR and p-rp S6. In contrast atomoxetine had minimal or no effects on these pathways except for an increase in p-mTOR at 24 h. A summary diagram depicting the gene and protein changes observed with acute formoterol treatment can be found in figure 4-4.

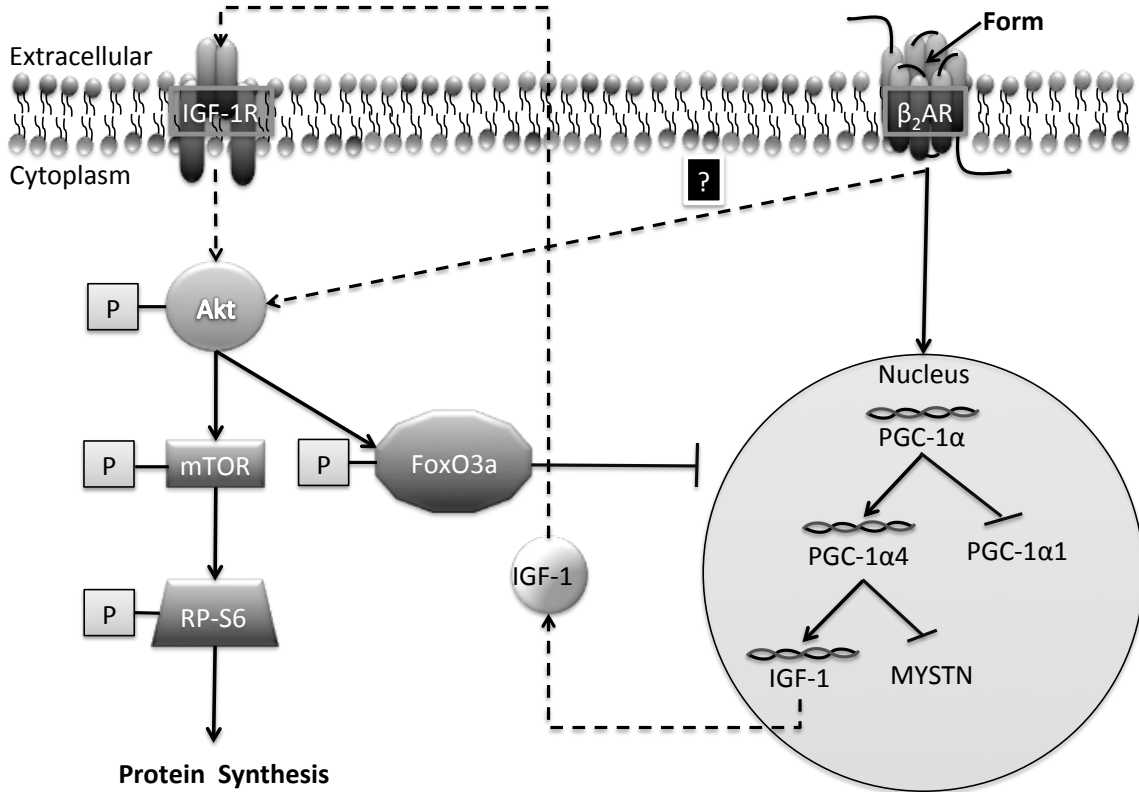


Fig. 4-4. Proposed mechanisms for acute treatment with formoterol in the skeletal muscle of mice. This diagram depicts the changes observed in gene and protein expression following acute treatment with formoterol (Form). Treatment with formoterol executes a discrete gene program associated with the PGC-1 α isoform involving subsequent increases in IGF-1 gene expression and the phosphorylation (represented by “P”) status of the Akt-mTOR-rp S6 axis, indicating activation. Concomitantly, inactivation is depicted by increased phosphorylation of FoxO3a with suppression of myostatin (MYSTN) gene expression. Solid shapes represent proteins (name displayed in white), helices within the nucleus represent genes (name displayed in black below helices), solid black arrowed lines are pathways conferred by our data and dotted arrowed lines are potential pathways not evaluated by our study. Both represent activation. Except for the arrowed line from Akt to FoxO3a, where phosphorylation inactivates FoxO3a. Akt phosphorylation can result from numerous downstream interactions associated with the activation of the β_2 -AR, which are not evaluated by our study. Therefore, we do not know what else might play a role in phosphorylating Akt and chose to represent this interaction with “question mark” and a dotted line. Lines that are blunted at the end represent inhibition.

Chronic treatment with atomoxetine does not induce muscle hypertrophy, but increases phosphorylation of Akt in the naïve mouse. Given that the muscle atrophy model involves administration of 7 daily doses, chronic treatment studies with formoterol and atomoxetine were initiated in naïve mice to serve as a comparison. After 7 daily treatments with formoterol, increases in protein expression were observed in p-Akt, p-FoxO3a, and p-rp S6 (Fig. 4-5B) and muscle mass by 15%. However, chronic treatment with atomoxetine had no effect on muscle mass (Fig. 4-5A). Atomoxetine increased p-Akt but had no effect on the downstream effector proteins p-FoxO3a, p-mTOR, or p-rp S6 (Figs. 4-5C-F).

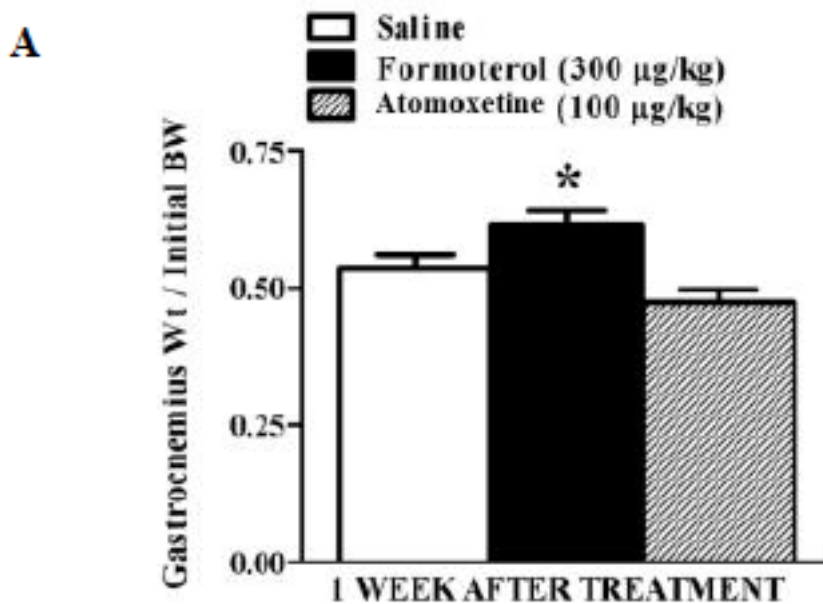


Fig. 4-5A. Chronic effects of atomoxetine and formoterol on muscle mass and protein synthesis signaling mechanisms in skeletal muscle of naïve mice. Mice were treated as described in Figure 1. (A) Normalized gastrocnemius muscle mass 7 days after the treatment of naïve mice with saline, formoterol or atomoxetine. Data are expressed as mean \pm SE (n = 4-5). * Significantly different from either saline-treated controls or all other groups of mice ($p \leq 0.05$).

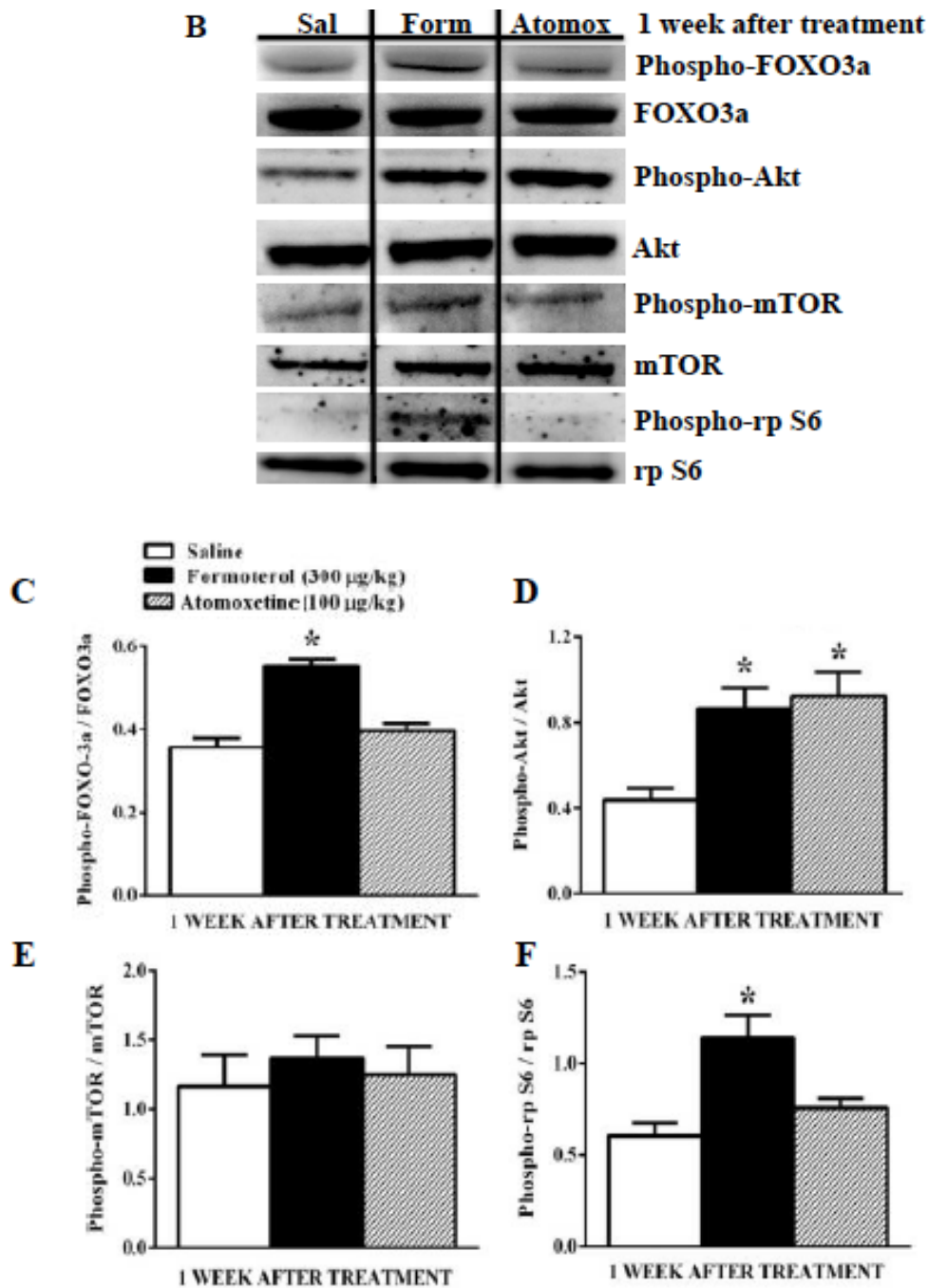


Fig. 4-5B-F. Chronic effects of atomoxetine and formoterol on muscle mass and protein synthesis signaling mechanisms in skeletal muscle of naïve mice. Mice were treated as described in Figure 1. **(B)**. Densitometric analysis of FoxO3a **(C)**, Akt **(D)**, mTOR **(E)** and ribosomal protein rp S6 **(F)** after saline, formoterol and atomoxetine. Data were normalized to vehicle and represented by relative fold change. Data are expressed as mean \pm SE (n = 4-5). * Significantly different from either saline-treated controls or all other groups of mice ($p \leq 0.05$).

Chronic treatment with formoterol and atomoxetine restores mitochondrial proteins, increases hypertrophy markers and restores gastrocnemius muscle mass in mice with dexamethasone-induced muscle atrophy. Using a previously described model of skeletal muscle atrophy [242], chronic treatment with dexamethasone caused a 17% reduction in gastrocnemius muscle mass in mice. Low doses of formoterol and atomoxetine prevented the loss of skeletal muscle mass (Fig. 4-6A). After 7 daily doses, treatment with neither dexamethasone nor atomoxetine had any effect on relative gene expression of PGC-1 α 1. However, formoterol significantly increased expression of PGC-1 α 1 (Fig. 4-6B).

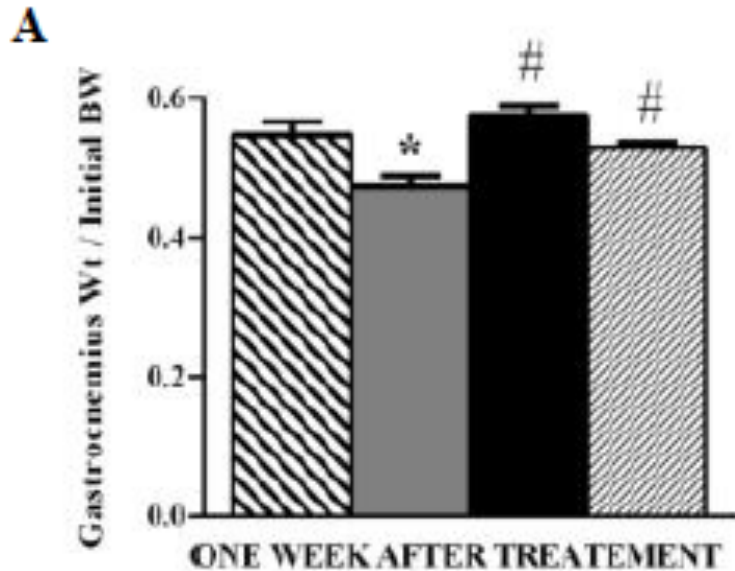
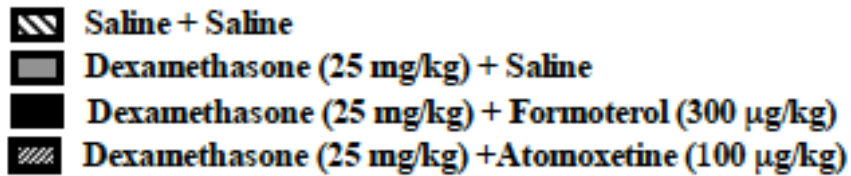


Fig. 4-6A. Chronic effects of atomoxetine and formoterol on skeletal muscle mass and mitochondrial proteins in dexamethasone-treated mice. Mice were co-administered with daily dose of 25 mg/kg water soluble-Dexamethasone ± 0.3 mg/kg of formoterol / 0.1mg/kg of atomoxetine or sterile saline, i.p. for 7 days. Appropriate saline controls were maintained throughout the experiment. Animals were euthanized after 7 days and gastrocnemius muscle was isolated from both right and the left hind limbs. (A) Normalized gastrocnemius muscle mass 7 days after the treatment of dexamethasone-treated mice with saline, formoterol or atomoxetine. Data were normalized by GAPDH. Data are expressed as mean ± SE (n = 4-5). * Significantly different from either saline-treated controls or all other groups of mice ($p \leq 0.05$). # Significantly different from dexamethasone-treated mice ($p \leq 0.05$).

Next, we determined if this increase was associated with a change in mtDNA or protein expression of nuclear and mitochondrial-encoded proteins, both markers of mitochondrial biogenesis. mtDNA copy number, as measured by ND1 gene expression, was not altered in any of the treatment groups (Fig. 4-6C). However, treatment with dexamethasone significantly decreased PGC-1 α protein expression one week after treatment and both formoterol and atomoxetine prevented the loss of PGC-1 α (Figs. 4-6D-E). ATP synthase β and mitochondrial cytochrome c oxidase subunit I (COX I) protein expression were increased following treatment with formoterol in dexamethasone-treated mice while there was no effect on NDUFB8 (Fig. 4-6D). Atomoxetine did not alter mitochondrial protein expression in dexamethasone-treated mice (Fig. 4-6E).

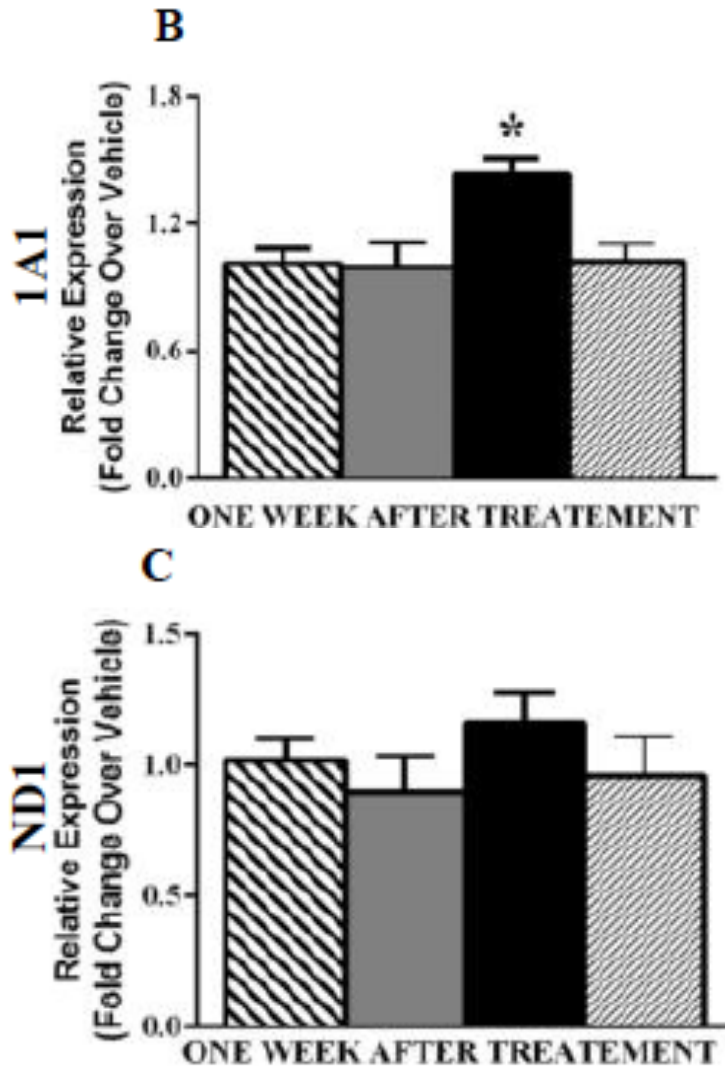


Fig. 4-6B-C. Chronic effects of atomoxetine and formoterol on skeletal muscle mass and mitochondrial proteins in dexamethasone-treated mice. Mice were co-administered with daily dose of 25 mg/kg water soluble-Dexamethasone \pm 0.3 mg/kg of formoterol / 0.1mg/kg of atomoxetine or sterile saline, i.p. for 7 days. Appropriate saline controls were maintained throughout the experiment. Gene expression analysis for PGC-1 α 1 (**B**) and ND1 (**C**). Data are expressed as mean \pm SE (n = 4-5). * Significantly different from either saline-treated controls or all other groups of mice ($p \leq 0.05$). # Significantly different from dexamethasone-treated mice ($p \leq 0.05$).

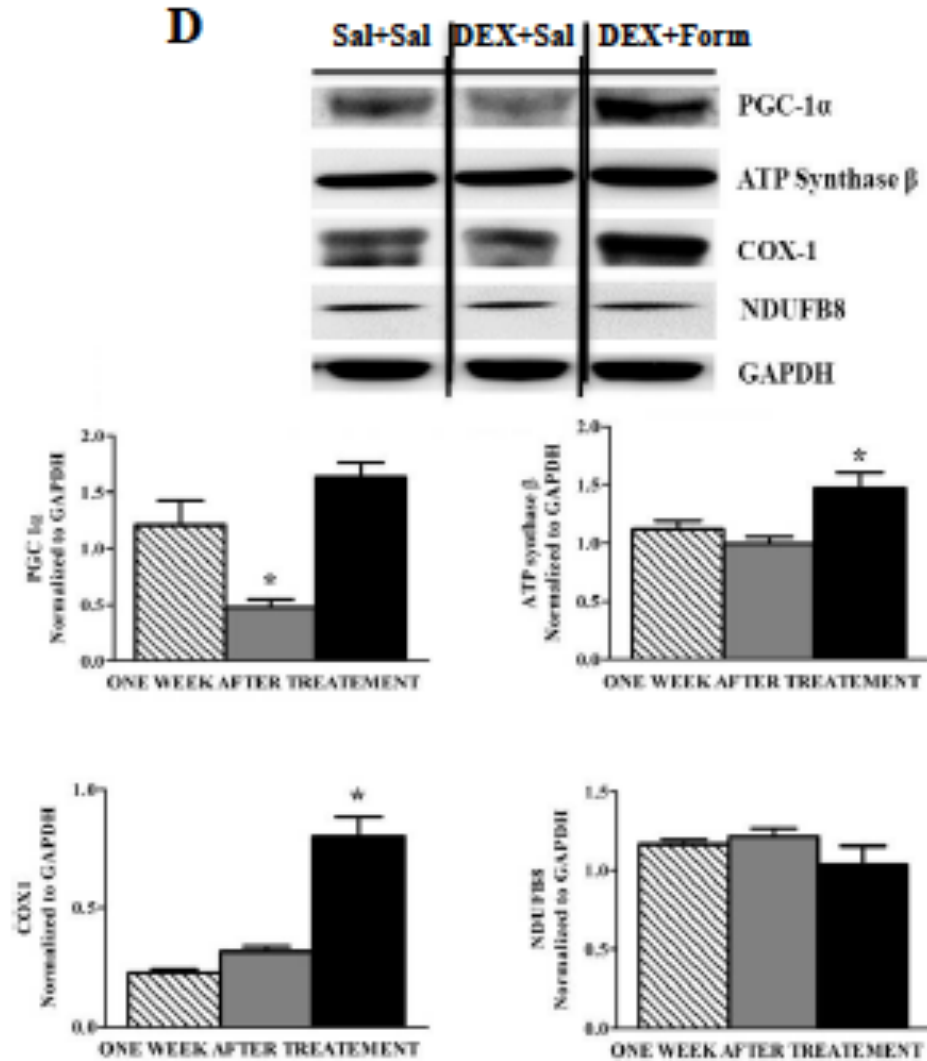


Fig. 4-6D. Chronic effects of atomoxetine and formoterol on skeletal muscle mass and mitochondrial proteins in dexamethasone-treated mice. Mice were co-administered with daily dose of 25 mg/kg water soluble-Dexamethasone \pm 0.3 mg/kg of formoterol / 0.1mg/kg of atomoxetine or sterile saline, i.p. for 7 days. Appropriate saline controls were maintained throughout the experiment. Representative immunoblots and respective densitometry for mitochondrial proteins: Total PGC1 α 1, ATP synthase β , COX-1 and NDUFB8 7 days after formoterol (**D**). Data were normalized by GAPDH. Data are expressed as mean \pm SE (n = 4-5). * Significantly different from either saline-treated controls or all other groups of mice ($p \leq 0.05$). # Significantly different from dexamethasone-treated mice ($p \leq 0.05$).

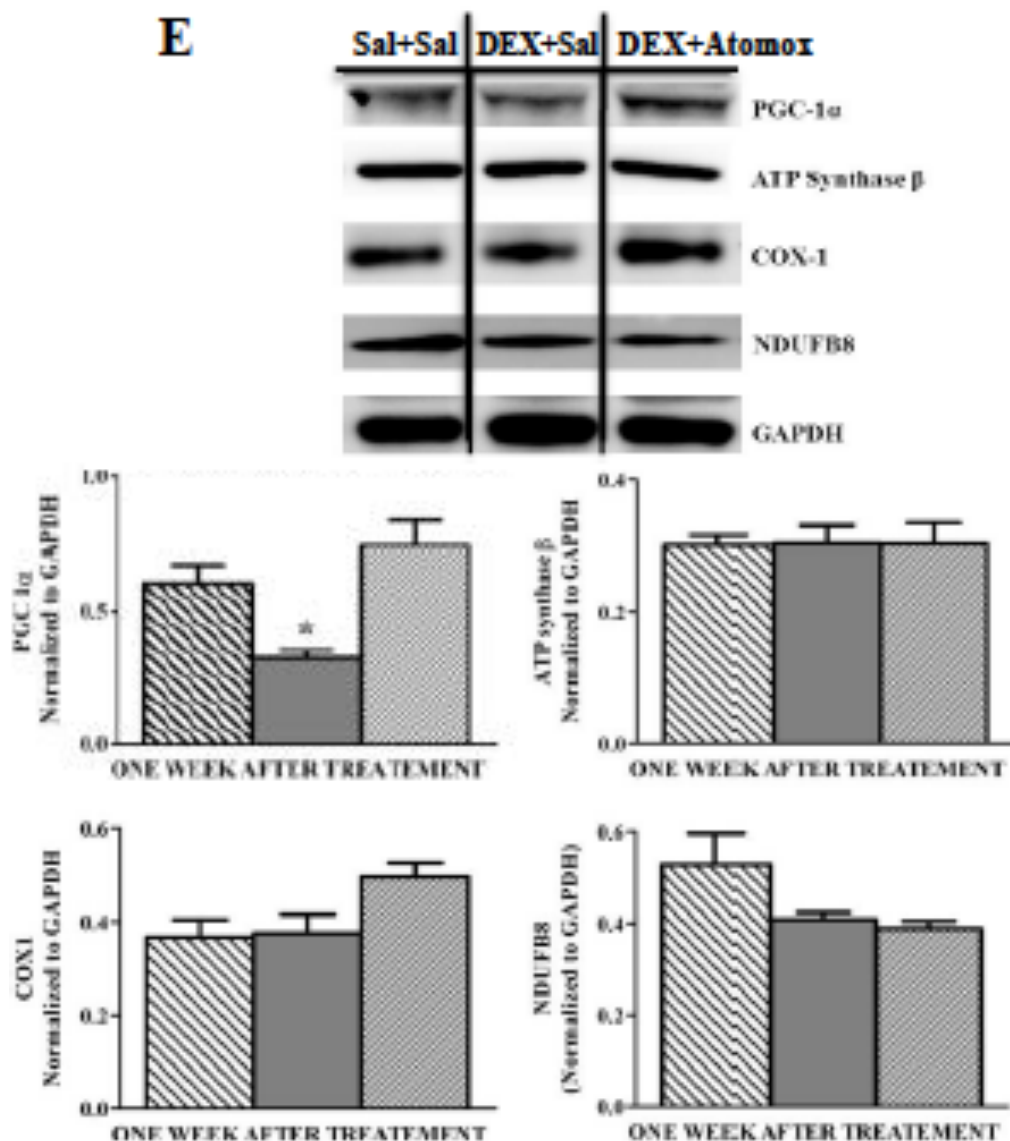


Fig. 4-6E. Chronic effects of atomoxetine and formoterol on skeletal muscle mass and mitochondrial proteins in dexamethasone-treated mice. Mice were co-administered with daily dose of 25 mg/kg water soluble-Dexamethasone \pm 0.3 mg/kg of formoterol / 0.1mg/kg of atomoxetine or sterile saline, i.p. for 7 days. Appropriate saline controls were maintained throughout the experiment. Representative immunoblots and respective densitometry for mitochondrial proteins: Total PGC1 α 1, ATP synthase β , COX-1 and NDUFB8 7 days after atomoxetine (0.1 mg/kg; E). Data were normalized by GAPDH. Data are expressed as mean \pm SE (n = 4-5). * Significantly different from either saline-treated controls or all other groups of mice ($p \leq 0.05$). # Significantly different from dexamethasone-treated mice ($p \leq 0.05$).

IGF-1 gene expression was increased with formoterol in dexamethasone-treated mice despite a significant decrease in PGC-1 α 4 isoform (Figs. 4-7A-B). However, atomoxetine had no effect on PGC-1 α 4, IGF-1, or myostatin in dexamethasone-treated mice (Figs. 4-7A-C). Formoterol and atomoxetine both consistently increased phosphorylation of Akt in dexamethasone-treated mice (Figs. 4-8A-D). However, only formoterol showed increases in Akt phosphorylation and increased mTOR phosphorylation (Fig. 4-8B). Surprisingly, formoterol decreased p-rp S6 and atomoxetine did not affect phosphorylation levels of mTOR and rp S6 (Fig. 4-8A-D). However, formoterol decreased MuRF-1 in dexamethasone-treated mice (Figs. 4-9A). Atomoxetine suppressed MuRF-1 protein expression in dexamethasone-treated mice (Figs. 4-9B).

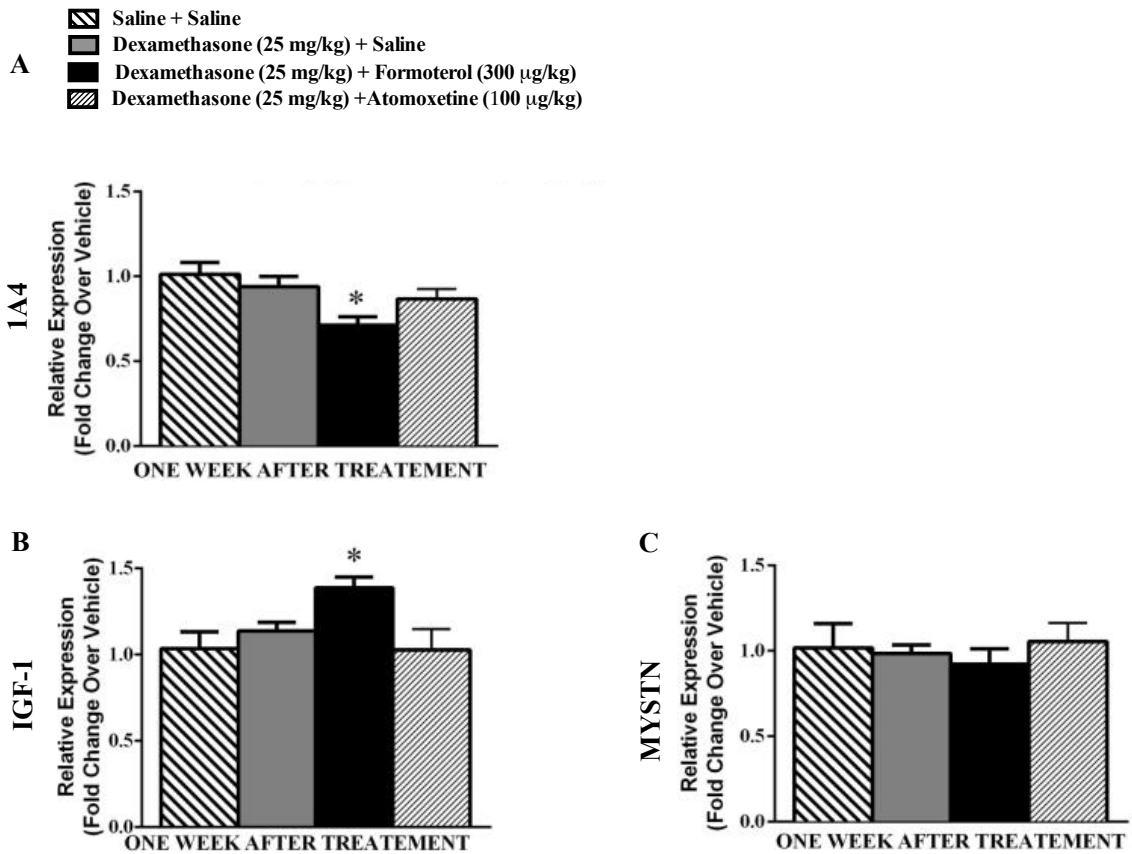
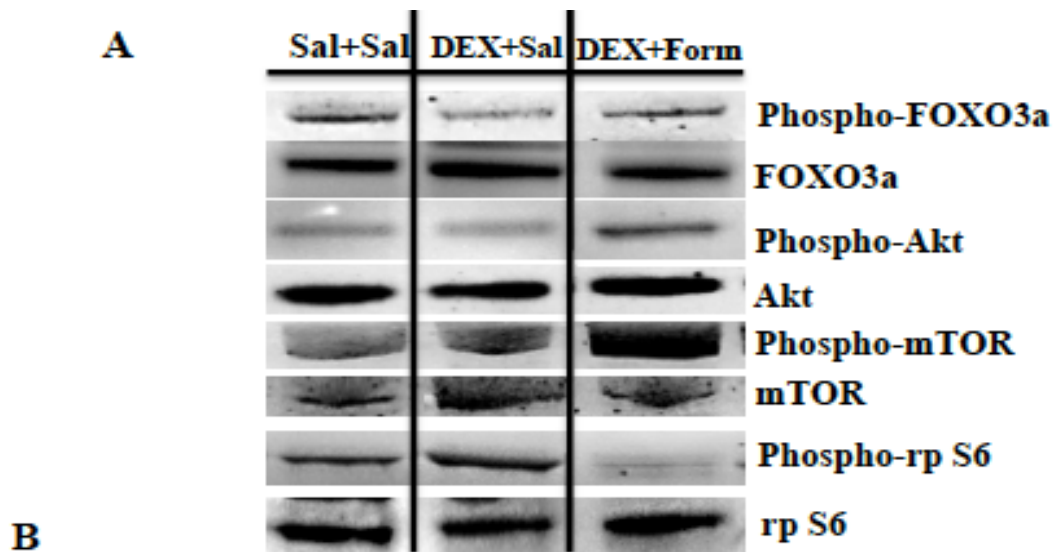


Fig. 4-7. Chronic effects of atomoxetine and formoterol on hypertrophy and atrophy associated proteins in skeletal muscle of dexamethasone-treated mice. Mice were treated as described in Figure 5. qPCR analysis of gene expression for proteins of muscle hypertrophy, PGC-1 α 4 (A) and IGF-1 (B), and atrophy, myostatin (MYSTN) (C). Data were normalized to vehicle and represented as a relative fold change. Data are expressed as mean \pm SE (n = 5). * Significantly different from untreated mice ($p \leq 0.05$).



B

Saline + Saline
 Dexamethasone (25 mg/kg) + Saline
 Dexamethasone (25 mg/kg) + Formoterol (300 µg/kg)

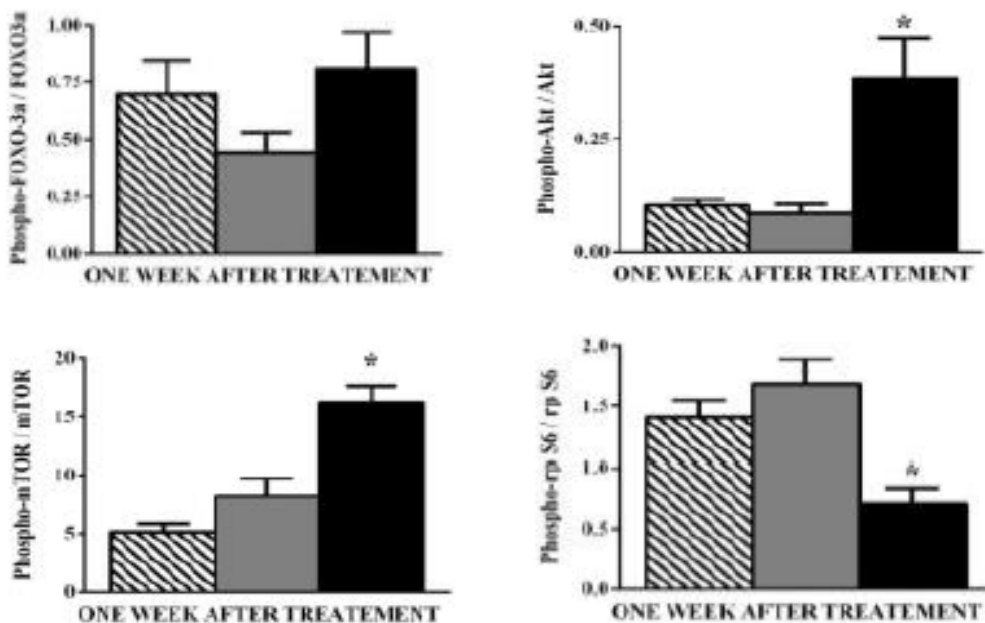


Fig. 4-8A-B. Chronic effects of atomoxetine and formoterol on protein synthesis signaling mechanisms in skeletal muscle of dexamethasone-treated mice. Mice were treated as described in Figure 5. Representative immunoblots and densitometric analysis for markers of muscle protein homeostasis: Total and phosphorylated forms of FoxO3a, Akt, mTOR and ribosomal protein rp S6 at 8 days after respective treatments with either formoterol (BD 0.3 mg/kg; **A, B**). Data were normalized to vehicle and represented as a relative fold change. Data are expressed as mean \pm SE (n = 4-5). * Significantly different from either saline-treated controls or all other groups of mice ($p \leq 0.05$).

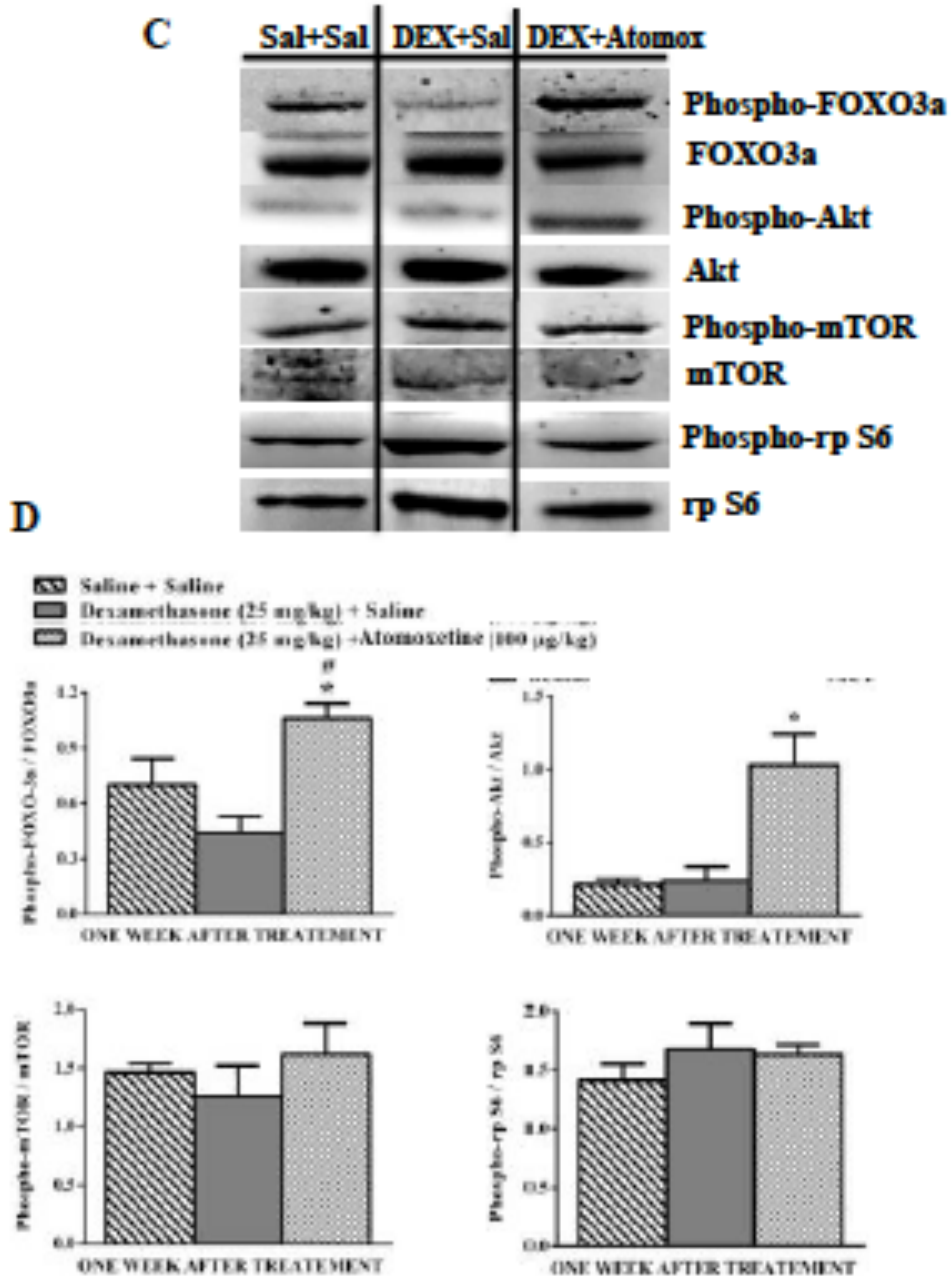


Fig. 4-8C-D Chronic effects of atomoxetine and formoterol on protein synthesis signaling mechanisms in skeletal muscle of dexamethasone-treated mice. Mice were treated as described in Figure 5. Representative immunoblots and densitometric analysis for markers of muscle protein homeostasis: Total and phosphorylated forms of FoxO3a, Akt, mTOR and ribosomal protein rp S6 at 8 days after respective treatments with either formoterol (BD 0.3 mg/kg; **A, B**). Data were normalized to vehicle and represented as a relative fold change. Data are expressed as mean \pm SE ($n = 4-5$). * Significantly different from either saline-treated controls or all other groups of mice ($p \leq 0.05$).

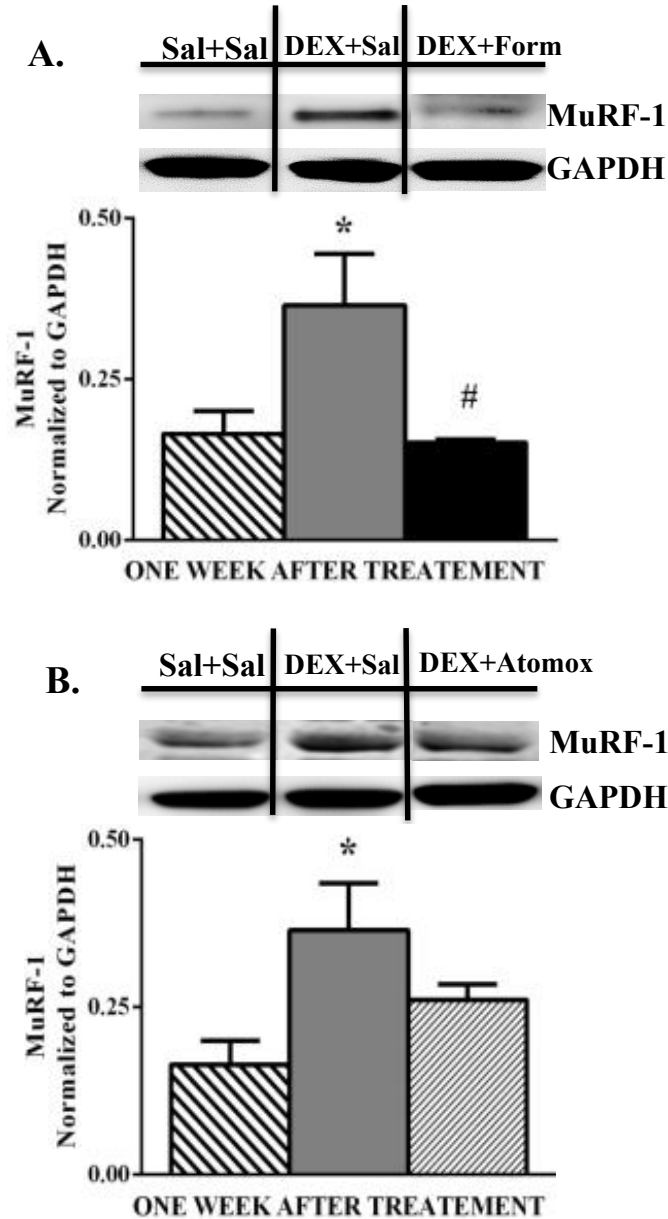


Fig. 4-9. Chronic effects of atomoxetine and formoterol on muscle atrophy markers in skeletal muscle of dexamethasone-treated mice. Mice were treated as described in Figure 5. Representative immunoblots and densitometric analysis for markers of skeletal muscle protein breakdown: MuRF-1 at 7 days after respective treatments with either formoterol (BD 0.3 mg/kg; **A**) or atomoxetine (0.1 mg/kg; **B**). Data were normalized by GAPDH. Data are expressed as mean \pm SE (n = 4-5). * Significantly different from saline-treated controls ($p \leq 0.05$). # Significantly different from dexamethasone-treated mice ($p \leq 0.05$).

DISCUSSION

Recently, alternative splice variants of the PGC-1 α gene have been identified [131]. The PGC-1 α isoforms differ in function due to their respective target set of genes; whereby, induction of the PGC-1 α 1 isoform regulates mitochondrial biogenesis and PGC-1 α 4 induces hypertrophy [131]. A low dose of formoterol (0.3 mg/kg), a long acting β_2 -AR agonist, stimulated alternative splicing of the PGC-1 α gene resulting in an increase in PGC-1 α 4 expression and suppression of PGC-1 α 1. As a result, the discrete gene program associated with PGC-1 α 4 was elicited, the IGF-1–Akt-mTOR-rp S6 axis and suppressed myostatin in the acute naïve animal model. Finally, chronic treatment with formoterol in naïve animals caused skeletal muscle hypertrophy and a similar activation of the Akt-mTOR-rp S6 axis and p-FoxO3a protein expression. Thus, low dose formoterol stimulates anabolism and prevents catabolism in skeletal muscle.

Despite differences in animal models with regards to dose, animal, and tissue type the observed increases in phosphorylation of FoxO3a and the activation of the Akt-mTOR-rp S6 axis is similar to what has been previously reported [239, 243]. Prior to the discovery of the PGC-1 α 4 isoform, Pearen et al. reported an increase in PGC-1 α , now called PGC-1 α 1, gene expression approximately 8 h post treatment with formoterol and no change in myostatin in the tibialis anterior of naïve C57BL/6 mice [238, 239]. In contrast, we determined that the up-regulation in total PGC-1 α (exon 2) gene expression observed at 8 h was driven primarily by PGC-1 α 4 and not the PGC-1 α 1 isoform. Given that PGC-1 α 4 is an inducer of IGF-1 [131], which then functions as a negative regulator of myostatin, myostatin gene expression decreased. The fact that all of the PGC-1 α splice variants

contain EX2, the disparity in the results between our studies and Pearen et al. may be explained by the incorporation of a sequence for exon 2 in the PGC-1 α primer used for their studies. Alternatively, the discrepancy could be the dissimilarities in the model including type of skeletal muscle tissue analyzed.

Recently, we reported that atomoxetine, an FDA approved NRI to treat ADHD, stimulates mitochondrial biogenesis in a high throughput screening assay in renal proximal tubules cells (RPTC) [132] and previous studies have reported that the pharmacological effects of atomoxetine may be through the β -adrenergic receptor system [244, 245]. Subsequent cheminformatic profiling of β_2 -AR agonists nisoxetine and atomoxetine was further carried out and elucidated four chemical moieties which are shared by atomoxetine and formoterol [132]. Despite chemical similarities, neither acute nor chronic treatments with atomoxetine in the naïve animal increased phosphorylated FoxO3a, activated the Akt-mTOR-rp S6 axis, or induced skeletal muscle hypertrophy. In addition, atomoxetine did not appear to modulate PGC-1 α 1/4 gene expression in gastrocnemius muscle, either acutely or chronically. However, in comparison to formoterol there was a similar increase in p-Akt protein expression after chronic treatment with atomoxetine. While the interpretation of this isolated finding is difficult given that there are numerous upstream modulators and downstream effectors of Akt activation [246], Akt phosphorylation is associated with skeletal muscle hypertrophy [227].

Therefore, we can infer from this observation that either atomoxetine is not an activator of the canonical signaling associated with direct β_2 -AR agonist or it elicits downstream signaling through an alternative pathway due to its pharmacological profile as a NRI.

In the atrophy model, treatment with formoterol stimulated muscle hypertrophy and atomoxetine was efficacious in preventing skeletal muscle atrophy. As expected, treatment with dexamethasone suppressed PGC-1 α 1 expression at 8 days; however, concomitant treatment with either formoterol or atomoxetine maintained PGC-1 α 1 levels equal to that of controls. Despite sustained expression of PGC-1 α 1, there was no evidence for mitochondrial biogenesis. It is important to note that PGC-1 α 1 and p-Akt prevent the de-phosphorylation of p-FoxO3a; thereby, limiting its entry to the nucleus and operating as a transcription factor to induce transcription of MuRF-1 [233]. This is supported by the observed increase in p-FoxO3a and decreased MURF-1 protein expression post treatment with either atomoxetine or formoterol as compared to dexamethasone treatment alone, further supporting evidence that atomoxetine possesses anti-atrophic properties. Finally, a summary diagram illustrating our findings in the dexamethasone study are summarized for both formoterol (Fig. 10) and atomoxetine (Fig. 11).

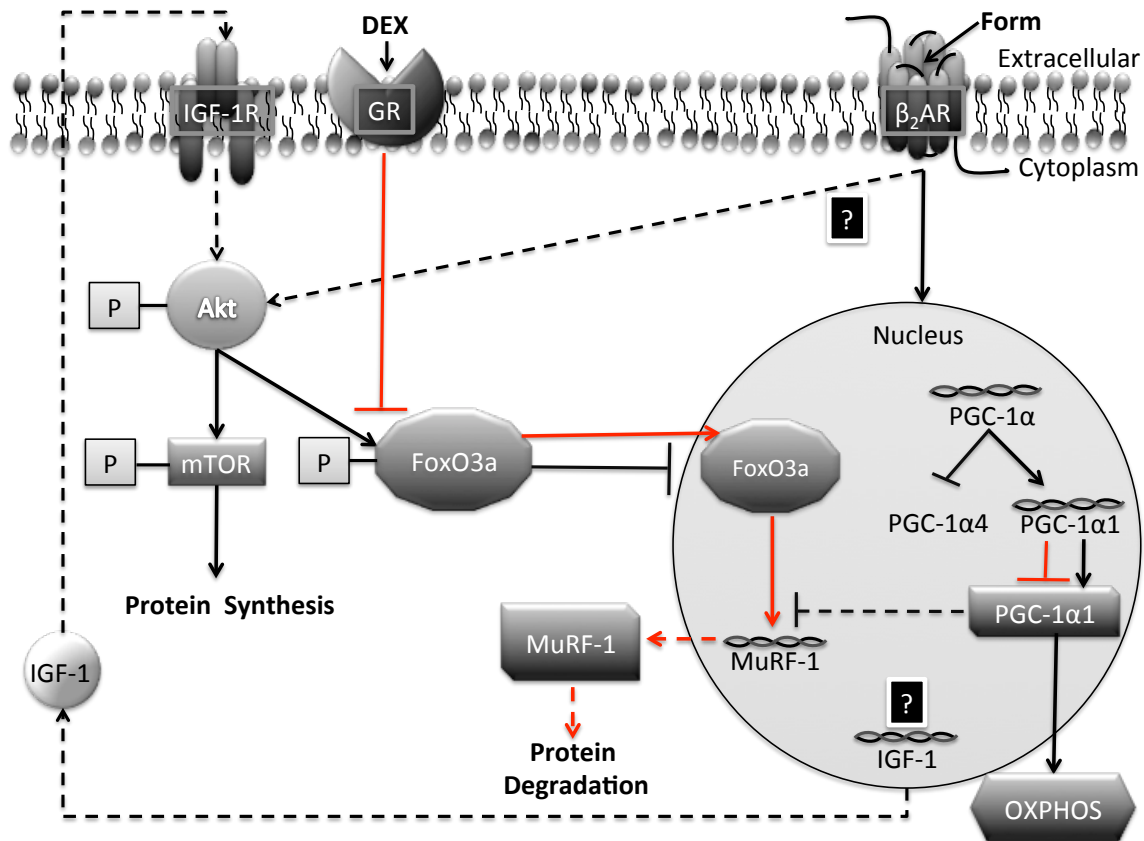


Fig. 10. Proposed mechanisms preventing muscle atrophy associated with chronic treatment of formoterol in skeletal muscle of dexamethasone-treated mice. This diagram depicts the changes observed in gene and protein expression following chronic treatment with formoterol (Form) in skeletal muscle of dexamethasone (DEX)-treated mice. Chronic treatment with formoterol sustained PGC-1 α 1 gene and protein expression leading to an increase in OXPHOS proteins. IGF-1 gene expression is increased, but it is unclear what is driving expression (denoted by “question mark” above IGF-1 gene). Formoterol was capable of sustaining an increase in the phosphorylation status of the Akt-mTOR axis, indicating activation and a possible mechanism for protein synthesis. We report concomitant inactivation of FoxO3a, depicted by increased phosphorylation with suppression of MuRF-1 gene expression, potentially blocking a major mechanism for protein degradation. In addition, the increase in PGC-1 α 1 observed with treatment may also be responsible for blocking the transcription of MuRF-1 and represent an anti-atrophic mechanism. The red lines shown are the proposed mechanisms for protein degradation in our study via treatment with dexamethasone. Solid shapes represent proteins (name displayed in white), helices within the nucleus represent genes (name displayed in black below helices), solid black lines are pathways conferred by our data, and dotted lines are potential pathways not evaluated by our study. Akt phosphorylation can result from numerous downstream interactions associated with the activation of the β_2 -AR, which were not evaluated by our study. Therefore, we do not know what else might play a role in phosphorylating Akt represented by a “question mark” and a dotted line. Lines that are blunted at the end represent inhibition.

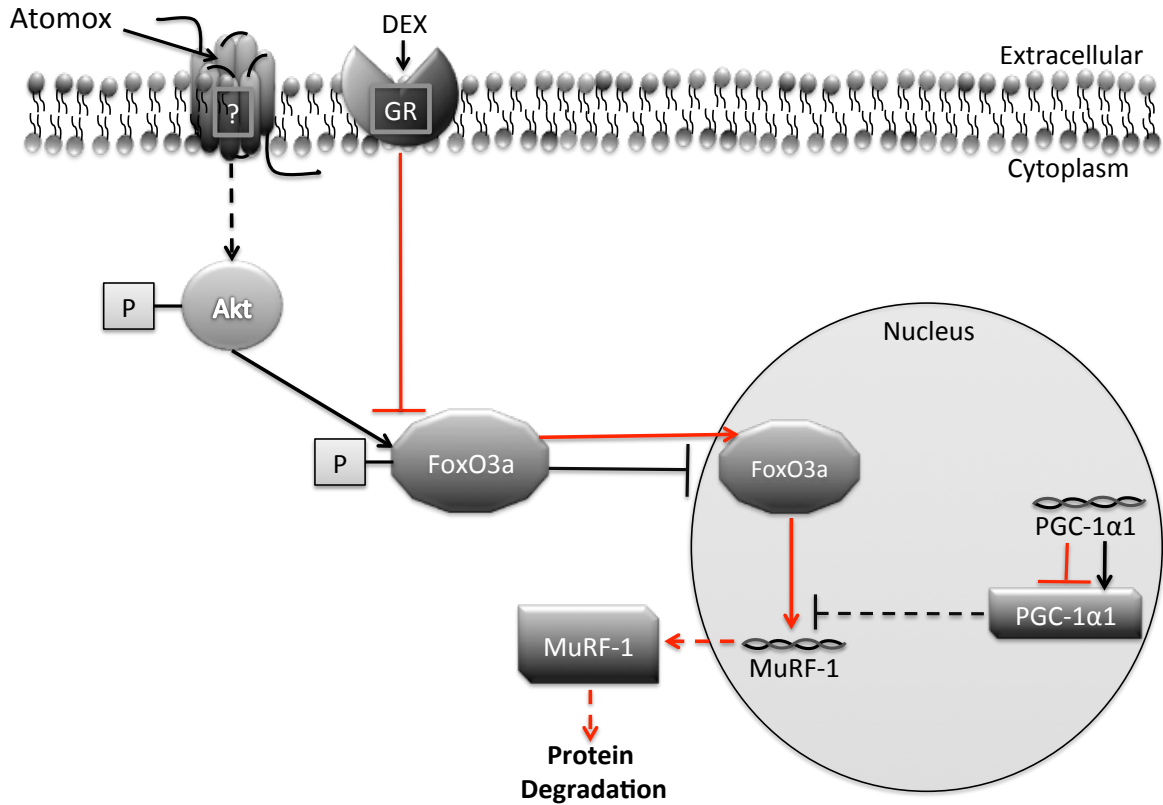


Fig. 11. Proposed mechanisms preventing muscle atrophy associated with chronic treatment of atomoxetine in skeletal muscle of dexamethasone-treated mice. This diagram depicts the changes observed in gene and protein expression following chronic treatment with atomoxetine (Atomox) in skeletal muscle of dexamethasone (DEX)-treated mice. Atomoxetine is capable of sustaining p-Akt, but not activating the entire axis. We report concomitant inactivation of FoxO3a, depicted by increased phosphorylation with suppression of MuRF-1 gene expression, potentially blocking a major mechanism for protein degradation. In addition, the increase in PGC-1 α 1 observed with Atomox treatment may also be responsible for blocking the transcription of MuRF-1 and represent an anti-atrophic mechanism. The red lines shown are the proposed mechanisms for protein degradation in our study via treatment with dexamethasone. Solid shapes represent proteins (name displayed in white), helices within the nucleus represent genes (name displayed in black below helices), solid black lines are pathways conferred by our data, and dotted lines are potential pathways not evaluated by our study. Akt phosphorylation can result from numerous downstream interactions associated with the activation of the β_2 -AR or the unidentified receptor for Atomox, which are not evaluated by our study. Therefore, we do not know what else might play a role in phosphorylating Akt and chose to represent this interaction with “question mark” and a dotted line. Lines that are blunted at the end represent inhibition.

Since atomoxetine is a NRI and norepinephrine has been demonstrated to modulate PGC-1 α 1 through the β ₂-AR [101], it is plausible that indirect β ₂-AR agonism of atomoxetine through norepinephrine as a possible mechanism for our observed results. However, norepinephrine is a less potent stimulator of the β ₂-AR than formoterol and the downstream signaling events may be more susceptible to internal regulation. This would explain the lack of observable changes in the naïve models.

In summary, the present study identifies formoterol as a potent inducer of skeletal muscle hypertrophy, which is associated with concomitant increases in PGC-1 α 4 and IGF-1, down regulation of myostatin, and activation of the Akt-mTOR-rp S6 axis. Formoterol also prevented catabolism, as evident by a decrease in MuRF-1. In addition, we report atomoxetine, used at a dose lower than what is clinically approved for ADHD, was efficacious in the prevention of skeletal muscle atrophy in a model of dexamethasone induced muscle atrophy. Furthermore, atomoxetine prevented muscle atrophy through sustained PGC-1 α 1 expression, Akt activation, increased p-FoxO3a and subsequent decrease in MuRF-1 protein expression.

While β ₂-AR agonists are potent catabolic agents, their potential clinical success to combat skeletal muscle atrophy is blunted by their potential side effects of altering cardiac muscle structure and function [239, 247-249]. In the naïve model, atomoxetine was unable to stimulate skeletal muscle hypertrophy. In addition, we report in the atrophy model that atomoxetine is not catabolic, but rather anti-atrophic.

These characteristics in combination with the hypertrophic cardiovascular events associated with formoterol makes atomoxetine a potential drug to prevent skeletal muscle atrophy.

Chapter 5:

CONCLUSIONS AND FUTURE DIRECTIONS

CONCLUSIONS

Acute kidney injury is characterized by a decrease in renal organ function. Injury to the proximal tubule epithelium is a primary component of AKI contributing to overall organ deterioration. Subcellular damage to the epithelium's mitochondria is a major pathophysiological mechanism driving the presence of malfunctioning proximal tubules. Successful recovery of renal function post AKI is dependent on restoration of the tubular epithelium. Thus, the mitochondrion represents a fundamental biological target upon which therapies can be developed for the improvement of renal function post AKI.

Studies simulating sublethal oxidant injury with the model oxidant TBHP in RPTC have established that within 24 h of injury mitochondrial function is maximally declined and slowly recovers over 6 days [128]. In addition, this study determined that overexpression of PGC-1 α in RPTC after injury accelerated recovery of mitochondrial and cellular functions, inferring the process of mitochondrial biogenesis is crucial to the successful recovery of injured cells [128]. A follow-up study was performed using the same oxidant model followed by post-treatment with the sirtuin 1 (SIRT1) activator and inducer of mitochondrial biogenesis, SRT1720. This compound was reported to accelerate the recovery of mitochondrial and

cellular function following oxidant injury [126]. Furthermore, in vivo experiments using two non-lethal rodent models inducing AKI, confirmed that there is a persistent disruption of mitochondrial homeostasis and sustained tubular damage after AKI 6 days after injury, even in the presence of mitochondrial recovery signals and improved glomerular filtration [95]. Despite the diverse nature of these approaches their findings support the hypothesis that the recovery of mitochondrial function is central to the overall restoration of cell structure and function in AKI. Given that no therapy currently exists in the clinic to promote recovery of kidney function, these novel findings established mitochondrial-targeted therapy, specifically the biogenic machinery, as a promising approach to restoring kidney function after acute kidney injury.

Very few pharmacological agents have been identified that can stimulate mitochondrial biogenesis. Therefore, our laboratory executed a drug discovery program to identify pharmacological compounds capable of inducing mitochondrial biogenesis. As part of this program, a unique high throughput screen was developed, which utilized primary RPTC and the Seahorse Biosciences extracellular flux analyzer (XF96) to evaluate the Sigma 1280 compound Library of Pharmacologically Active Compounds (LOPAC).

From this screen our laboratory identified multiple molecular hits. In particular, one of the hits was further investigated based on the receptor it targeted, the A₁ AR. We explored both agonists and antagonists of the A₁ AR and concluded that only

the agonists were capable of stimulating mitochondrial biogenesis. Interestingly, we determined that the A₁ AR partial agonist CVT-2759, at a lower dose, was more efficacious in the promotion of mitochondrial biogenesis than the full agonist CCPA. This is a significant finding as it not only demonstrates the G_{i/o} receptor family as being capable of stimulating mitochondrial biogenesis, but additionally because it describes fine biochemical tuning to maximize the response with CVT-2759, an agent that is also superior to CCPA to in its side effect profile. Given the complex and arduous nature of the characterization process for these compounds, our efforts were put into formoterol; one of the most potent hits identified from this screen to further develop and evaluate in an I/R induced model of AKI. However, we can conclude from these studies involving CCPA and formoterol that our drug discovery approach is effective in identifying pharmacological agents capable of stimulating mitochondrial biogenesis and with that comes the identification of relevant biological drug targets.

As previously described, formoterol is a specific long-acting β_2 -AR agonist approved by the FDA to treat asthma. Validation studies using RPTC revealed that low nanomolar doses of formoterol were potent for stimulating mitochondrial biogenesis [159]. In addition, further in vivo validation for mitochondrial biogenesis was achieved when male C57BL/6 mice were exposed to a single formoterol dose (0.1 mg/kg) over a 24 h time period and had a robust increase in mitochondrial biogenic machinery [159]. This effect was blocked in vitro when pretreated with both a non-specific β -AR and specific β_2 -AR antagonist [159].

The conclusion from these results was that formoterol, through the β_2 -AR, is a potent inducer of mitochondrial biogenesis in RPTC and healthy mice.

The aforementioned findings lead us to execute a series of experiments evaluating the efficacy of formoterol to restore kidney function after insult in an established model of I/R induced AKI. As reported in Chapter 3, treatment with formoterol restored renal function, rescued renal tubules from injury, and diminished necrosis after I/R-induced AKI. Concomitantly, formoterol stimulated mitochondrial biogenesis and restored the expression and function of mitochondrial proteins.

Ultimately, from these data we successfully the proof of principle that a novel drug therapy to treat AKI, and potentially other acute organ failures, works by restoring mitochondrial function and accelerating the recovery of renal function after injury has occurred.

There are many other conclusions and new questions that can be derived from this work. To start we have validated that normophysiological mechanisms, which stimulate the mitochondrial biogenesis process, can be used for target identification and exploited pharmacologically to stimulate biogenesis. For example, it is established that cold exposure, in mammals, triggers a thermogenic response involving catecholamine-mediated activation the β -AR family of GPCRs, which subsequently stimulates the mitochondrial biogenic machinery. Thus, given the mechanism of action associated with formoterol we have confirmed the β_2 -AR as a viable target for future drug discovery efforts aimed at rapid recovery from

maximal renal dysfunction. Beyond target validation, we have established a point of origin for drug development whereby the formoterol pharmacophore now serves as a lead chemical structure that can be optimized through medicinal chemistry in obtainment of a novel molecular agent with greater efficacy.

With regards to our target, the β_2 -AR, it can be concluded that it plays a major role in orchestrating cellular repair responses, as evident by the robust down regulation of KIM-1. Since KIM-1 is a sensitive and highly selective biomarker for proximal tubule injury, it is reasonable to infer that the associated repair mechanism(s) is responsible for recovery of overall renal function. Though mitochondrial biogenesis occurs concomitantly with renal repair, it is important to note that at this time our data is corollary and not causal. Therefore, “opening the doors” for future discovery elucidating how the signaling from the β_2 -AR stimulates recovery mechanisms decreasing KIM-1 expression and if those mechanisms are dependent on mitochondrial biogenesis. Thereby potentially identifying new biological drug targets.

Finally, previous studies established formoterol as an effective agent against skeletal muscle hypertrophy and the proposed mechanism was thought to be through mitochondrial biogenesis. A recent study published by our laboratory identified the structure of atomoxetine, an FDA approved NRI, to be composed of essential moieties capable of mitochondrial biogenesis. Therefore, we tested if atomoxetine was capable of also capable of preventing skeletal muscle atrophy.

We concluded that formoterol selectively induces PGC-1 α isoform expression in a tissue specific and time dependent manner. In contrast to renal cortical tissue, skeletal muscle responded to acute treatment with formoterol by robustly inducing the expression of the PGC-1 α 4 isoform upon acute exposure to formoterol, which executed a discrete gene program resulting in skeletal muscle hypertrophy. We determined that hypertrophy was mediated through the induction of IGF-1 and suppression of myostatin and not mitochondrial biogenesis. Concomitantly, there was no change in expression of OXPHOS components. Therefore, we concluded that short-term exposure to formoterol (i.e.-24 h) does not alter skeletal muscle metabolism. However, in response to chronic formoterol exposure (i.e.-7 days) skeletal muscle induces mitochondrial biogenic components such as PGC-1 α 1 and components of the OXPHOS system. Therefore, long-term exposure to formoterol may affect metabolism. We were also able to determine that chronic formoterol exposure does not only produce hypertrophy, but is also anti-atrophic as PGC-1 α 1 expression may also be working within a pathway involving Akt activation, increased p-FoxO3a and subsequent decrease in MuRF-1 protein expression. These mechanisms are beneficial in the prevention of skeletal muscle atrophy.

However, because formoterol is both hypertrophic and anti-atrophic it is associated with deleterious side effects such as cardiac hypertrophy. Alternatively, we proposed that chronic treatment with atomoxetine prevented skeletal muscle atrophy through the PGC-1 α 1 expression may also be working within a pathway involving Akt activation, increased p-FoxO3a and subsequent decrease in MuRF-1

protein expression PGC-1 α 1 and p-Akt prevent the de-phosphorylation of p-FoxO3a; thereby, limiting its entry to the nucleus and operating as a transcription factor to induce transcription of MuRF-1.

FUTURE DIRECTION

Gene expression experiments have been carried out in the I/R animal groups described in chapter 2, which shows a marginal increase in transcriptional expression of total PGC-1 α in the I/R + formoterol vs. I/R + vehicle groups, and insignificant differences between gene expression of NDUFB8 and COX I in the I/R animals (Fig. 5-1), but a complete restoration of NDUFB8 and COX I protein expression only in I/R animals subjected to formoterol treatment (Fig. 3-3) suggest that post-transcriptional modification(s) preventing protein translation and not transcriptional regulation, as a possible mechanism driving the disparity in ETC protein expression.

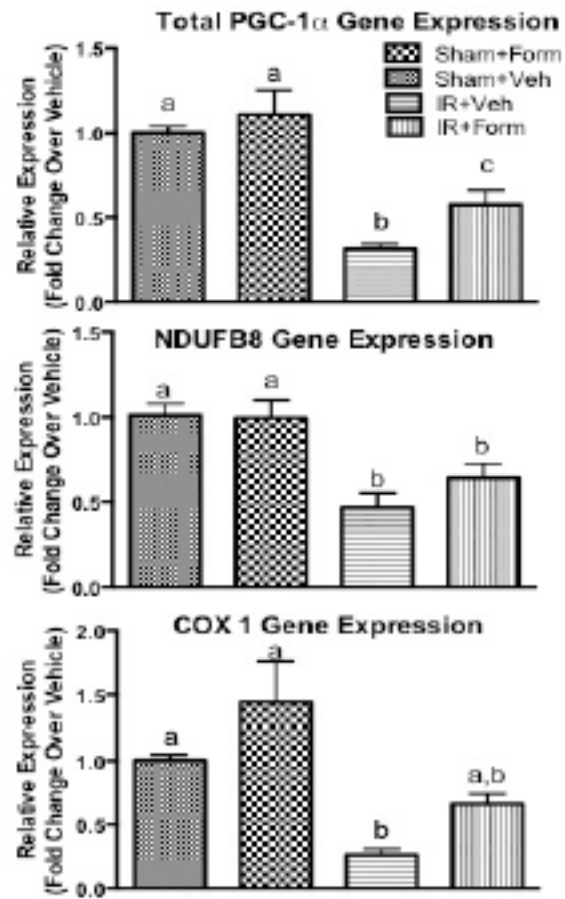


Fig. 5-1. Formoterol restores ETC protein expression and mitochondrial function after I/R injury. Mice were treated with formoterol (0.3 mg/kg) i.p. daily for five days starting 24 h after I/R euthanized at 144 h post surgery. Gene expression of PGC-1 α , NDUFB8, and COX I were assessed in the kidney via RT-PCR. P<0.5, N=6.

A possible post-transcriptional modification is the presence of microRNA (miRNA) targeting of NDUFB8 and COX I mRNA in the I/R + vehicle group, preventing protein translation. There are hundreds of miRNAs that have been defined in the literature, which decrease ETC subunit protein expression. Picking the correct one to evaluate is complex. Similar results, with regards to a decrease in COX I gene expression in the presence of normal to high protein expression, were obtained in cardiomyocytes when miR181c was over expressed [250]. It has also been shown that miR210 degrades NDUFB8 expression [251]. However, evaluation of expression of either of these isoforms in 144 h post I/R injury in tissue samples revealed there was no change in miR expression (Fig. 5-2). Future experiments should be carried out, which are more comprehensive in design and seek to obtain a comprehensive analysis of possible miR targets.

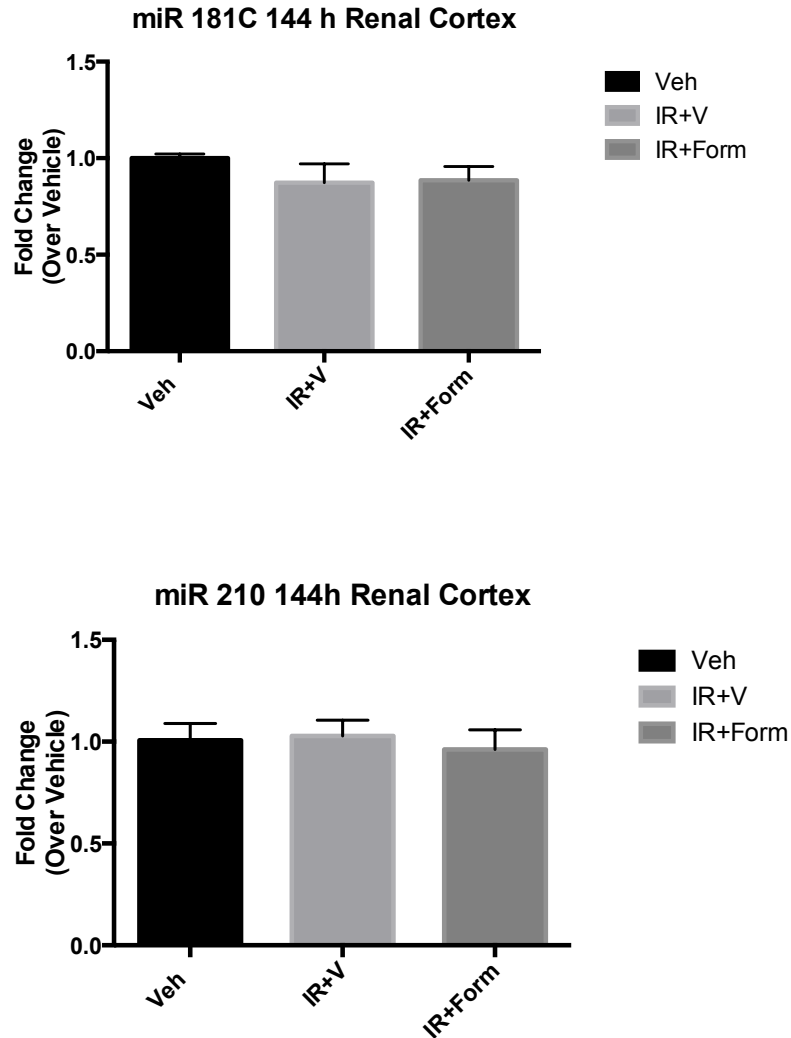


Fig. 5-2. miR181c and miR210 expression after I/R injury. Mice were treated with formoterol (0.3 mg/kg) i.p. daily for five days starting 24 h after I/R euthanized at 144 h post surgery. Gene expression of miR181c and miR210 were assessed in the kidney via qPCR. $P < 0.5$, $N = 6$.

Despite 5 days of reperfusion post ischemic insult, chronic hypoxia may still exist as defined by the chronic hypoxia hypothesis formulated by Fine et al [252]. Their hypothesis postulated that primary glomerular injury leads to reduced post-glomerular flow, which culminates in peritubular capillary loss. This creates a hypoxic environment that produces a fibrotic response that further propagates injury by affecting adjacent unaffected capillaries [252]. In hypoxic physiologic conditions, such as ischemia, the hypoxia-inducible factor 1 alpha (HIF-1 α) separates from its binding partner the von Hippel-Lindau (VHL) protein, becomes activated, and promotes the synthesis of the mitochondrial protease LON. It is established in the literature that LON expression is induced by activation of HIF-1 α during hypoxia and is known to degrade the COX I subunit of complex IV in the ETC, while increasing the expression of COX 2 [253]. The lab of Gregg Semenza hypothesize this phenomenon to be a pro-survival mechanism which allows optimization of electron transfer through and reduction of reactive oxygen species (ROS) from the ETC [253]. In addition, miR181c activity also causes a shift from COX I to COX 2 protein expression [250]. This mechanism may also explain the reduction observed in NDUFB8 expression post I/R injury. Therefore, LON and HIF-1 α expression was evaluated in 144 h renal cortical lysate samples and there was no change in LON and a complete depletion of the HIF-1 α protein in the I/R + veh group (5-3). Given the results from the miR181c experiments and those on Fig. 5-3, this pathway should not be further evaluated, but future experiments should confirm the results with the HIF-1 α protein data, as this is the opposite of what one would expect. However, degradation by proteases or the proteasome should not be ruled out.

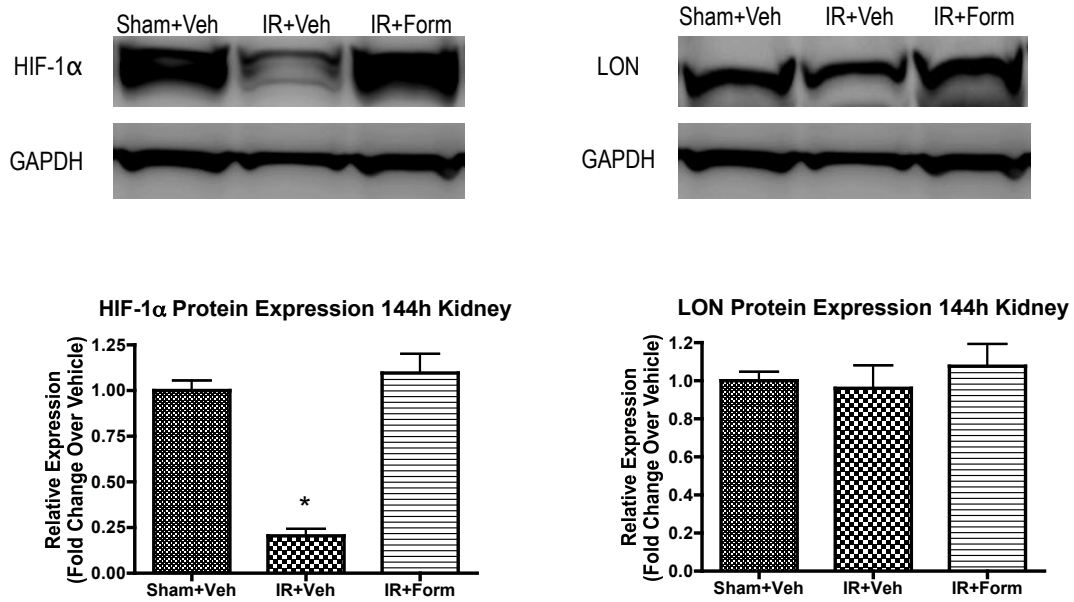


Fig. 5-3. LON and HIF-1 α expression after I/R injury. Mice were treated with formoterol (0.3 mg/kg) i.p. daily for five days starting 24 h after I/R euthanized at 144 h post surgery. Gene expression of miR181c and miR210 were assessed in the kidney via qPCR. $P < 0.5$, $N = 6$.

Several groups have shown PGC-1 α to be degraded by the proteasome during times of oxidative stress. Previous work in our laboratory has shown the half-life of PGC-1 α to be approximately 37 min, however, degradation is dependent on post-translational modifications [254]. Even though the abundance in genes or proteins of PGC-1 α in the presence of I/R + vehicle versus I/R + formoterol was equal, blocking protein translation and evaluating PGC-1 α protein expression can provide insight not only into if gene expression or proteasomal degradation is responsible for accumulation, but also why the presence of ETC proteins are higher in animals treated with formoterol after I/R injury. Further analysis focusing on the degradation of NDUFB and COX I should be carried out to elucidate if the accumulation in these proteins is regulated by mechanisms other than the state of PGC-1 α and canonical mitochondrial biogenesis signaling.

LIST OF REFERENCES

1. DiPiro, J.T., *Pharmacotherapy : a pathophysiologic approach*. 7th ed. 2008, New York: McGraw-Hill Medical. xxxii, 2559 p.
2. Lote, C.J., *Principles of renal physiology*. 5th ed. 2012, New York: Springer. xv, 204 p.
3. Reilly, R.F. and D.H. Ellison, *Mammalian distal tubule: physiology, pathophysiology, and molecular anatomy*. *Physiol Rev*, 2000. **80**(1): p. 277-313.
4. Brenner, B.M., *Functional and structural determinants of glomerular filtration. A brief historical perspective*. *Fed Proc*, 1977. **36**(12): p. 2599-601.
5. Vallon, V., C. Miracle, and S. Thomson, *Adenosine and kidney function: potential implications in patients with heart failure*. *Eur J Heart Fail*, 2008. **10**(2): p. 176-87.
6. Jankowski, M., *Purinergic regulation of glomerular microvasculature and tubular function*. *J Physiol Pharmacol*, 2008. **59 Suppl 9**: p. 121-35.
7. Wright, E.M., D.D. Loo, and B.A. Hirayama, *Biology of human sodium glucose transporters*. *Physiol Rev*, 2011. **91**(2): p. 733-94.
8. Jamison, R.L., *Short and long loop nephrons*. *Kidney Int*, 1987. **31**(2): p. 597-605.
9. Layton, A.T., et al., *The mammalian urine concentrating mechanism: hypotheses and uncertainties*. *Physiology (Bethesda)*, 2009. **24**: p. 250-6.
10. Bellomo, R., J.A. Kellum, and C. Ronco, *Acute kidney injury*. *Lancet*, 2012. **380**(9843): p. 756-66.
11. Hoste, E.A., et al., *The epidemiology of cardiac surgery-associated acute kidney injury*. *Int J Artif Organs*, 2008. **31**(2): p. 158-65.
12. Kunzendorf, U., et al., *Novel aspects of pharmacological therapies for acute renal failure*. *Drugs*, 2010. **70**(9): p. 1099-114.
13. Ricci, Z., D. Cruz, and C. Ronco, *The RIFLE criteria and mortality in acute kidney injury: A systematic review*. *Kidney Int*, 2008. **73**(5): p. 538-46.
14. Rewa, O. and S.M. Bagshaw, *Acute kidney injury-epidemiology, outcomes and economics*. *Nat Rev Nephrol*, 2014. **10**(4): p. 193-207.
15. Susantitaphong, P., et al., *World incidence of AKI: a meta-analysis*. *Clin J Am Soc Nephrol*, 2013. **8**(9): p. 1482-93.
16. Kellum, J.A., R. Bellomo, and C. Ronco, *Kidney attack*. *JAMA*, 2012. **307**(21): p. 2265-6.
17. Shusterman, N., et al., *Risk factors and outcome of hospital-acquired acute renal failure. Clinical epidemiologic study*. *Am J Med*, 1987. **83**(1): p. 65-71.
18. Chertow, G.M., et al., *Acute kidney injury, mortality, length of stay, and costs in hospitalized patients*. *J Am Soc Nephrol*, 2005. **16**(11): p. 3365-70.
19. Pannu, N. and M.K. Nadim, *An overview of drug-induced acute kidney injury*. *Crit Care Med*, 2008. **36**(4 Suppl): p. S216-23.
20. Bentley, M.L., H.L. Corwin, and J. Dasta, *Drug-induced acute kidney injury in the critically ill adult: recognition and prevention strategies*. *Crit Care Med*, 2010. **38**(6 Suppl): p. S169-74.

21. Brown, J.R. and C.A. Thompson, *Contrast-induced acute kidney injury: the at-risk patient and protective measures*. *Curr Cardiol Rep*, 2010. **12**(5): p. 440-5.
22. McCullough, P.A., *Contrast-induced acute kidney injury*. *J Am Coll Cardiol*, 2008. **51**(15): p. 1419-28.
23. Nash, K., A. Hafeez, and S. Hou, *Hospital-acquired renal insufficiency*. *Am J Kidney Dis*, 2002. **39**(5): p. 930-6.
24. Streetman, D.S., et al., *Individualized pharmacokinetic monitoring results in less aminoglycoside-associated nephrotoxicity and fewer associated costs*. *Pharmacotherapy*, 2001. **21**(4): p. 443-51.
25. Slaughter, R.L. and D.M. Cappelletty, *Economic impact of aminoglycoside toxicity and its prevention through therapeutic drug monitoring*. *Pharmacoeconomics*, 1998. **14**(4): p. 385-94.
26. Heyman, S.N., et al., *Early renal medullary hypoxic injury from radiocontrast and indomethacin*. *Kidney Int*, 1991. **40**(4): p. 632-42.
27. Schneider, V., et al., *Association of selective and conventional nonsteroidal antiinflammatory drugs with acute renal failure: A population-based, nested case-control analysis*. *Am J Epidemiol*, 2006. **164**(9): p. 881-9.
28. Arany, I. and R.L. Safirstein, *Cisplatin nephrotoxicity*. *Semin Nephrol*, 2003. **23**(5): p. 460-4.
29. Kawai, Y., et al., *Relationship of intracellular calcium and oxygen radicals to Cisplatin-related renal cell injury*. *J Pharmacol Sci*, 2006. **100**(1): p. 65-72.
30. Dobyas, D.C., et al., *Mechanism of cis-platinum nephrotoxicity: II. Morphologic observations*. *J Pharmacol Exp Ther*, 1980. **213**(3): p. 551-6.
31. Sutton, T.A., C.J. Fisher, and B.A. Molitoris, *Microvascular endothelial injury and dysfunction during ischemic acute renal failure*. *Kidney Int*, 2002. **62**(5): p. 1539-49.
32. Laberke, H.G. and A. Bohle, *Acute interstitial nephritis: correlations between clinical and morphological findings*. *Clin Nephrol*, 1980. **14**(6): p. 263-73.
33. Thadhani, R., M. Pascual, and J.V. Bonventre, *Acute renal failure*. *N Engl J Med*, 1996. **334**(22): p. 1448-60.
34. Liano, F. and J. Pascual, *Epidemiology of acute renal failure: a prospective, multicenter, community-based study*. *Madrid Acute Renal Failure Study Group*. *Kidney Int*, 1996. **50**(3): p. 811-8.
35. Bonventre, J.V. and L. Yang, *Cellular pathophysiology of ischemic acute kidney injury*. *J Clin Invest*, 2011. **121**(11): p. 4210-21.
36. Devarajan, P., *Update on mechanisms of ischemic acute kidney injury*. *J Am Soc Nephrol*, 2006. **17**(6): p. 1503-20.
37. Le Dorze, M., et al., *The role of the microcirculation in acute kidney injury*. *Curr Opin Crit Care*, 2009. **15**(6): p. 503-8.
38. Karlberg, L., et al., *Impaired medullary circulation in postischemic acute renal failure*. *Acta Physiol Scand*, 1983. **118**(1): p. 11-7.
39. Mason, J., J. Torhorst, and J. Welsch, *Role of the medullary perfusion defect in the pathogenesis of ischemic renal failure*. *Kidney Int*, 1984. **26**(3): p. 283-93.
40. Conger, J., *Hemodynamic factors in acute renal failure*. *Adv Ren Replace Ther*, 1997. **4**(2 Suppl 1): p. 25-37.
41. Brooks, D.P., *Role of endothelin in renal function and dysfunction*. *Clin Exp*

- Pharmacol Physiol, 1996. **23**(4): p. 345-48.
42. Kurata, H., et al., *Protective effect of nitric oxide on ischemia/reperfusion-induced renal injury and endothelin-1 overproduction*. Eur J Pharmacol, 2005. **517**(3): p. 232-9.
 43. da Silveira, K.D., et al., *ACE2-angiotensin-(1-7)-Mas axis in renal ischaemia/reperfusion injury in rats*. Clin Sci (Lond), 2010. **119**(9): p. 385-94.
 44. Kwon, O., S.M. Hong, and G. Ramesh, *Diminished NO generation by injured endothelium and loss of macula densa nNOS may contribute to sustained acute kidney injury after ischemia-reperfusion*. Am J Physiol Renal Physiol, 2009. **296**(1): p. F25-33.
 45. Kelly, K.J., et al., *Intercellular adhesion molecule-1-deficient mice are protected against ischemic renal injury*. J Clin Invest, 1996. **97**(4): p. 1056-63.
 46. Bonventre, J.V. and A. Zuk, *Ischemic acute renal failure: an inflammatory disease?* Kidney Int, 2004. **66**(2): p. 480-5.
 47. Kimura, T., et al., *Autophagy protects the proximal tubule from degeneration and acute ischemic injury*. J Am Soc Nephrol, 2011. **22**(5): p. 902-13.
 48. Bagnasco, S., et al., *Lactate production in isolated segments of the rat nephron*. Am J Physiol, 1985. **248**(4 Pt 2): p. F522-6.
 49. Bonventre, J.V. and J.M. Weinberg, *Recent advances in the pathophysiology of ischemic acute renal failure*. J Am Soc Nephrol, 2003. **14**(8): p. 2199-210.
 50. Bonventre, J.V., *Mechanisms of ischemic acute renal failure*. Kidney Int, 1993. **43**(5): p. 1160-78.
 51. Sutton, T.A. and B.A. Molitoris, *Mechanisms of cellular injury in ischemic acute renal failure*. Semin Nephrol, 1998. **18**(5): p. 490-7.
 52. Bush, K.T., S.H. Keller, and S.K. Nigam, *Genesis and reversal of the ischemic phenotype in epithelial cells*. J Clin Invest, 2000. **106**(5): p. 621-6.
 53. Brown, D., R. Lee, and J.V. Bonventre, *Redistribution of villin to proximal tubule basolateral membranes after ischemia and reperfusion*. Am J Physiol, 1997. **273**(6 Pt 2): p. F1003-12.
 54. Molitoris, B.A., R. Dahl, and A. Geerdes, *Cytoskeleton disruption and apical redistribution of proximal tubule Na(+)-K(+)-ATPase during ischemia*. Am J Physiol, 1992. **263**(3 Pt 2): p. F488-95.
 55. Heyman, S.N., C. Rosenberger, and S. Rosen, *Experimental ischemia-reperfusion: biases and myths-the proximal vs. distal hypoxic tubular injury debate revisited*. Kidney Int, 2010. **77**(1): p. 9-16.
 56. Bhalodia, Y., et al., *Renoprotective activity of benincasa cerifera fruit extract on ischemia/reperfusion-induced renal damage in rat*. Iran J Kidney Dis, 2009. **3**(2): p. 80-5.
 57. Shanley, P.F., et al., *Topography of focal proximal tubular necrosis after ischemia with reflow in the rat kidney*. Am J Pathol, 1986. **122**(3): p. 462-8.
 58. Singbartl, K., S.B. Forlow, and K. Ley, *Platelet, but not endothelial, P-selectin is critical for neutrophil-mediated acute postischemic renal failure*. FASEB J, 2001. **15**(13): p. 2337-44.
 59. Schroedl, C., et al., *Hypoxic but not anoxic stabilization of HIF-1alpha requires mitochondrial reactive oxygen species*. Am J Physiol Lung Cell Mol Physiol, 2002. **283**(5): p. L922-31.

60. Giaccia, A.J., M.C. Simon, and R. Johnson, *The biology of hypoxia: the role of oxygen sensing in development, normal function, and disease*. Genes Dev, 2004. **18**(18): p. 2183-94.
61. Vaidya, V.S., M.A. Ferguson, and J.V. Bonventre, *Biomarkers of acute kidney injury*. Annu Rev Pharmacol Toxicol, 2008. **48**: p. 463-93.
62. Waikar, S.S., R.A. Betensky, and J.V. Bonventre, *Creatinine as the gold standard for kidney injury biomarker studies?* Nephrol Dial Transplant, 2009. **24**(11): p. 3263-5.
63. Charlton, J.R., D. Portilla, and M.D. Okusa, *A basic science view of acute kidney injury biomarkers*. Nephrol Dial Transplant, 2014.
64. Han, W.K., et al., *Kidney Injury Molecule-1 (KIM-1): a novel biomarker for human renal proximal tubule injury*. Kidney Int, 2002. **62**(1): p. 237-44.
65. Ichimura, T., et al., *Kidney injury molecule-1 (KIM-1), a putative epithelial cell adhesion molecule containing a novel immunoglobulin domain, is up-regulated in renal cells after injury*. J Biol Chem, 1998. **273**(7): p. 4135-42.
66. Dieterle, F., et al., *Renal biomarker qualification submission: a dialog between the FDA-EMEA and Predictive Safety Testing Consortium*. Nat Biotechnol, 2010. **28**(5): p. 455-62.
67. Hales, K.G., *The machinery of mitochondrial fusion, division, and distribution, and emerging connections to apoptosis*. Mitochondrion, 2004. **4**(4): p. 285-308.
68. Sue, C.M. and E.A. Schon, *Mitochondrial respiratory chain diseases and mutations in nuclear DNA: a promising start?* Brain Pathol, 2000. **10**(3): p. 442-50.
69. McKenzie, M., et al., *Analysis of mitochondrial subunit assembly into respiratory chain complexes using Blue Native polyacrylamide gel electrophoresis*. Anal Biochem, 2007. **364**(2): p. 128-37.
70. Scarpulla, R.C., *Transcriptional paradigms in mammalian mitochondrial biogenesis and function*. Physiol Rev, 2008. **88**(2): p. 611-38.
71. Basile, D.P., M.D. Anderson, and T.A. Sutton, *Pathophysiology of acute kidney injury*. Compr Physiol, 2012. **2**(2): p. 1303-53.
72. Brooks, C., et al., *Regulation of mitochondrial dynamics in acute kidney injury in cell culture and rodent models*. J Clin Invest, 2009. **119**(5): p. 1275-85.
73. Feldkamp, T., A. Kribben, and J.M. Weinberg, *Assessment of mitochondrial membrane potential in proximal tubules after hypoxia-reoxygenation*. Am J Physiol Renal Physiol, 2005. **288**(6): p. F1092-102.
74. Hall, A.M. and R.J. Unwin, *The not so 'mighty chondrion': emergence of renal diseases due to mitochondrial dysfunction*. Nephron Physiol, 2007. **105**(1): p. p1-10.
75. Iwano, M., et al., *Evidence that fibroblasts derive from epithelium during tissue fibrosis*. J Clin Invest, 2002. **110**(3): p. 341-50.
76. Weinberg, J.M., et al., *Mitochondrial dysfunction during hypoxia/reoxygenation and its correction by anaerobic metabolism of citric acid cycle intermediates*. Proc Natl Acad Sci U S A, 2000. **97**(6): p. 2826-31.
77. Vanholder, R., et al., *Rhabdomyolysis*. Journal of the American Society of Nephrology : JASN, 2000. **11**(8): p. 1553-61.
78. Nath, K.A., et al., *Intracellular targets in heme protein-induced renal injury*.

- Kidney international, 1998. **53**(1): p. 100-11.
79. Zager, R.A., *Mitochondrial free radical production induces lipid peroxidation during myohemoglobinuria*. Kidney international, 1996. **49**(3): p. 741-51.
 80. Tran, M., et al., *PGC-1alpha promotes recovery after acute kidney injury during systemic inflammation in mice*. J Clin Invest, 2011. **121**(10): p. 4003-14.
 81. Jung, K. and R. Reszka, *Mitochondria as subcellular targets for clinically useful anthracyclines*. Advanced drug delivery reviews, 2001. **49**(1-2): p. 87-105.
 82. Lewis, W., B.J. Day, and W.C. Copeland, *Mitochondrial toxicity of NRTI antiviral drugs: an integrated cellular perspective*. Nature reviews. Drug discovery, 2003. **2**(10): p. 812-22.
 83. Mingatto, F.E., et al., *The critical role of mitochondrial energetic impairment in the toxicity of nimesulide to hepatocytes*. The Journal of pharmacology and experimental therapeutics, 2002. **303**(2): p. 601-7.
 84. Bonventre, J.V. and J.M. Weinberg, *Recent advances in the pathophysiology of ischemic acute renal failure*. Journal of the American Society of Nephrology : JASN, 2003. **14**(8): p. 2199-210.
 85. Weinberg, J.M., et al., *Glycine-protected, hypoxic, proximal tubules develop severely compromised energetic function*. Kidney international, 1997. **52**(1): p. 140-51.
 86. Rivera, M.I., et al., *Early morphological and biochemical changes during 2-Br-(diglutathion-S-yl)hydroquinone-induced nephrotoxicity*. Toxicology and applied pharmacology, 1994. **128**(2): p. 239-50.
 87. Nowak, G., et al., *Differential effects of EGF on repair of cellular functions after dichlorovinyl-L-cysteine-induced injury*. The American journal of physiology, 1999. **276**(2 Pt 2): p. F228-36.
 88. Schnellmann, R.G., *Mechanisms of t-butyl hydroperoxide-induced toxicity to rabbit renal proximal tubules*. The American journal of physiology, 1988. **255**(1 Pt 1): p. C28-33.
 89. Kozlov, A.V., et al., *Mitochondrial dysfunction and biogenesis: do ICU patients die from mitochondrial failure?* Annals of intensive care, 2011. **1**(1): p. 41.
 90. Funk, J.A. and R.G. Schnellmann, *Persistent disruption of mitochondrial homeostasis after acute kidney injury*. American journal of physiology. Renal physiology, 2012. **302**(7): p. F853-64.
 91. Weinberg, J.M., et al., *Mitochondrial dysfunction during hypoxia/reoxygenation and its correction by anaerobic metabolism of citric acid cycle intermediates*. Proceedings of the National Academy of Sciences of the United States of America, 2000. **97**(6): p. 2826-31.
 92. Feldkamp, T., A. Kribben, and J.M. Weinberg, *Assessment of mitochondrial membrane potential in proximal tubules after hypoxia-reoxygenation*. American journal of physiology. Renal physiology, 2005. **288**(6): p. F1092-102.
 93. Crompton, M., *The mitochondrial permeability transition pore and its role in cell death*. Biochem J, 1999. **341** (Pt 2): p. 233-49.
 94. Humphreys, B.D., et al., *Fate tracing reveals the pericyte and not epithelial origin of myofibroblasts in kidney fibrosis*. Am J Pathol, 2010. **176**(1): p. 85-97.
 95. Funk, J.A. and R.G. Schnellmann, *Persistent disruption of mitochondrial homeostasis after acute kidney injury*. Am J Physiol Renal Physiol, 2012. **302**(7):

- p. F853-64.
96. Puigserver, P. and B.M. Spiegelman, *Peroxisome proliferator-activated receptor-gamma coactivator 1 alpha (PGC-1 alpha): transcriptional coactivator and metabolic regulator*. *Endocr Rev*, 2003. **24**(1): p. 78-90.
 97. Wenz, T., et al., *Activation of the PPAR/PGC-1alpha pathway prevents a bioenergetic deficit and effectively improves a mitochondrial myopathy phenotype*. *Cell Metab*, 2008. **8**(3): p. 249-56.
 98. Nisoli, E., et al., *Mitochondrial biogenesis as a cellular signaling framework*. *Biochem Pharmacol*, 2004. **67**(1): p. 1-15.
 99. Liu, C. and J.D. Lin, *PGC-1 coactivators in the control of energy metabolism*. *Acta Biochim Biophys Sin (Shanghai)*, 2011. **43**(4): p. 248-57.
 100. Puigserver, P., et al., *A cold-inducible coactivator of nuclear receptors linked to adaptive thermogenesis*. *Cell*, 1998. **92**(6): p. 829-39.
 101. Wu, Z., et al., *Mechanisms controlling mitochondrial biogenesis and respiration through the thermogenic coactivator PGC-1*. *Cell*, 1999. **98**(1): p. 115-24.
 102. Scarpulla, R.C., *Nucleus-encoded regulators of mitochondrial function: integration of respiratory chain expression, nutrient sensing and metabolic stress*. *Biochim Biophys Acta*, 2012. **1819**(9-10): p. 1088-97.
 103. Scarpulla, R.C., R.B. Vega, and D.P. Kelly, *Transcriptional integration of mitochondrial biogenesis*. *Trends Endocrinol Metab*, 2012. **23**(9): p. 459-66.
 104. Evans, M.J. and R.C. Scarpulla, *Interaction of nuclear factors with multiple sites in the somatic cytochrome c promoter. Characterization of upstream NRF-1, ATF, and intron Sp1 recognition sequences*. *J Biol Chem*, 1989. **264**(24): p. 14361-8.
 105. Scarpulla, R.C., *Nuclear control of respiratory chain expression in mammalian cells*. *J Bioenerg Biomembr*, 1997. **29**(2): p. 109-19.
 106. Eichner, L.J. and V. Giguere, *Estrogen related receptors (ERRs): a new dawn in transcriptional control of mitochondrial gene networks*. *Mitochondrion*, 2011. **11**(4): p. 544-52.
 107. Dufour, C.R., et al., *Genome-wide orchestration of cardiac functions by the orphan nuclear receptors ERRalpha and gamma*. *Cell Metab*, 2007. **5**(5): p. 345-56.
 108. Gopalakrishnan, L. and R.C. Scarpulla, *Differential regulation of respiratory chain subunits by a CREB-dependent signal transduction pathway. Role of cyclic AMP in cytochrome c and COXIV gene expression*. *J Biol Chem*, 1994. **269**(1): p. 105-13.
 109. Vercauteren, K., et al., *PGC-1-related coactivator: immediate early expression and characterization of a CREB/NRF-1 binding domain associated with cytochrome c promoter occupancy and respiratory growth*. *Mol Cell Biol*, 2006. **26**(20): p. 7409-19.
 110. Herzig, R.P., S. Scacco, and R.C. Scarpulla, *Sequential serum-dependent activation of CREB and NRF-1 leads to enhanced mitochondrial respiration through the induction of cytochrome c*. *J Biol Chem*, 2000. **275**(17): p. 13134-41.
 111. Li, R., et al., *Sp1 activates and inhibits transcription from separate elements in the proximal promoter of the human adenine nucleotide translocase 2 (ANT2) gene*. *J Biol Chem*, 1996. **271**(31): p. 18925-30.

112. Basu, A., et al., *Regulation of murine cytochrome oxidase Vb gene expression in different tissues and during myogenesis. Role of a YY-1 factor-binding negative enhancer.* J Biol Chem, 1997. **272**(9): p. 5899-908.
113. Seelan, R.S. and L.I. Grossman, *Structural organization and promoter analysis of the bovine cytochrome c oxidase subunit VIIc gene. A functional role for YY1.* J Biol Chem, 1997. **272**(15): p. 10175-81.
114. Gulick, T., et al., *The peroxisome proliferator-activated receptor regulates mitochondrial fatty acid oxidative enzyme gene expression.* Proc Natl Acad Sci U S A, 1994. **91**(23): p. 11012-6.
115. Monsalve, M., et al., *Direct coupling of transcription and mRNA processing through the thermogenic coactivator PGC-1.* Mol Cell, 2000. **6**(2): p. 307-16.
116. Wu, C.G., et al., *Mechanism for controlling the monomer-dimer conversion of SARS coronavirus main protease.* Acta Crystallogr D Biol Crystallogr, 2013. **69**(Pt 5): p. 747-55.
117. Gleyzer, N., K. Vercauteren, and R.C. Scarpulla, *Control of mitochondrial transcription specificity factors (TFB1M and TFB2M) by nuclear respiratory factors (NRF-1 and NRF-2) and PGC-1 family coactivators.* Mol Cell Biol, 2005. **25**(4): p. 1354-66.
118. Mootha, V.K., et al., *Erralpha and Gabpa/b specify PGC-1alpha-dependent oxidative phosphorylation gene expression that is altered in diabetic muscle.* Proc Natl Acad Sci U S A, 2004. **101**(17): p. 6570-5.
119. Handschin, C. and B.M. Spiegelman, *Peroxisome proliferator-activated receptor gamma coactivator 1 coactivators, energy homeostasis, and metabolism.* Endocr Rev, 2006. **27**(7): p. 728-35.
120. Fernandez-Marcos, P.J. and J. Auwerx, *Regulation of PGC-1alpha, a nodal regulator of mitochondrial biogenesis.* Am J Clin Nutr, 2011. **93**(4): p. 884S-90.
121. Herzig, S., et al., *CREB regulates hepatic gluconeogenesis through the coactivator PGC-1.* Nature, 2001. **413**(6852): p. 179-83.
122. Nisoli, E., et al., *Can endogenous gaseous messengers control mitochondrial biogenesis in mammalian cells? Prostaglandins Other Lipid Mediat,* 2004. **73**(1-2): p. 9-27.
123. Nisoli, E., et al., *Calorie restriction promotes mitochondrial biogenesis by inducing the expression of eNOS.* Science, 2005. **310**(5746): p. 314-7.
124. Schaeffer, P.J., et al., *Calcineurin and calcium/calmodulin-dependent protein kinase activate distinct metabolic gene regulatory programs in cardiac muscle.* J Biol Chem, 2004. **279**(38): p. 39593-603.
125. Austin, S. and J. St-Pierre, *PGC1alpha and mitochondrial metabolism--emerging concepts and relevance in ageing and neurodegenerative disorders.* J Cell Sci, 2012. **125**(Pt 21): p. 4963-71.
126. Funk, J.A., S. Odejinmi, and R.G. Schnellmann, *SRT1720 induces mitochondrial biogenesis and rescues mitochondrial function after oxidant injury in renal proximal tubule cells.* J Pharmacol Exp Ther, 2010. **333**(2): p. 593-601.
127. Nowak, G., et al., *Activation of ERK1/2 pathway mediates oxidant-induced decreases in mitochondrial function in renal cells.* Am J Physiol Renal Physiol, 2006. **291**(4): p. F840-55.
128. Rasbach, K.A. and R.G. Schnellmann, *PGC-1alpha over-expression promotes*

- recovery from mitochondrial dysfunction and cell injury*. Biochem Biophys Res Commun, 2007. **355**(3): p. 734-9.
129. Nowak, G., et al., *Recovery of cellular functions following oxidant injury*. Am J Physiol, 1998. **274**(3 Pt 2): p. F509-15.
 130. Rasbach, K.A. and R.G. Schnellmann, *Signaling of mitochondrial biogenesis following oxidant injury*. J Biol Chem, 2007. **282**(4): p. 2355-62.
 131. Ruas, J.L., et al., *A PGC-1alpha isoform induced by resistance training regulates skeletal muscle hypertrophy*. Cell, 2012. **151**(6): p. 1319-31.
 132. Peterson, Y.K., et al., *beta2-Adrenoceptor agonists in the regulation of mitochondrial biogenesis*. Bioorg Med Chem Lett, 2013. **23**(19): p. 5376-81.
 133. Rasmussen, S.G., et al., *Crystal structure of the beta(2) adrenergic receptor-Gs protein complex*. Nature, 2011.
 134. Seifert, R., et al., *Efficient adenylyl cyclase activation by a beta2-adrenoceptor-G(i)alpha2 fusion protein*. Biochem Biophys Res Commun, 2002. **298**(5): p. 824-8.
 135. Scarpulla, R.C., *Metabolic control of mitochondrial biogenesis through the PGC-1 family regulatory network*. Biochimica et biophysica acta, 2011. **1813**(7): p. 1269-78.
 136. Yuzlenko, O. and K. Kiec-Kononowicz, *Potent adenosine A1 and A2A receptors antagonists: recent developments*. Curr Med Chem, 2006. **13**(30): p. 3609-25.
 137. Sachdeva, S. and M. Gupta, *Adenosine and its receptors as therapeutic targets: An overview*. Saudi Pharm J, 2013. **21**(3): p. 245-53.
 138. Birk, A.V., et al., *The mitochondrial-targeted compound SS-31 re-energizes ischemic mitochondria by interacting with cardiolipin*. J Am Soc Nephrol, 2013. **24**(8): p. 1250-61.
 139. Jo, S.K., M.H. Rosner, and M.D. Okusa, *Pharmacologic treatment of acute kidney injury: why drugs haven't worked and what is on the horizon*. Clin J Am Soc Nephrol, 2007. **2**(2): p. 356-65.
 140. Wenz, T., et al., *Activation of the PPAR/PGC-1 β Pathway Prevents a Bioenergetic Deficit and Effectively Improves a Mitochondrial Myopathy Phenotype*. Cell Metabolism, 2008. **8**(3): p. 249-256.
 141. Rasbach, K.A. and R.G. Schnellmann, *PGC-1alpha over-expression promotes recovery from mitochondrial dysfunction and cell injury*. Biochemical and biophysical research communications, 2007. **355**(3): p. 734-9.
 142. Canto, C. and J. Auwerx, *PGC-1alpha, SIRT1 and AMPK, an energy sensing network that controls energy expenditure*. Curr Opin Lipidol, 2009. **20**(2): p. 98-105.
 143. Lagouge, M., et al., *Resveratrol improves mitochondrial function and protects against metabolic disease by activating SIRT1 and PGC-1alpha*. Cell, 2006. **127**(6): p. 1109-22.
 144. Nemoto, S., M.M. Fergusson, and T. Finkel, *SIRT1 functionally interacts with the metabolic regulator and transcriptional coactivator PGC-1{alpha}*. J Biol Chem, 2005. **280**(16): p. 16456-60.
 145. Rasbach, K.A. and R.G. Schnellmann, *Isoflavones promote mitochondrial biogenesis*. J Pharmacol Exp Ther, 2008. **325**(2): p. 536-43.
 146. Beeson, C.C., G.C. Beeson, and R.G. Schnellmann, *A high-throughput*

- respirometric assay for mitochondrial biogenesis and toxicity*. Anal Biochem, 2010. **404**(1): p. 75-81.
147. Pejznochova, M., et al., *The developmental changes in mitochondrial DNA content per cell in human cord blood leukocytes during gestation*. Physiol Res, 2008. **57**(6): p. 947-55.
148. Medeiros, D.M., *Assessing mitochondria biogenesis*. Methods, 2008. **46**(4): p. 288-94.
149. Chazotte, B., *Labeling mitochondria with MitoTracker dyes*. Cold Spring Harb Protoc, 2011. **2011**(8): p. 990-2.
150. Gohil, V.M., et al., *Binding of 10-N-nonyl acridine orange to cardiolipin-deficient yeast cells: implications for assay of cardiolipin*. Anal Biochem, 2005. **343**(2): p. 350-2.
151. Kelly, D.P. and R.C. Scarpulla, *Transcriptional regulatory circuits controlling mitochondrial biogenesis and function*. Genes Dev, 2004. **18**(4): p. 357-68.
152. Goffart, S. and R.J. Wiesner, *Regulation and co-ordination of nuclear gene expression during mitochondrial biogenesis*. Exp Physiol, 2003. **88**(1): p. 33-40.
153. Arany, Z., et al., *Gene expression-based screening identifies microtubule inhibitors as inducers of PGC-1 α and oxidative phosphorylation*. Proc Natl Acad Sci U S A, 2008. **105**(12): p. 4721-6.
154. Pacholec, M., et al., *SIRT1720, SIRT2183, SIRT1460, and resveratrol are not direct activators of SIRT1*. J Biol Chem, 2010. **285**(11): p. 8340-51.
155. Nowak, G. and R.G. Schnellmann, *Improved culture conditions stimulate gluconeogenesis in primary cultures of renal proximal tubule cells*. Am J Physiol, 1995. **268**(4 Pt 1): p. C1053-61.
156. Nowak, G. and R.G. Schnellmann, *L-ascorbic acid regulates growth and metabolism of renal cells: improvements in cell culture*. Am J Physiol, 1996. **271**(6 Pt 1): p. C2072-80.
157. Jesinkey, S.R., et al., *Formoterol restores mitochondrial and renal function after ischemia-reperfusion injury*. J Am Soc Nephrol, 2014. **25**(6): p. 1157-62.
158. Gerencser, A.A., et al., *Quantitative microplate-based respirometry with correction for oxygen diffusion*. Anal Chem, 2009. **81**(16): p. 6868-78.
159. Wills, L.P., et al., *The beta2-adrenoceptor agonist formoterol stimulates mitochondrial biogenesis*. J Pharmacol Exp Ther, 2012. **342**(1): p. 106-18.
160. Wills, L.P., et al., *High-throughput respirometric assay identifies predictive toxicophore of mitochondrial injury*. Toxicol Appl Pharmacol, 2013. **272**(2): p. 490-502.
161. Vallon, V. and H. Osswald, *Adenosine receptors and the kidney*. Handb Exp Pharmacol, 2009(193): p. 443-70.
162. Maemoto, T., et al., *Species differences in brain adenosine A1 receptor pharmacology revealed by use of xanthine and pyrazolopyridine based antagonists*. Br J Pharmacol, 1997. **122**(6): p. 1202-8.
163. Ukena, D., et al., *Species differences in structure-activity relationships of adenosine agonists and xanthine antagonists at brain A1 adenosine receptors*. FEBS Lett, 1986. **209**(1): p. 122-8.
164. Joo, J.D., et al., *Acute and delayed renal protection against renal ischemia and reperfusion injury with A1 adenosine receptors*. Am J Physiol Renal Physiol,

2007. **293**(6): p. F1847-57.
165. Kim, J., et al., *Endogenous A1 adenosine receptors protect against hepatic ischemia reperfusion injury in mice*. Liver Transpl, 2008. **14**(6): p. 845-54.
 166. Schenone, S., et al., *A1 receptors ligands: past, present and future trends*. Curr Top Med Chem, 2010. **10**(9): p. 878-901.
 167. Albasanz, J.L., et al., *Up-regulation of adenosine receptors in the frontal cortex in Alzheimer's disease*. Brain Pathol, 2008. **18**(2): p. 211-9.
 168. Boison, D., *Adenosine as a modulator of brain activity*. Drug News Perspect, 2007. **20**(10): p. 607-11.
 169. Boison, D., *Adenosine-based modulation of brain activity*. Curr Neuropharmacol, 2009. **7**(3): p. 158-9.
 170. Brust, T.B., et al., *p38 mitogen-activated protein kinase contributes to adenosine A1 receptor-mediated synaptic depression in area CA1 of the rat hippocampus*. J Neurosci, 2006. **26**(48): p. 12427-38.
 171. *HOTLINE III: End of the line for rolofylline?* Eur Heart J, 2009. **30**(23): p. 2819-20.
 172. Voors, A.A., et al., *Effects of the adenosine A1 receptor antagonist rolofylline on renal function in patients with acute heart failure and renal dysfunction: results from PROTECT (Placebo-Controlled Randomized Study of the Selective Adenosine A1 Receptor Antagonist Rolofylline for Patients Hospitalized with Acute Decompensated Heart Failure and Volume Overload to Assess Treatment Effect on Congestion and Renal Function)*. J Am Coll Cardiol, 2011. **57**(19): p. 1899-907.
 173. Mitrovic, V., et al., *Cardio-renal effects of the A1 adenosine receptor antagonist SLV320 in patients with heart failure*. Circ Heart Fail, 2009. **2**(6): p. 523-31.
 174. Ellenbogen, K.A., et al., *Trial to evaluate the management of paroxysmal supraventricular tachycardia during an electrophysiology study with tecadenoson*. Circulation, 2005. **111**(24): p. 3202-8.
 175. Dhalla, A.K., et al., *A1 adenosine receptor: role in diabetes and obesity*. Handb Exp Pharmacol, 2009(193): p. 271-95.
 176. Zablocki, J.A., et al., *Partial A(1) adenosine receptor agonists from a molecular perspective and their potential use as chronic ventricular rate control agents during atrial fibrillation (AF)*. Curr Top Med Chem, 2004. **4**(8): p. 839-54.
 177. Zannikos, P.N., S. Rohatagi, and B.K. Jensen, *Pharmacokinetic-pharmacodynamic modeling of the antilipolytic effects of an adenosine receptor agonist in healthy volunteers*. J Clin Pharmacol, 2001. **41**(1): p. 61-9.
 178. Wu, L., et al., *A partial agonist of the A(1)-adenosine receptor selectively slows AV conduction in guinea pig hearts*. Am J Physiol Heart Circ Physiol, 2001. **280**(1): p. H334-43.
 179. Lee, H.T., et al., *A1 adenosine receptor knockout mice exhibit increased renal injury following ischemia and reperfusion*. Am J Physiol Renal Physiol, 2004. **286**(2): p. F298-306.
 180. Lee, H.T., et al., *Renal tubule necrosis and apoptosis modulation by A1 adenosine receptor expression*. Kidney Int, 2007. **71**(12): p. 1249-61.
 181. Park, S.W., et al., *Protection against acute kidney injury via A(1) adenosine receptor-mediated Akt activation reduces liver injury after liver ischemia and*

- reperfusion in mice*. J Pharmacol Exp Ther, 2010. **333**(3): p. 736-47.
182. Kim, M., et al., *Selective renal overexpression of human heat shock protein 27 reduces renal ischemia-reperfusion injury in mice*. Am J Physiol Renal Physiol, 2010. **299**(2): p. F347-58.
 183. Kim, M., et al., *Kidney-specific reconstitution of the A1 adenosine receptor in A1 adenosine receptor knockout mice reduces renal ischemia-reperfusion injury*. Kidney Int, 2009. **75**(8): p. 809-23.
 184. Park, S.W., et al., *Selective intrarenal human A1 adenosine receptor overexpression reduces acute liver and kidney injury after hepatic ischemia reperfusion in mice*. Lab Invest, 2010. **90**(3): p. 476-95.
 185. Lee, H.T. and C.W. Emala, *Protective effects of renal ischemic preconditioning and adenosine pretreatment: role of A(1) and A(3) receptors*. Am J Physiol Renal Physiol, 2000. **278**(3): p. F380-7.
 186. Lee, H.T., et al., *A1 adenosine receptor activation inhibits inflammation, necrosis, and apoptosis after renal ischemia-reperfusion injury in mice*. J Am Soc Nephrol, 2004. **15**(1): p. 102-11.
 187. Chakrabarti, S.K., et al., *S-[(1 and 2)-phenyl-2-hydroxyethyl]cysteine-induced alterations in renal mitochondrial function in male Fischer-344 rats*. Toxicol Appl Pharmacol, 1998. **151**(1): p. 123-34.
 188. Nath, K.A., et al., *Intracellular targets in heme protein-induced renal injury*. Kidney Int, 1998. **53**(1): p. 100-11.
 189. Cummings, B.S., et al., *Cytotoxicity of trichloroethylene and S-(1, 2-dichlorovinyl)-L-cysteine in primary cultures of rat renal proximal tubular and distal tubular cells*. Toxicology, 2000. **150**(1-3): p. 83-98.
 190. Nowak, G., et al., *Differential effects of EGF on repair of cellular functions after dichlorovinyl-L-cysteine-induced injury*. Am J Physiol, 1999. **276**(2 Pt 2): p. F228-36.
 191. Bellomo, R., J.A. Kellum, and C. Ronco, *Acute kidney injury*. Lancet. **380**(9843): p. 756-66.
 192. Kellum, J.A., R. Bellomo, and C. Ronco, *Kidney attack*. Jama. **307**(21): p. 2265-6.
 193. Funk, J.A., S. Odejinmi, and R.G. Schnellmann, *SRT1720 induces mitochondrial biogenesis and rescues mitochondrial function after oxidant injury in renal proximal tubule cells*. J Pharmacol Exp Ther. **333**(2): p. 593-601.
 194. Funk, J.A. and R.G. Schnellmann, *Persistent disruption of mitochondrial homeostasis after acute kidney injury*. Am J Physiol Renal Physiol. **302**(7): p. F853-64.
 195. Hall, A.M., et al., *Multiphoton imaging reveals differences in mitochondrial function between nephron segments*. J Am Soc Nephrol, 2009. **20**(6): p. 1293-302.
 196. Sharfuddin, A.A. and B.A. Molitoris, *Pathophysiology of ischemic acute kidney injury*. Nat Rev Nephrol. **7**(4): p. 189-200.
 197. Weinberg, J.M., et al., *Glycine-protected, hypoxic, proximal tubules develop severely compromised energetic function*. Kidney Int, 1997. **52**(1): p. 140-51.
 198. Tran, M., et al., *PGC-1alpha promotes recovery after acute kidney injury during systemic inflammation in mice*. J Clin Invest. **121**(10): p. 4003-14.
 199. Szeto, H.H., et al., *Mitochondria-targeted peptide accelerates ATP recovery and*

- reduces ischemic kidney injury*. Journal of the American Society of Nephrology : JASN, 2011. **22**(6): p. 1041-52.
200. Liu, C. and J.D. Lin, *PGC-1 coactivators in the control of energy metabolism*. Acta Biochim Biophys Sin (Shanghai). **43**(4): p. 248-57.
 201. Arany, Z., et al., *HIF-independent regulation of VEGF and angiogenesis by the transcriptional coactivator PGC-1alpha*. Nature, 2008. **451**(7181): p. 1008-12.
 202. Barger, J.L., et al., *A low dose of dietary resveratrol partially mimics caloric restriction and retards aging parameters in mice*. PLoS One, 2008. **3**(6): p. e2264.
 203. Suliman, H.B., et al., *Lipopolysaccharide stimulates mitochondrial biogenesis via activation of nuclear respiratory factor-1*. J Biol Chem, 2003. **278**(42): p. 41510-8.
 204. Sutherland, L.N., et al., *Exercise and adrenaline increase PGC-1{alpha} mRNA expression in rat adipose tissue*. J Physiol, 2009. **587**(Pt 7): p. 1607-17.
 205. Wang, H., et al., *CCAAT/enhancer binding protein-beta is a transcriptional regulator of peroxisome-proliferator-activated receptor-gamma coactivator-1alpha in the regenerating liver*. Mol Endocrinol, 2008. **22**(7): p. 1596-605.
 206. Yin, W., et al., *Rapidly increased neuronal mitochondrial biogenesis after hypoxic-ischemic brain injury*. Stroke, 2008. **39**(11): p. 3057-63.
 207. Wills, L.P., et al., *The beta2-adrenoceptor agonist formoterol stimulates mitochondrial biogenesis*. J Pharmacol Exp Ther. **342**(1): p. 106-18.
 208. Peterson, Y.K., et al., *beta-Adrenoceptor agonists in the regulation of mitochondrial biogenesis*. Bioorganic & medicinal chemistry letters, 2013.
 209. van Timmeren, M.M., et al., *Tubular kidney injury molecule-1 (KIM-1) in human renal disease*. J Pathol, 2007. **212**(2): p. 209-17.
 210. Chawla, L.S., et al., *The severity of acute kidney injury predicts progression to chronic kidney disease*. Kidney Int. **79**(12): p. 1361-9.
 211. Nakhoul, N. and V. Batuman, *Role of proximal tubules in the pathogenesis of kidney disease*. Contrib Nephrol. **169**: p. 37-50.
 212. Fluck, M., *Functional, structural and molecular plasticity of mammalian skeletal muscle in response to exercise stimuli*. J Exp Biol, 2006. **209**(Pt 12): p. 2239-48.
 213. Fanzani, A., et al., *Molecular and cellular mechanisms of skeletal muscle atrophy: an update*. J Cachexia Sarcopenia Muscle, 2012. **3**(3): p. 163-79.
 214. Schakman, O., et al., *Glucocorticoid-induced skeletal muscle atrophy*. Int J Biochem Cell Biol, 2013. **45**(10): p. 2163-72.
 215. Slee, A.D., *Exploring metabolic dysfunction in chronic kidney disease*. Nutr Metab (Lond), 2012. **9**(1): p. 36.
 216. Metter, E.J., et al., *Skeletal muscle strength as a predictor of all-cause mortality in healthy men*. J Gerontol A Biol Sci Med Sci, 2002. **57**(10): p. B359-65.
 217. Pocock, S.J., et al., *Weight loss and mortality risk in patients with chronic heart failure in the candesartan in heart failure: assessment of reduction in mortality and morbidity (CHARM) programme*. Eur Heart J, 2008. **29**(21): p. 2641-50.
 218. He, W.A., et al., *NF-kappaB-mediated Pax7 dysregulation in the muscle microenvironment promotes cancer cachexia*. J Clin Invest, 2013. **123**(11): p. 4821-35.
 219. Bonaldo, P. and M. Sandri, *Cellular and molecular mechanisms of muscle*

- atrophy*. Disease models & mechanisms, 2013. **6**(1): p. 25-39.
220. Sacheck, J.M., et al., *Rapid disuse and denervation atrophy involve transcriptional changes similar to those of muscle wasting during systemic diseases*. FASEB journal : official publication of the Federation of American Societies for Experimental Biology, 2007. **21**(1): p. 140-55.
 221. Lee, S.J., *Regulation of muscle mass by myostatin*. Annu Rev Cell Dev Biol, 2004. **20**: p. 61-86.
 222. McPherron, A.C., A.M. Lawler, and S.J. Lee, *Regulation of skeletal muscle mass in mice by a new TGF-beta superfamily member*. Nature, 1997. **387**(6628): p. 83-90.
 223. Bodine, S.C., et al., *Identification of ubiquitin ligases required for skeletal muscle atrophy*. Science, 2001. **294**(5547): p. 1704-8.
 224. Gomes, M.D., et al., *Atrogin-1, a muscle-specific F-box protein highly expressed during muscle atrophy*. Proc Natl Acad Sci U S A, 2001. **98**(25): p. 14440-5.
 225. Adams, G.R., *Autocrine and/or paracrine insulin-like growth factor-I activity in skeletal muscle*. Clin Orthop Relat Res, 2002(403 Suppl): p. S188-96.
 226. Adams, G.R., *Invited Review: Autocrine/paracrine IGF-I and skeletal muscle adaptation*. J Appl Physiol (1985), 2002. **93**(3): p. 1159-67.
 227. Schiaffino, S., et al., *Mechanisms regulating skeletal muscle growth and atrophy*. FEBS J, 2013. **280**(17): p. 4294-314.
 228. Musaro, A., et al., *Localized Igf-1 transgene expression sustains hypertrophy and regeneration in senescent skeletal muscle*. Nat Genet, 2001. **27**(2): p. 195-200.
 229. Sandri, M., et al., *Foxo transcription factors induce the atrophy-related ubiquitin ligase atrogin-1 and cause skeletal muscle atrophy*. Cell, 2004. **117**(3): p. 399-412.
 230. Senf, S.M., S.L. Dodd, and A.R. Judge, *FOXO signaling is required for disuse muscle atrophy and is directly regulated by Hsp70*. Am J Physiol Cell Physiol, 2010. **298**(1): p. C38-45.
 231. Brault, J.J., J.G. Jespersen, and A.L. Goldberg, *Peroxisome proliferator-activated receptor gamma coactivator 1alpha or 1beta overexpression inhibits muscle protein degradation, induction of ubiquitin ligases, and disuse atrophy*. J Biol Chem, 2010. **285**(25): p. 19460-71.
 232. Schreiber, S.N., et al., *The estrogen-related receptor alpha (ERRalpha) functions in PPARgamma coactivator 1alpha (PGC-1alpha)-induced mitochondrial biogenesis*. Proc Natl Acad Sci U S A, 2004. **101**(17): p. 6472-7.
 233. Sandri, M., et al., *PGC-1alpha protects skeletal muscle from atrophy by suppressing FoxO3 action and atrophy-specific gene transcription*. Proc Natl Acad Sci U S A, 2006. **103**(44): p. 16260-5.
 234. Sato, S., et al., *Muscle plasticity and beta(2)-adrenergic receptors: adaptive responses of beta(2)-adrenergic receptor expression to muscle hypertrophy and atrophy*. Journal of biomedicine & biotechnology, 2011. **2011**: p. 729598.
 235. Kline, W.O., et al., *Rapamycin inhibits the growth and muscle-sparing effects of clenbuterol*. Journal of applied physiology, 2007. **102**(2): p. 740-7.
 236. Joassard, O.R., et al., *Regulation of Akt-mTOR, ubiquitin-proteasome and autophagy-lysosome pathways in response to formoterol administration in rat skeletal muscle*. The international journal of biochemistry & cell biology, 2013.

- 45(11): p. 2444-55.
237. Bymaster, F.P., et al., *Atomoxetine increases extracellular levels of norepinephrine and dopamine in prefrontal cortex of rat: a potential mechanism for efficacy in attention deficit/hyperactivity disorder*. *Neuropsychopharmacology*, 2002. **27**(5): p. 699-711.
238. Pearen, M.A., et al., *The orphan nuclear receptor, NOR-1, a target of beta-adrenergic signaling, regulates gene expression that controls oxidative metabolism in skeletal muscle*. *Endocrinology*, 2008. **149**(6): p. 2853-65.
239. Pearen, M.A., et al., *Expression profiling of skeletal muscle following acute and chronic beta2-adrenergic stimulation: implications for hypertrophy, metabolism and circadian rhythm*. *BMC genomics*, 2009. **10**: p. 448.
240. Wills, L.P., et al., *The beta2-adrenoceptor agonist formoterol stimulates mitochondrial biogenesis*. *The Journal of pharmacology and experimental therapeutics*, 2012. **342**(1): p. 106-18.
241. Joassard, O.R., A.C. Durieux, and D.G. Freyssenet, *beta2-Adrenergic agonists and the treatment of skeletal muscle wasting disorders*. *Int J Biochem Cell Biol*, 2013. **45**(10): p. 2309-21.
242. Wada, S., et al., *Translational suppression of atrophic regulators by microRNA-23a integrates resistance to skeletal muscle atrophy*. *J Biol Chem*, 2011. **286**(44): p. 38456-65.
243. Koopman, R., et al., *Cellular mechanisms underlying temporal changes in skeletal muscle protein synthesis and breakdown during chronic {beta}-adrenoceptor stimulation in mice*. *J Physiol*, 2010. **588**(Pt 23): p. 4811-23.
244. Mirbolooki, M.R., et al., *Targeting presynaptic norepinephrine transporter in brown adipose tissue: a novel imaging approach and potential treatment for diabetes and obesity*. *Synapse*, 2013. **67**(2): p. 79-93.
245. Springer, J.P., B.P. Kropp, and K.B. Thor, *Facilitatory and inhibitory effects of selective norepinephrine reuptake inhibitors on hypogastric nerve-evoked urethral contractions in the cat: a prominent role of urethral beta-adrenergic receptors*. *J Urol*, 1994. **152**(2 Pt 1): p. 515-9.
246. Hemmings, B.A. and D.F. Restuccia, *PI3K-PKB/Akt pathway*. *Cold Spring Harb Perspect Biol*, 2012. **4**(9): p. a011189.
247. Carbo, N., et al., *Comparative effects of beta2-adrenergic agonists on muscle waste associated with tumour growth*. *Cancer Lett*, 1997. **115**(1): p. 113-8.
248. Soppa, G.K., et al., *Effects of chronic administration of clenbuterol on function and metabolism of adult rat cardiac muscle*. *Am J Physiol Heart Circ Physiol*, 2005. **288**(3): p. H1468-76.
249. Ryall, J.G., M.N. Sillence, and G.S. Lynch, *Systemic administration of beta2-adrenoceptor agonists, formoterol and salmeterol, elicit skeletal muscle hypertrophy in rats at micromolar doses*. *Br J Pharmacol*, 2006. **147**(6): p. 587-95.
250. Das, S., et al., *Nuclear miRNA regulates the mitochondrial genome in the heart*. *Circ Res*, 2012. **110**(12): p. 1596-603.
251. Colleoni, F., et al., *Suppression of mitochondrial electron transport chain function in the hypoxic human placenta: a role for miRNA-210 and protein synthesis inhibition*. *PLoS One*, 2013. **8**(1): p. e55194.

252. Fine, L.G., C. Orphanides, and J.T. Norman, *Progressive renal disease: the chronic hypoxia hypothesis*. *Kidney Int Suppl*, 1998. **65**: p. S74-8.
253. Fukuda, R., et al., *HIF-1 regulates cytochrome oxidase subunits to optimize efficiency of respiration in hypoxic cells*. *Cell*, 2007. **129**(1): p. 111-22.
254. Rasbach, K.A., P.T. Green, and R.G. Schnellmann, *Oxidants and Ca²⁺ induce PGC-1alpha degradation through calpain*. *Arch Biochem Biophys*, 2008. **478**(2): p. 130-5.